Anders Opheim Heggseth

Passivation and Reactivation of Aluminium Sacrificial Anodes

Master's thesis in Materials Science and Engineering
Supervisor: Ole Øystein Knudsen
June 2019

Master's thesis

NTNU
Norwegian University of Science and Technology
Faculty of Engineering
Department of Mechanical and Industrial Engineering

NTNU
Norwegian University of
Science and Technology

Anders Opheim Heggseth

Passivation and Reactivation of Aluminium Sacrificial Anodes

Master's thesis in Materials Science and Engineering
Supervisor: Ole Øystein Knudsen
June 2019

Norwegian University of Science and Technology
Faculty of Engineering
Department of Mechanical and Industrial Engineering

NTNU
Norwegian University of
Science and Technology

PREFACE

This master's thesis describes the attempt of passivating aluminium anodes by cathodic polarization. The goal has been to passivate anodes while investigating the process, as well as inspect at which circumstances the anodes will reactivate. While observing the process, it has also been attempted to obtain good methods for further investigation of this phenomenon. The project has been a collaboration between NTNU and FORCE Technology, and the report is the basis for evaluation of the course TMM4960 at the Norwegian University of Science and Technology, NTNU.

I would like to thank my supervisor Professor Ole Øystein Knudsen for excellent help and guidance throughout the project duration. I would also like to thank Gro Østensen Lauvstad, Harald Osvoll and Magnus Myhr from FORCE Technology for valuable discussion and inputs. In addition, I would like to thank Skarpenord AS for supplying the material used in the project.

Trondheim, June 2019

Anders Opheim Heggseth

ABSTRACT

A new non-contact inspection method called FIGS® has been developed in recent years. This technique is based on field gradient measurements and will assess the condition of the corrosion protection system of different subsea assets [5]. This new method of inspection has resulted in the discovery of aluminium anodes with low to no activity, in addition to cathodic behaving aluminium anodes. Based on this, it has been projected that a difference in operating potential between anodes on the same structure can cause low potential anodes to cathodically polarize anodes with higher potential, and thereby passivating them. This hypothesis has been tested in this report, where it has been attempted to passivate aluminium anodes in the lab, as well as investigating conditions for reactivation.

A long-term potentiostatic experiment where aluminium anode samples were polarized to different cathodic potentials was performed. The current density was logged throughout the experiment. After 27 and 120 days of exposure, linear polarization resistance was recorded and used for corrosion rate calculations. Polarization curves were recorded after the potentiostatic experiment was ended. A handful of samples were also further investigated in the scanning electron microscope, in order to investigate which oxides that might have been formed. Short-term galvanostatic experiments with different experiment durations were also performed, where polarization curves also were obtained after the galvanostatic polarization.

The cathodic current density measurements decreased slightly throughout the long-term potentiostatic experiment. This could indicate partial passivation, but it is difficult to know if passivation had occurred based solely on this. Polarization curves gave clear indications of some sort of passivation, as most of the samples had a decrease current density at a given potential compared to the polarization curve of non-exposed samples. The series that was subjected to the largest cathodic polarization indicated the highest degree of passivation.

Corrosion rate measurements showed that that the results from each series varied to a large degree, as well as variations between series and samples was small. This indicates that the corrosion rates were almost unaffected by cathodic polarization, even though the anodes ability to provide cathodic current up to a given potential was decreased. However, the corrosion rate of exposed samples decreased compared

to the corrosion rate of non-exposed samples but did not seem to give any information on the degree of passivation.

The polarization curves carried out after the short-term experiments showed a decrease in current density at a given potential as well, compared to polarization curve of non-exposed samples. This indicates passivation, where the degree of passivation seemed to increase with experiment duration.

Most of the passivated samples reactivated somewhere between -900 and -950 $mV_{Ag/AgCl}$, where this interval did not seem to be dependent on the degree of passivation. This indicates that if an anode used for cathodic protection is passivated to some degree, the anode will reactivate before the potential reaches a level where active corrosion is possible for steel structures. The material was permanently activated after being anodically polarized to the reactivation potential or higher.

Scanning electron microscope results showed that a layer was present on the sample surface, which mainly consisted of oxygen and aluminium. Traces of calcareous deposits were also found, and the greatest amount of deposits was found at samples subjected to the highest cathodic polarization. However, in general, the amount of calcareous deposits were very small, indicating that these findings have little influence on the electrochemical properties of the material.

SAMANDRAG

Ein ny inspeksjonsmetode ved navn FIGS® har i dei seinare år blitt utvikla. Denne metoden nyttar seg av felt-gradient målingar og vurderar tilstanden på korrosjonsbeskyttelsesystemet til forskjellige undervasstrukturar og røyrledningar utan fysisk kontakt [5]. Denne teknologien har ført til funn av aluminiumsanodar som viser lite til ingen aktivitet, samt katodiske anodar. Basert på dette har det blitt presentert ein mogleg forklaring der potensialforskjell mellom anodar på same struktur kan føra til at anodar med lågt potensial vil polarisera andre anodar med høgare potensial katodisk, og dermed passivera dei. Denne forklaringa har blitt undersøkt i denne rapporten, der det er forsøkt å passivera aluminiumsanodar under kontrollerte former. Reaktivering har også blitt undersøkt.

Eit lengre potensiostatisk forsøk der aluminiumsanoder vart katodisk polarisert til ulike potensial har blitt gjennomført. Gjennom forsøket vart straumtettheita logga. Etter 27 og 120 dagar vart det gjennomført lineær polarisasjonsmotstand på prøvane til videre utrekning av korrosjonshastigheta. Ved slutten av eksperimentet vart det teke polarisasjonskurvar av prøvane. Eit utval av prøvar vart også undersøkt i eit elektronmikroskop, der målet var å avdekka kva oksid som var danna på overflata av prøvane. Kortare galvanostatiske forsøk med ulik varigheit vart også gjennomført, der polarisasjonskurvar av prøvane vart tatt opp til slutt i forsøket.

Straumtettheita avtok noko utover i det potentiostatiske langtidseksperimentet. Dette indikerer delvis passivering, men det er ikkje mogleg å konkludera basert på desse resultata aleine. Polarisasjonskurvene gav tydelege teikn på ein form for passivering, då straumtettheita ved et gitt potensial var redusert samanlikna med polarisasjonskurva til ueksponerte prøvar. Polarisasjonskurvane viste også ein typisk passiv-aktiv form med låg straumtettheit til eit bestemt aktiveringspotensial, der straumtettheita plutseleg auka. Serien som var utsett for størst katodisk polarisering viste høgast grad av passivering.

Korrosjonshastigheita varierte meir innad i seriane enn på tvers av seriane. Dette kan tyde på at korrosjonshastigheta ikkje er vesentleg påverka på katodisk polarisering, sjølv om prøvane sin evne til å levera katodisk straum opp til eit visst potensial er redusert. Korrosjonshastigheten var likevel tydelig redusert sammenlikna med ueksponerte prøvar.

Polarisasjonskurvane frå dei korte galvanostatiske eksperimenta viste også ein nedgang i straumtettheit ved eit gitt potensial samanlikna med polarisasjonskurvene til prøvar som ikkje var katodisk polarisert. Dette tyder på passivering. Resultata viste at grad av passivering var avhengig av varigheita på den galvanostatiske polariseringa.

Dei fleste av dei passiverte prøvane reaktiverte ein plass mellom -900 og -950 $mV_{Ag/AgCl}$, der dette reaktiveringspotensialet ikkje virka å være avhengig av grad av passivering. Dette tyder på at dersom ein anode brukt til katodisk beskyttelse blir passivert til ein viss grad, vil materialet reaktivera før stålstrukturen oppnår eit potensial som tillèt aktiv korrosjon. Materialet ser også ut til å verta permanent aktivert etter å ha vorte utsett for anodisk polarisering til reaktiveringspotensial eller høgare.

Resultat frå elektronmikroskopi viser at belegget som blir danna på overflata til prøvane hovudsakeleg består av oksygen og aluminium. Spor av kalkbelegg er også funne, der mengda ser ut til å auke ved aukande katodisk polarisering.

CONTENTS

ABBREVIATIONS

Ag/AgCl = Silver, silver chloride

b_a = Anodic Tafel constant

b_c = Cathodic Tafel constant

CP = Cathodic Protection

EDS = Energy-Dispersive X-ray Spectroscopy

F = Faradays constant

LPR = Linear Polarization Resistance

OCP = Open Circuit Potential

SEM = Scanning Electron Microscope

SHE = Standard Hydrogen Electrode

DNV = Det Norske Veritas

ISO = International Organization for Standardization

NORSOK = Norsk Sokkels Konkurranseposisjon

LIST OF FIGURES

LIST OF TABLES

1. INTRODUCTION

1.1 BACKGROUND AND MOTIVATION

Inspection of sacrificial anodes used in cathodic protection subsea has typically been performed by stabbing, which is a method where a probe is stabbed on to the material to provide contact measurements. A new non-contact inspection method called FIGS® has been developed in recent years. This technique is based on field gradient measurements, and will assess the condition of the corrosion protection system of different subsea assets [5]. The new method of inspection has resulted in observations of a substantial number of anodes showing low to no activity on pipelines in areas with very low current demand. It has also been observed that some anodes behave cathodically. As permanently passive anodes potentially could lead to problems if the need for cathodic protection increases, it is of great interest to know more about the process, as well as if anodes will reactivate.

1.2 PROBLEM DESCRIPTION

It is known from inspection by stabbing that the potential of anodes varies to some degree [6]. The ISO 15589-2 recommended practice require aluminium anodes to have a potential of maximum -1050 mV $_{SCE}$, but does not include requirements of the lower limit of potential [7]. The producer of aluminium anodes, Skarpenord, has stated that quality testing is performed to ensure that the potential does not exceed -1100 mV $_{SCE}$ [8]. This could indicate that there is a possibility that anodes on a pipeline, in theory, could experience a difference of 50 mV in operating potential. Studies also indicate that the values used for current density and coating breakdown in cathodic protection design standards is very conservative, which can cause anodes to deliver less current than designed for, or even no current at all [1, 9].

The experimental work in this thesis is based on the following observation. CP designs based on common standard and recommended practice are intended to be conservative, i.e. the number of anodes installed is commonly seen to exceed the number of anodes actually required. This conservative number of anodes in combination with very low current demand for protection in pipeline sections not affected by drain towards connected structures implies that a substantial number of anodes will deliver very small amounts of current. Considering that the open-circuit potential (OCP) may vary somewhat between anodes installed

on a pipeline, anodes with more negative OCP could, in theory, start to supply current to neighbour anodes with slightly more positive potential, thereby polarizing these anodes in the cathodic direction (i.e. cathodically protecting them). Different reactions can then occur (as a result of cathodic polarization) such as the formation of calcareous deposits or other kinds of layer, and thereby possibly passivate the cathodically polarized anodes. As a consequence, for well-protected pipelines with low current demand, anodes can be seen as anodic or cathodic with an FG sensor such as FIGS®, but may also not be seen at all (i.e. no anodic or cathodic activity, passive). This could explain the observation of passive and cathodic behaving anodes on pipelines, where the hypothesis is that the anodes initially becomes cathodic, and eventually becomes passive as a consequence of the cathodic polarization. As the current transferred between anodes most likely is very low, it is reasonable to believe that this is a very time-consuming process with a timespan of years or even decades.

Another likely explanation why anodes do not seem to appear active can simply be because the anodes do not have any exposed steel to protect as a result of conservative CP design standards, causing the anode to only be exposed at its own open-circuit potential (OCP) and appear passive.

The problem will be investigated by mimicking the suspected potential difference by polarizing the anode in cathodic direction by doing a potentiostatic experiment while observing how the material reacts. Short-term galvanostatic polarization test will also be performed. Investigation in the SEM will also be of great interest, since this hopefully will disclose what kind of layer that is formed on the surface of the possibly passivated sample.

1.3 PROJECT SCOPE

1.3.1 OBJECTIVES

The main objective of this study is to investigate if passivation of aluminium anodes can occur based on the projected explanation, why it occurs, and characterize the passivating surface layer. It is also of great interest to find at which circumstances the anodes will reactivate. Parallel to these objectives, different methods for further studying of passivation will be investigated.

1.3.2 RESEARCH QUESTIONS

The most important question of this thesis is if and to which degree anodes will passivate after being cathodically polarized with realistic experimental conditions. By performing different electrochemical measurements such as linear polarization resistance, polarization curves, and continuous current logging will this question hopefully be answered. Another interesting question is what kind of surface layer that is formed on the possibly passivated samples, where Al_2O_3 and calcareous deposits are expected to be possibilities. The SEM will also hopefully answer this and disclose what kind of deposits that are present on the possibly passivated surface layer. It is also of interest to investigate if passivated anodes will reactivate, and possibly what is required for reactivation. Another important question which hopefully also will be answered based on literature is whether a potential difference between anodes is possible, and which variations that could cause these.

1.3.3 LIMITATIONS

Only one type of aluminium anodes will be tested in this thesis, where the alloy composition is given. This will exclude the effect of different alloying elements, and only passivation of this alloy will be investigated. As previously mentioned, the discovery of passive behaving anodes seems to be rather new. As a result, there is little previous work done regarding the process and cause of passivating aluminium anodes. Because of this, large parts of the theory focus on possible reasons for why the potential can vary between anodes on the same pipeline, as the presented explanation relies on this.

1.4 THESIS STRUCTURE

Literature regarding reasons for a potential difference between aluminium anodes is the main part of the state-of-the-art section. Theory regarding other relevant subjects such as current demand for cathodic protection, calcareous deposit formation and cathodic corrosion of aluminium is also included.

Experiment details and approach is described in Section 3. The long-term experiment was initiated in the specialization project, and the method is included in this thesis as well [10]. The galvanostatic experiment method is further explained, as well as the details regarding post-test treatment of all experiment samples.

The results are divided into three different parts, where the first part contains results from the long-term potentiostatic experiment. The second part will present short-term galvanostatic experiments. The last section of the results will contain results from the SEM.

The thesis will end with a discussion, which will address the different research questions based on the results, and the conclusions will be presented in the last section. Experimental findings which are not included in the results are presented in the appendix.

2. STATE OF THE ART

2.1 EFFECT OF ALLOYING ELEMENTS AND IMPURITIES

Today there are three elements mainly used for cathodic protection; zinc, magnesium and aluminium based anodes, where each of them provides different advantages and disadvantages. Due to its low density, availability, high current capacity, low specific weight and low-cost have aluminium based anodes has become the preferred galvanic anode in seawater. Aluminium possesses a thermodynamic potential of -1.663 V_{SHE}, but this theoretical driving potential is not realized. Due to its passive oxide, structural aluminium alloys have a pitting potential of about -700 mV_{SCE} in seawater. This is neither negative enough to polarize steel below its protection potential, nor will aluminium undergoing pitting be able to provide much current for cathodic protection [3].

By alloying aluminium with certain element, the protective oxide layer can be destabilized and thus permitting continuous uniform corrosion. The alloying elements that are used in aluminium can be categorized in two groups. The first category is called modifiers, and include elements such as zinc, magnesium, cadmium or barium. These are added to lower the anode potential by 0.1 to 0.3 V and are added in concentrations up to 10 wt.%. The presence of zinc will result in the formation of a second phase which destabilize the formation of Al_2O_3 and prevents homogeneous passive layer on the passive layer of aluminium [3, 11, 12].

The second category of alloying elements is de-passivators, which are elements such as indium, mercury and tin. They are added in smaller concentrations up to 0.5% to further decreases the anode potential [3, 13]. These small additions act as activators that prevent large areas of electrochemically inactive material and hence increases efficiency [14, 15]. The most used aluminium alloying elements in marine services are zinc (3-6%) and indium (0.04-0.015%). These additions will activate the aluminium and provide both the necessary potential and capacity for cathodic protection of steel in seawater [15]. The aluminium anode composition requirements from the NORSOK M-503 cathodic protection standard is shown in figure 2.1.

ELEMENT		MAX %	MIN %
Zinc	(Zn)	5.5	2.5
Indium	(In)	0.040	0.015
Iron	(Fe)	0.09	-
Silicon	(Si)	0.10	-
Copper	(Cu)	0.005	-
Others	(Each)	0.02	
Aluminium	(Al)	Remainder	

Figure 2.1: Chemical composition requirements for aluminium anode material [1]

Indium is usually only added in a small content of about 0.03%, and studies done by Zazoua and Azzouz show that the presence of indium significantly favours the reactivity of aluminium in natural seawater [16]. In addition to lowering the driving potential, indium will also supress hydrogen evolution which is increased by the addition of zinc. The use of indium-based anodes is preferred today because they are easy to manufacture, non-hazardous and give uniform dissolution [3].

Presence of less than 300 ppm mercury in the aluminium alloy will lower the operational potential of the sacrificial anode in chloride media [17]. Even though aluminium anodes containing mercury out-performs both tin and indium based anodes, it is not used today because of the environmental hazard of mercury [3]. Tin was also previously often used for activation. Because of the non-uniform corrosion, adherent corrosion products, parameters varying heavily with current density and the need of very accurate composition control, it is no longer preferred [3].

Studies performed by Ponchel and Horst with Al-Zn showed that iron and copper are two detrimental impurities that can affect the current capacity of aluminium anodes [18]. After their work strict controls on the purity of aluminium stocks were introduced, where copper had the lowest weight tolerance of 0.01%, while iron could be accepted up to 0.1% [19]. They found that iron was beneficial for current capacity until a threshold was reached where the effect became negative. Iron also lead to more uniform corrosion [3].

Silicone can affect current capacity but has a more gradual effect and can be accepted at higher concentrations. Silicone can also lower the potential, as well as causing irregular corrosion patterns and increase time before the anode reaches operating potential. Figure 2.2 shows the effect of silicone content on potential and current capacity for a Al-Zn-In alloy containing 0.14% Fe [3].

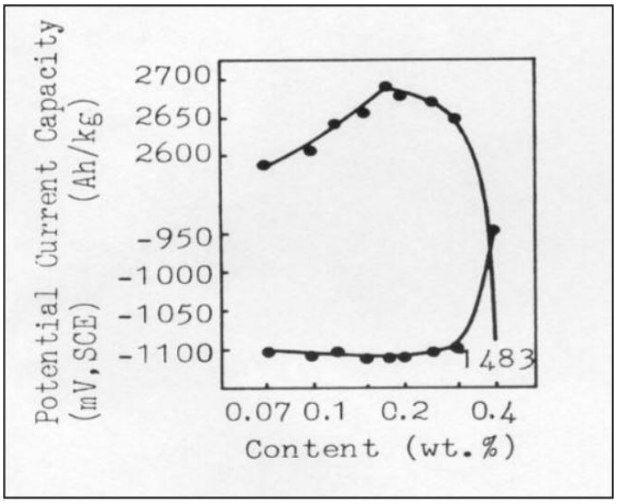

Figure 2.2: Effect of silicone content on an Al-Zn-In alloy containing 0.14% Fe [3]

2.2 PASSIVATION OF ALUMINIUM ANODES

Activated aluminum anodes used in cathodic protection can under certain conditions become passive. The mechanism behind this is not well known, but most likely is a non-conductive film developed on the surface of the material, causing the material to no longer be able to supply current [20].

As of now there is little, or no work done on passivation of aluminum anode alloys, and the cause of it. However, W.H. Hartt has done work where he concluded that partial anode passivation was the cause of why the potential of steel shifted towards higher values as current density decreased [9].

2.3 MICROSTRUCTURE OF ALUMINIUM ANODES

Optimisation of alloy microstructure is claimed to have positive influence on the electrochemical capacity of aluminium anodes [21]. Several factors such as unwanted trace elements, their distribution in the alloy

microstructure and the grain size distribution can have an impact on the current efficiency. Different microstructure characteristics such as anode size, mould construction and temperature can also have an effect on the electrochemical properties of the material [21].

Work performed by Salinas, Garcia and Bessone show that microstructure can affect the operating potential [22]. However, the effect of modifying the microstructure is dependent on the amount of zinc present in the alloy. For lower contents of zinc (below 3 wt%) is the operating potential strongly affected by solidification macrostructure of the alloy. Under nonequilibrium casting conditions for an Al-Zn alloy, a combination of the two solid phases α (Al) and β (Zn) are expected, where these are the two main solid solutions in the Al-Zn binary-phase diagram as shown in figure 2.3. Alloys with Zn contents of around 1% will have an undefined α–phase distribution which will cause a fluctuating operating potential. In alloys with 5 wt% Zn, a good α-phase distribution was observed, and the operating potential will therefore be independent of microstructure. If the content of zinc exceeds 5 wt%, it is the α/β – phase relationship which defines the operating potential [22].

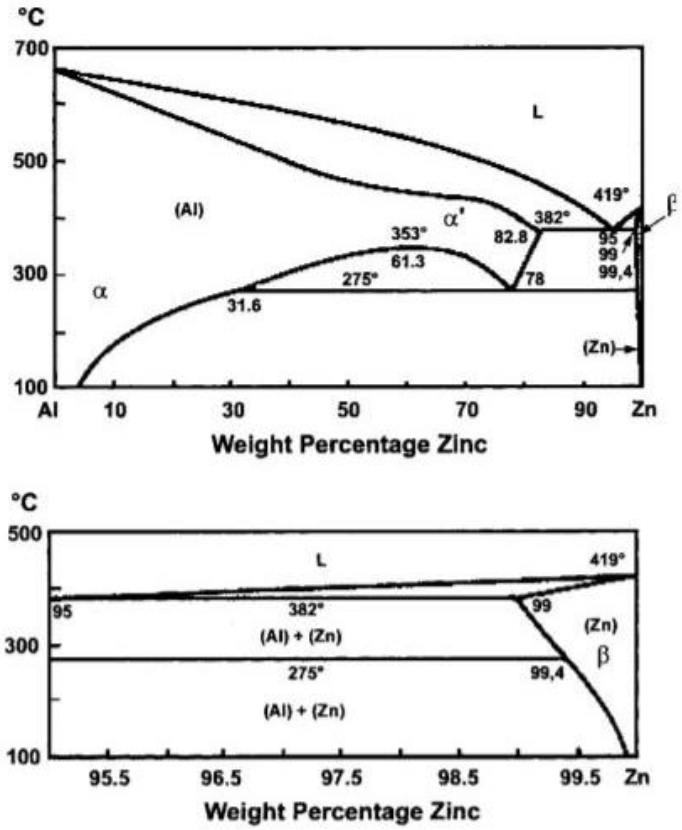

Figure 2.3: Binary-phase diagram for Al-Zn system [22]

Cold works can also be applied to the aluminium anode to increase anode efficiency. Experiments done by Asmara shows this, where the efficiency of aluminium anodes were increased as the material was subjected to cold work up to 40% [13].

2.4 ENVIRONMENT VARIABLES AND ANODE CURRENT DENSITIES EFFECT ON POTENTIAL

Experiments were performed on an Al-Zn-Sn-Bi-Ga alloy by Murai, Tamura and Miura at varying temperatures and anode current densities [23]. Very high anode current densities (10 A/m^2) shifted the anode potential from -1080 mV_{SCE} to -1055 mV_{SCE}, where this happened for all temperatures up to around 60 °C. At 80 °C the anode potential increased to -1020 mV_{SCE}. The same effect was seen at somewhat lower current densities (3 A/m^2), but there was no change in potential until temperature exceeded 50 °C. Murai, Tamura and Miura correlated the increase of potential at higher temperatures with the growth of boehmite, which is an aluminium oxide hydroxide [3].

Similar results were obtained on Al-Zn-In alloys by Kobayashi and Tamura [3]. They tested the alloy at different temperatures at 10 A/m^2, and the results showed an increase in potential when exceeding 50 °C and up to 100 °C, as the potential went from -1100 mV_{SCE} to -1000 mV_{SCE}. The same was found by Wroe and May [3] where the operating potential for an Al-Zn-In alloy increased from -1120 mV_{SCE} at 5°C to -1074 mV_{SCE} at 95 °C.

Gibson investigated correlation between operating potential and the current density over time, where he observed how different current densities affected the operating potential for an Al-Zn-In aluminium alloy exposed for 7 days [3]. Current densities from 0.1 A/m^2 to 6 A/m^2 had no impact on the operating potential at 20 C°, as shown in figure 2.4. Not until 60 A/m^2 cathodic current density, a notable shift in operating potential was noticed. At 60 A/m^2 the Al-Zn-in alloy was polarized 43 mV.

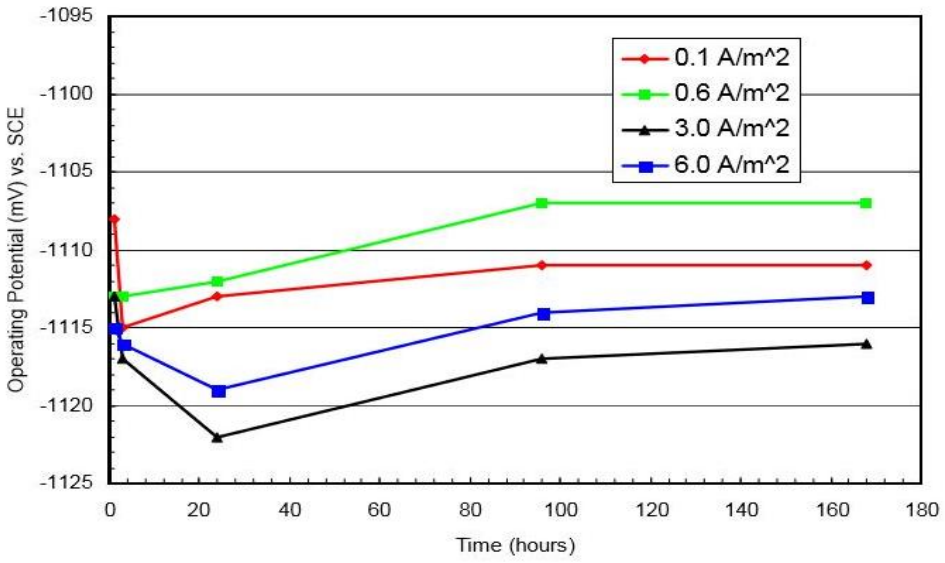

Figure 2.4: Operating potential versus time for varying current densities at 20 °C [3]

Gibson also did experiments on how current density affects the operating potential at different temperatures. In these experiments he tested operating potential vs current densities at 20, 40, 60 and 80 °C. His results showed that the potential was almost unaffected by current densities at all temperatures except at 80 °C, where the anode polarized 20 mV when current densities was increased from 0.1 A/m^2 to 6 A/m^2 as shown in Figure 2.5.

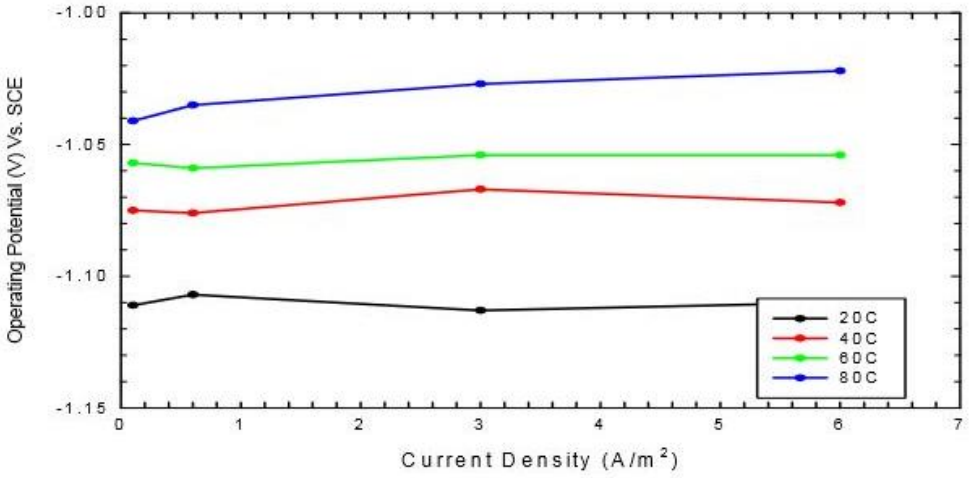

Figure 2.5: Operating potential versus current densities for varying temperatures [3]

Gibson tested one aluminium alloy containing indium and one that did not, and he found that the indium addition may be reason for why the potential increase as temperature increases [3]. The commercially available alloy containing indium that they tested had an increase in potential as temp increased, but the alloy with less indium used for comparison reacted oppositely.

Another study done on Al-Zn-In-Si and Al-Zn-Hg anodes by Schrieber and Murray showed the same, where the anode potential became more noble as temperature increased [24]. They tested these materials at different temperatures and at 3 and 7% NaCl, where they found that increased brine concentration would lower the operating potential.

The effect of electrolyte salinity has also been investigated. Al-Zn-In-Si tested in 15% brine by Smith, Reding and Riley [3]. Their work showed that the potential was higher in 15% brine than in seawater, as potential increased from -1080 mV_{SCE} vs -1060 mV_{SCE}. Additional studies also showed that an increase in potential as salinity decreased, indicating that the potential is related to the resistivity of the environment [3].

2.5 CURRENT DEMAND FOR CATHODIC PROTECTION OF COATED STEEL

Cathodic protection standards used in the North Sea are suggested to be very conservative compared to actual measured data with respect to current demand. The NORSOK M-503 uses current densities between 80 – 100 mA/m^2 for bare steel surfaces at temperatures up to 25°C [1]. Jelinek, et al. reported 20 mA/m^2 steel exposed in the North Sea, supporting that the standards used are very conservative [25]. Lauvstad et al. also found the same, where they by using field gradient measurements calculated final current density to be 50 mA/m^2 [26]. The DNV-RP-B401 cathodic protection design standard required a current density of 140 mA/m^2, again confirming that the standard is very conservative.

Steel used in marine environments are usually coated. The coating will degrade, which is taken into account by the coating breakdown factor. The term coating breakdown is related to the coatings ability to insulate the steel from seawater, and thereby affecting the current demand of the material. Studies show that the actual coating breakdown on coated steel samples is significantly lower than predicted in breakdown models such as DNV RP-B-401. Conservative predictions are made in these models, which expects a linear increase in current demand of the steel. However, testing shows that this does not seem to be the case [2].

Knudsen and Steinsmo has done several experiments on how coating degradation affects current demand under simulated field conditions [2]. One of their experiments was performed on 450 µm thick coating. Their experiments showed that the coating breakdown after five years was close to zero, and for all coatings tested less than 1%. The DNV model predicts coating breakdown between 6-8% after five years. Figure 2.6 shows the results from Knudsen and Steinsmo's experiments where they are compared to the NORSOK M-501 coating system No. 7 coating breakdown predictions. All other experiments presented in their paper had the same results, where DNV coating breakdown models were very conservative in comparison with experimental results [2].

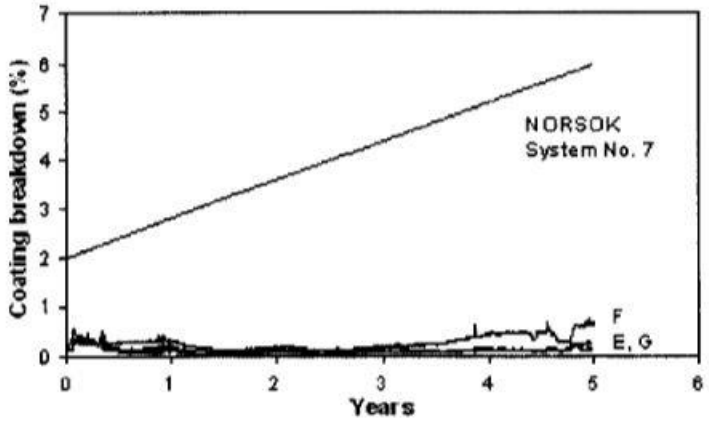

Figure 2.6: Measured coating breakdown for some of Knudsen and Steinsmo's experiments compared to the NORSOK system No. 7 coating breakdown predictions [2]

2.6 CALCAREOUS DEPOSIT FORMATION

As a cathodic current is impressed to a material submerged in seawater an increase in local pH will occur due to the cathodic reactions and the production of OH^- ions it causes. The inorganic carbonic equilibrium in the electrolyte adjacent to the metallic surface will then change. The term calcareous deposit formation describes Mg and Ca containing compounds, which will be further described.

At potentials more positive than -1.0 V, the oxygen reduction reaction (2.1) is the dominant cathodic half reaction. If the potential is more negative than -1.0 V the hydrogen evolution reaction as shown in equation (2.2) is the dominant one [27].

$$O_2 + 2H_2O + 4e^- \rightarrow 4OH^- \quad (2.1)$$

$$2H_2O + 2e^- \rightarrow H_2 + 2OH^- \quad (2.2)$$

The pH of seawater is controlled by the carbonate system. The cathodic half reactions shown in equation (2.1) and (2.2) will shift the pH, and the inorganic carbon equilibria expressed by equation (2.3), (2.4) and (2.5) is shifted to the right [9].

$$CO_2 + H_2O \rightarrow H_2CO_3 \quad (2.3)$$

$$H_2CO_3 \rightarrow HCO_3{}^- + H^+ \quad (2.4)$$

$$HCO_3{}^- \rightarrow CO_3{}^{2-} + H^+ \quad (2.5)$$

These changes combined with the presence of Ca^{2+} and Mg^{2+} ions in seawater and the hydroxyl ions from (2.1) and (2.2) will cause formation of the calcareous deposits $CaCO_3$ shown in (2.6) and $Mg(OH)_2$ shown in (2.7). These will precipitate on the metallic surface.

$$Ca^{2+} + CO_3{}^{2-} \rightarrow CaCO_3 \quad (2.6)$$

$$Mg^{2+} + 2OH^- \rightarrow Mg(OH)_2 \quad (2.7)$$

Deposition generally occurs at a pH between 8 and 10. All hydroxyl ions will be used for precipitation of $CaCO_3$ until pH reaches a value of 9.3, because precipitation of magnesium hydroxide is not possible before this pH threshold is reached [27].

As the calcareous deposit film is formed, it acts as a physical barrier between the material and the seawater. As a result the material will require less current to be polarized because of the physical barrier protecting the surface and decrease the current density [27]. Similar to organic paints are the calcareous deposits poor electron conductors and will not support oxygen reduction at the surface. Studies done by Yang states that calcareous deposits are formed under all conditions of cathodic protection, regardless of the degree of protection [28].

However, Solis and Ganesca states that application of a high current value will result in a more protective calcareous deposit than if a more gradual polarization is applied [27]. The general trend for steel in seawater polarized to -880 mV shown by Hartt, is that the current density remains between 400 - 450 mA/m^2 for about 35 hours, but then decreases to near 20 mA/m^2 after 100 hours [9].

Other studies states that for aluminium alloys, the calcareous deposits play a less important role for determining the current requirements regarding cathodic protection. Gundersen and Nisancioglu found in their studies that very thin layers of calcareous deposits were formed on aluminium, compared to steel [29]. Egtvedt did studies on cathodically protected TSA in seawater, where she found that the layer on the TSA surface consisted of two layers. The inner layer consisted of only aluminium oxide, while the outer layer, consisted of a mixture of aluminium oxide and magnesium hydroxide. The outer layer was a few times thicker than the inner layer [30]. Knudsen also did similar discoveries, where he found that TSA cathodically polarized in seawater did grow some calcareous deposits, but in small amounts. His experiments also showed that a layer of aluminium oxide was grown on the TSA surface [31].

2.7 CATHODIC CORROSION OF ALUMINIUM

When aluminium is cathodically polarized, the reduction of hydrogen and oxygen will as previously mentioned increase hydroxide ion formation at the aluminium surface. This will increase the pH and thereby causing cathodic corrosion. Van de Ven and Koelmanns has suggested that the cathodic dissolution rate of aluminium which is determined by the concentration of hydroxide ions, is strongly dependent of the hydrogen evolution rate as the production of OH^- is proportional with the production of H_2 [4, 32].

Moon and Pyun did experiments regarding the suggested explanation for cathodic corrosion for pure aluminium. They found that corrosion rate increases as applied cathodic current density increases in natural solutions. However, they did not observe the same for alkaline and acidic solutions where current density had no effect on corrosion rate. One of their results is presented in Figure 2.7, where corrosion rate of pure aluminium is plotted as a function of applied current density at 20 °C for different solutions. It is not the applied cathodic current itself that increase the cathodic corrosion, but the increased hydroxide ion concentration as a result of hydrogen and oxygen reduction. They also found that an oxide film is spontaneously formed, and still exists at the surface even under cathodic polarization.

In a 0.5M NaOH alkaline solution will the extra production of hydroxide ion not affect corrosion, because the concentration already is high. However, in natural solutions will the increased hydroxyl ion production change the concentration so that corrosion rate increases. Moon and Pyun concluded that Van de Ven and Koelmanns was right, and that increasing cathodic polarization will increase the dissolution of pure aluminium. This as a result of increased hydroxide ion concentrations because of increased hydrogen evolution [4].

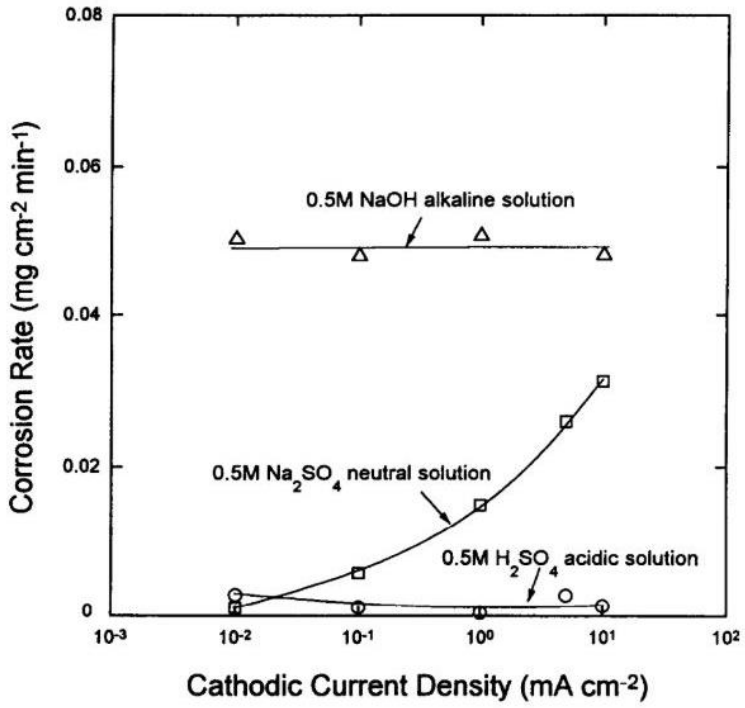

Figure 2.7: Cathodic current density effect on the corrosion rate in natural, alkaline and acidic solution [4]

2.8 METHOD

2.8.1 CHOICE OF METHODS

As a result of limited previous work regarding passivation of aluminium anodes, an important part of this thesis is to investigate relevant methods for further work. Two different methods for controlled cathodic polarization are possible, and both will be used in the experimental work of this thesis. Potentiostatic polarization is the first alternative, where the material is connected to a potentiostat and cathodically

polarized by being subjected to a potential difference that is held constant. During the experiment, the cathodic current transfer will be measured. Galvanostatic polarization is the other possible polarization methods, which is performed with a potentiostat that transfer a pre-defined current to the material, which is held constant, while the potential is measured.

Potentiostatic polarization will be used for the main long-term experiment because of the simplicity of the experiment setup with many samples. Galvanostatic polarization would require a more complicated setup with the same number of samples. The potentiostatic polarization will also be the most realistic experiment as the hypothesis of this thesis is based on a potential difference between connected anodes, which is what the potentiostatic polarization will provide. However, the experiment will not be completely realistic, as the potential difference is held constant during the experiment.

However, galvanostatic polarization does have its benefits compared to the potentiostatic polarization. During the experiment, galvanostatic polarization will provide better control of the reaction speed as this is dependent on the current density, which is constant. Parallel to the main long-term experiment, several small-scale experiments will be carried out in order to investigate how experiment duration affects anode passivation. Galvanostatic polarization will be used for these experiments in order to look for obvious differences in the passivating methods.

Linear polarization resistance will be recorded two times during the long-term experiment in order to observe how the corrosion rate develops during the experiment. These measurements will be carried out to compare the corrosion rate of possibly passivated samples and the corrosion rate of non-exposed samples, as well as investigating if the corrosion rate decreased throughout the experiment duration. A reduction could indicate some sort of passivation. How corrosion rate is obtained from LPR is described in 2.8.2. Several post-test treatments will be carried out in order to investigate how the anode material has reacted to the different passivation methods. Polarization curves will be recorded after the experiments are ended. The objective is to compare the polarization curves of possibly passivated samples with the polarization curves of non-exposed aluminium anodes, in order to see if the behaviour of the polarization curves changes after being subjected potentiostatic and galvanostatic polarization. A reduction in the anodic current density of the anode will indicate partial passivation. A potential where the current rapidly increases will indicate that the anode re-activates.

SEM will be used to characterize the surface layer. Samples will be investigated in order to look for calcareous deposits, which mainly consists of $MgCO_3$ and $Ca(OH)_2$. It is also expected to find some kind of aluminium oxide in the surface layer. One sample will be inspected in SEM without recording a polarization curve before inspection. This will be done in order to see if there are any differences in the surface layer between the sample that was directly extracted from the experiment and the samples that were anodically polarized to -600 $mV_{Ag/AgCl}$ before inspection.

2.8.2 MEASURING CORROSION RATE BY LPR

Corrosion rate can be calculated by recording linear polarization resistance (LPR). The LPR method is a more efficient method than calculating the corrosion rate from recording polarization curves. In addition, it does not destroy the sample in the same manner that recording a polarization curve does, since recording polarization curves require to polarizes the sample far away from the OCP. To be able to make an approximation of the corrosion rate from LPR measurements, the Tafel constants from a polarization curve of the material must be known. The LPR method polarizes the sample with a small potential difference such as 20 mV from OCP both anodic and cathodic, while the current is measured [33].

By using the linear relationship between the change in potential and change in net current in this small range the polarization resistance R_P [Ω] can be found as shown in Equation 2.8.

$$R_P = \frac{\Delta E}{\Delta I} = \frac{B}{i_{Corr}} \tag{2.8}$$

By using the known anodic and cathodic Tafel constants, B can be calculated as shown in Equation 2.9. This makes it possible to find I_{Corr} as shown in Equation 2.10 from combining Equation 2.8 and 2.9.

$$B = \frac{b_a \cdot |b_c|}{2.3(b_a + |b_c|)} \tag{2.9}$$

Further the corrosion current can be calculated using the Stern-Geary Equation 2.10.

$$I_{Corr} = \frac{b_a \cdot |b_c|}{2.3 \cdot R_P \cdot (b_a + |b_c|)} \tag{2.10}$$

The corrosion rate can then be calculated by using Faraday`s law while also introducing the surface area [A] of the sample to convert the corrosion current [I_{Corr}] to the corrosion current density [i_{Corr}]. This is shown in Equation 2.11 where K is a constant used to obtain corrosion rates in mm/year [34].

$$CR = K \cdot \frac{i_{Corr} \cdot M}{\eta \cdot \rho \cdot A} \tag{2.11}$$

Where:

ΔE – Change in potential	η – Electrons exchanged*	b_a – Anodic Tafel constant [V/decade]
ΔI – Change in current	ρ – Density [g/cm^3]	b_c – Cathodic Tafel constant [V/decade]
		M – Atomic weight of metal [g/mol]

3. EXPERIMENTAL WORK

This Section will describe all the experimental work that has been done as part of this thesis. The long-term potentiostatic experiment carried out at SINTEF Sealab was done in potentiostatic mode. Several small scale galvanostatic experiments was also carried out. The test matrix and sample preparation is described in Section 3.1 and 3.2, respectively, while the long-term potentiostatic experiments and the small-scale experiments are described in Section 3.3 and 3.4, respectively. Polarization curves was recorded for most of the samples from both the main experiment and the small-scale experiment, and the details around this procedure are described in Section 3.5. The LPR measurements are described in Section 3.6. Five samples from the long-term experiment was investigated by SEM as described in Section 3.7.

3.1 TEST MATRIX

3.1.1 LONG-TERM EXPERIMENT

The test matrix for the experiment initiated in the specialisation project is presented in Table 3.1. Four different series were included in this experiment. The experiment setup is presented in Section 3.3.1. Realistic potential differences based on acceptable variations in recommended practice and the quality control of anodes were used for two of the series, which was polarized -10 mV and -30 mV from OCP. One series with a -80 mV difference from OCP was also included in an attempt to accelerate the possible passivation process. One series which was exposed at OCP was also added for reference.

Table 3.1: Experiment matrix presenting the anode sample size, the different potential differences and the number of parallels

Sample	Potential	Number of parallells
Anode sample 1x1x3cm	OCP	6
	-10 mV from OCP	6
	-30 mV from OCP	6
	-80 mV from OCP	6

3.1.2 SMALL-SCALE EXPERIMENT

The test matrix for the short-term experiment is presented in Table 3.2. The experiment setup is shown in Section 3.4. Three different experiment durations were chosen where an anode sample was galvanostatically polarized with a cathodic current of -50 µA. One sample exposed at OCP was also included in each experiment beaker for reference. All experiments were performed with three parallels.

Table 3.2: Experiment matrix presenting the different parallel details of the galvanostatic experiment

Sample	Test no.	Sample no.	Current	Current density	Duration	Number of parallels
Anode sample 1x1x3cm	1	1.1	-50 µA	38 mA/m^2	2 days	3
		1.2	No current	-	2 days	3
	2	2.1	-50 µA	38 mA/m^2	5 days	3
		2.2	No current	-	5 days	3
	3	3.1	-50 µA	38 mA/m^2	10 days	3
		3.2	No current	-	10 days	3

3.2 SAMPLE PREPARATION

The anode material used in the experiments is a “Coral ‘A’ High Grade” sacrificial anode, which was provided by Skarpenord. The chemical composition of the material is shown in Table 3.3 and the data sheet is found in Appendix A3. The anode was cut into approximately 1x1x3cm samples using a Struers labotom 5. Samples were then grinded with an ATM Saphir 330 grinding machine to even the surface, and remains of the original moulded surface was removed. Holes were drilled in the top of the sample, and isolated copper wires were pushed into the hole where the inserted part was uninsulated. After inserting the wire, the surface around the hole was deformed so that the wire was attached properly. Further, silicone was added at the joint to ensure only the aluminium where exposed to seawater. Figure 3.1 and 3.2 shows a prepared sample connected to the wire and the intersection between sample and cable.

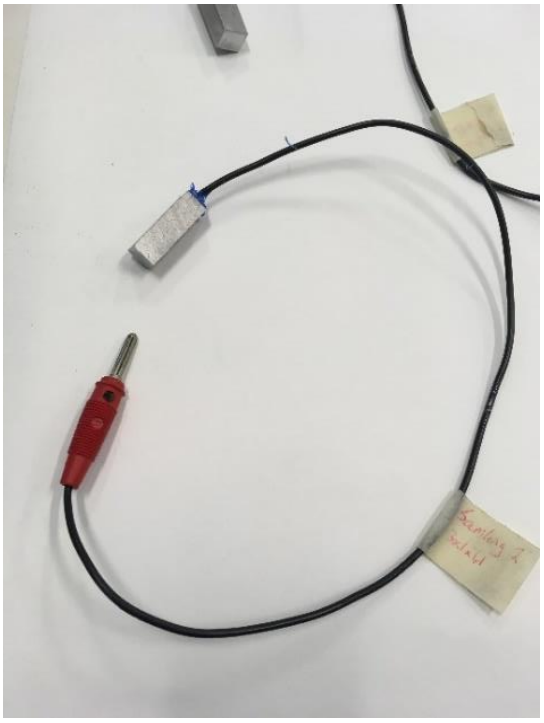

Figure 3.1: Anode material sample connected to cable

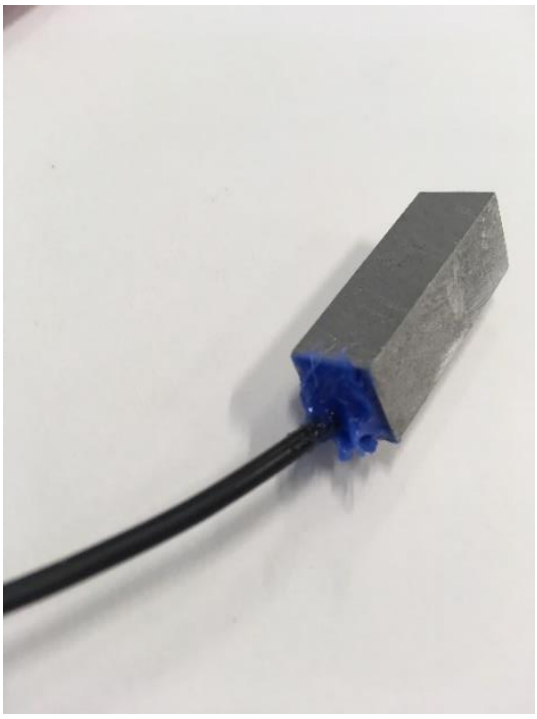

Figure 3.2: Intersection between the anode material and cable isolated with silicone

Table 3.3: Chemical composition of the anode material provided by Skarpenord

Element	Al [%]	Zn [%]	Si [%]	In [%]	Fe [%]	Cu [%]
Avg	96,1	3.84	0.0385	0.0225	0.0385	0.0012
Element	Cd [%]	Cr [%]	Pb [%]	Sn [%]	Mg [%]	Mn [%]
Avg	0.0001	0	0	0.004	0.0004	0.0002

As shown in Table 3.1, four series with different potentials were tested. Six parallel samples were tested at each given potential, so that 24 anode samples had to be prepared. Three extra samples were used as reference electrodes. Six samples were also prepared for all the small-scale experiments. A total of 33 samples were prepared.

Prior to the experiment, all the sample dimensions for the long-term experiment was measured. These measurements were later used to determine the surface area in order to calculate the current density and corrosion rate. The area of samples used as reference electrode was not measured. The area of the different samples is shown in Table 1-5 in Appendix A1.

3.3 LONG-TERM POTENTIOSTATIC EXPERIMENTS

3.3.1 EXPERIMENTAL SETUP

Because the electrochemical reactions will affect the composition of the electrolyte, the experiment had to be carried out with a continuous replacement of the seawater. The experiment was therefore conducted at SINTEF Sealab, where there is access on natural seawater which is pumped from 80 meters depth in the Trondheim fjord.

A large container was filled with natural seawater, where a drain was attached on the top of one of the container walls. Close to stagnant conditions is ensured as natural seawater is continuous filling the container while old seawater is drained out. All six samples within each potential category were placed in one row. The references electrode used in the experiment for series 1-3 consisted of three 1x1x3 aluminium anode samples. Three anode material samples were used to minimize variations. Three metal plates with thermally sprayed zinc, one for each of the three potentiostats were placed at the bottom of the tub as counter electrodes.

Each potential series was connected to a resistor box, which each of the anode material samples also were connected to. For measurements, a datalogger was used. This device measured the potential over a resistor. To keep the potential drop less than 1mV, the resistors applied for each series differed, where series 1 (-10 mV) and 2 (-30 mV) had a resistance of 100 Ω, and series 3 (-80mV) had a 1 Ω resistor. The potential for series 4 was measured versus an Ag/AgCl saturated KCl reference electrode. Potential

measurements logging was performed on the working electrode on all three potentiostats as well. All logging was done with one-hour intervals in the beginning and changed to six hours after 20 days.

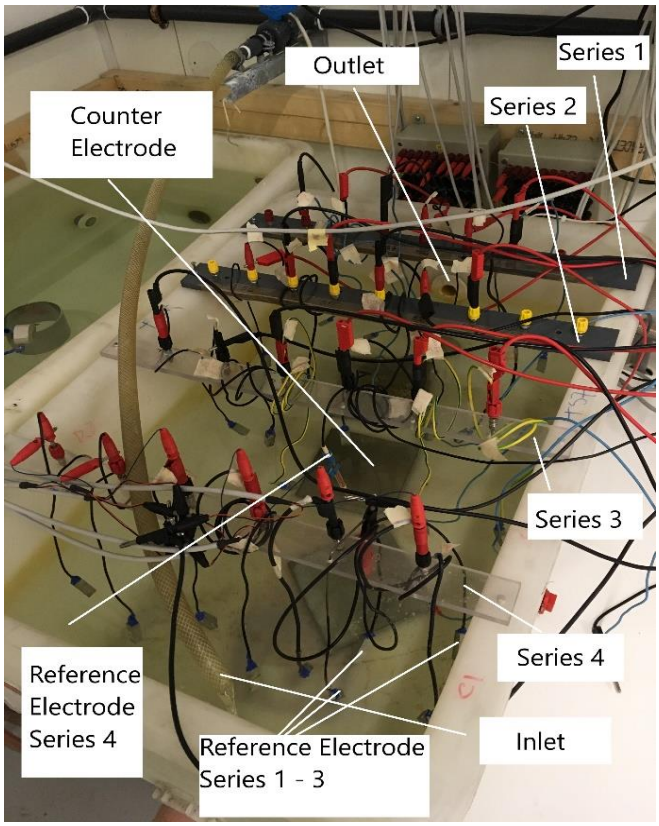

Figure 3.3: Experiment setup for the potentiostatic experiment

3.3.2 SAMPLE EXTRACTION

Samples from the long-term experiment was extracted in three rounds, where two samples from each series was removed in each set. The first set of samples was extracted after 135 days, the second set after 166 days, and the last set after 190 days. Polarization curves of all samples was obtained before they were extracted as outlined in Section 3.5.1. One sample of each series from the first set of sample removal was used for further investigation in the SEM. One sample from the last set was removed without anodic polarization for further analysis in the SEM. This is further explained in Section 3.7.

3.4 SHORT-TERM GALVANOSTATIC EXPERIMENTS

Parallel to the long-term tests, several short-term galvanostatic tests were performed, with test samples prepared as outlined in Section 3.2. After these tests were carried out, anodic polarization curves were recorded, ref. Section 3.5.2.

A portable Gamry Reference 600 potentiostat was used for this experiment. The sample was connected to the Gamry in room temperature with artificial seawater as electrolyte. A small piece of platinum was used for counter electrode, and an Ag/AgCl saturated KCI reference electrode was used. The experiment setup is shown in Figure 3.4. Three different durations were tested where the current was constant for all tests. Three parallels were added for each duration, and nine tests in total was performed. The experiment matrix is presented in Table 3.2 in Section 3.1.2.

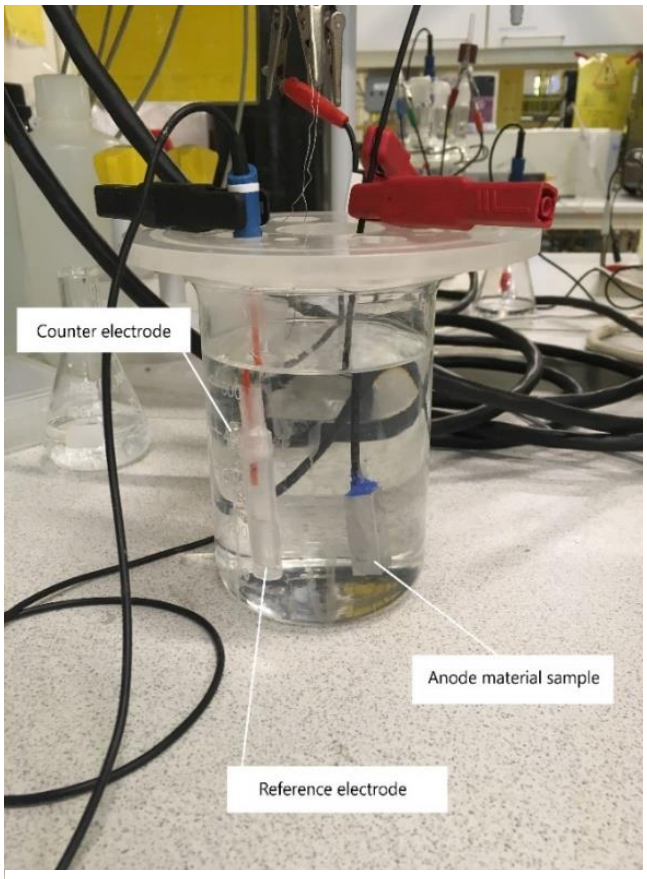

Figure 3.4: Experiment setup for the galvanostatic experiments

The galvanostatic tests was performed by using a galvanostatic current of -50 µA. Galvanostatic experiments performed in the specialisation project with varying cathodic current indicated that test performed with -50 µA, which corresponds to a potential difference of around 100 mV gave clear signs of passivation [10]. Based on these results, more experiments at this current was performed with varying duration to investigate the effect of exposure duration. An anode sample was also exposed at OCP in the same beaker as each of the test for comparison. Between the different galvanostatic tests, the surface of the samples was grinded to ensure reproducible conditions.

3.5 POLARIZATION CURVES

Anodic polarization curves were recorded in order to see how the material reacted to the cathodic polarization. The polarization curves were recorded from OCP to -600 $mV_{Ag/AgCl}$ for all samples, where a scanning speed of 1 mV/s was used.

3.5.1 LONG-TERM POTENTIOSTATIC EXPERIMENTS

Before each wave of samples were extracted from the long-term experiment, polarization curves of all samples were recorded. A portable Gamry Reference 600 potentiostat was connected to the samples, where the same reference electrode and counter electrode as used in the long-term experiment was used for recording the polarization curves. Each sample was disconnected from the potentiostat for a minimum of thirty minutes prior to recording the polarization curves, in order for samples to stabilize at OCP. When the second set of samples were removed, the polarization curve of sample 3 in series 3 was recorded 4 times consecutively to see if the sample were permanently reactivated. One sample of each of the four series was also polarized with a lower scanning rate during the last set of sample removal, in order to see if a longer polarization duration would affect the curve. For these polarization curves, a scanning speed of 0.1 mV/s was used.

3.5.2 GALVANOSTATIC EXPERIMENTS

Polarization curves were recorded both of non-exposed anode material and samples subjected to the galvanostatic experiments. Polarization curves of all samples exposed to galvanostatic polarization was performed after each individual experiment duration, as well as polarization curves of the anode samples exposed at OCP included in the experiments. In addition, nine polarization curves were recorded of non-exposed samples for comparison. Between each recording of polarization curves of the non-exposed material, the surface was grinded down to ensure reproducible conditions. The polarization curve of the non-exposed material was used for comparison both for the long-term experiments and the short-term experiment. A Gamry potentiostat was used to record the polarization curves, where the experiment had the same setup as the galvanostatic experiment in 3.4. A scanning rate of 1 mV/s was used for all the mentioned polarization curves.

3.6 LINEAR POLARIZATION RESISTANCE

LPR measurements were carried out on all the samples in the long-term experiment after 27 and 127 days of exposure. LPR were also performed on non-exposed samples, where 6 parallels were used. The same setup explained in Section 3.4 was used for LPR on non-exposed samples, and samples were grinded between each test to obtain reproducible conditions. The constants used for calculating the corrosion rates are shown in Appendix A2, and the area of the samples used for measuring corrosion rate can be found in Table 1-5 in Appendix A1.

For the LPR measurements from the long-term experiment, a portable Gamry Reference 600 potentiostat was used. The device was used to polarize the samples 20 mV in both anodic and cathodic direction while current was measured. A scan-rate of 0.167 mV/sec was used. Before the LPR recording, the samples were decoupled from the polarization for approximately 30 minutes so that the samples potential could stabilize at OCP. LPR measurements were conducted using a Ag/AgCl saturated reference electrode and with the same counter electrode as used in the long-term experiment, ref, Section 3.3.1. LPR of the samples was done without extracting them from the tub to minimize the disturbance of the experiment, as the long-term experiment continued after LPR was performed.

3.7 SCANNING ELECTRON MICROSCOPE

One sample from each of the long-term experiment was further investigated in the SEM in order to see if any deposits was formed on the anode surface. After the first wave of recording polarization curves and extraction, the cross-section of one sample from each series was prepared for further inspection. After samples were removed from the experiment tub, they were dried and cross sectioned with a Struers Minitom. Further, the samples were moulded with the cross section pointing upwards. The moulded samples were grinded down a few millimetres in order to avoid impact on the surface deposit from the cutting procedure. Samples were then grinded and polished. Before inspection in SEM, the epoxy was covered with a layer of aluminium foil and sample was coated with a thin layer of carbon in order to ensure conductivity of the sample and thereby avoid charging. One of the prepared samples are shown in Figure 3.5.

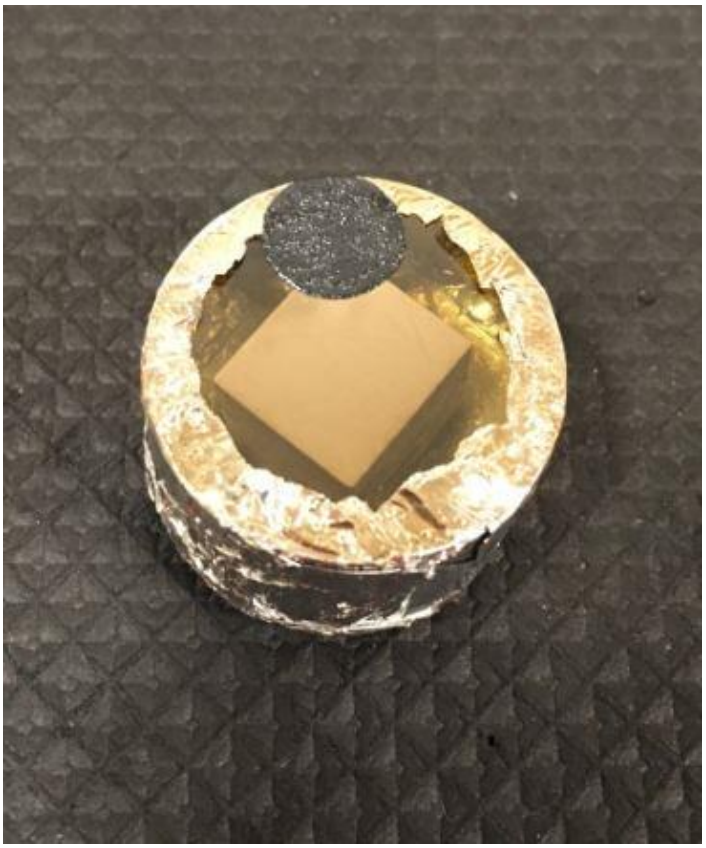

Figure 3.5: Sample moulded and prepared for inspection in SEM

The same preparation procedure was used on one additional sample from series 3 after the last extraction of samples in the long-term experiment. This sample was removed without recording a anodic polarization curve and was further investigated in the SEM.

Mapping and spot analysis were performed in EDS mode in the SEM, where one mapping analysis was performed on three sides of the sample, for all four samples. The mapping procedure was limited to look for aluminium, oxygen, calcium and magnesium. Spot analysis was also performed in three to four spots on each area, where spot placement in the coating area was chosen.

4 RESULTS

This Section will present all the results from the electrochemical experiments, as well as results from the analysis performed in the SEM. Results from the long-term potentiostatic experiment will be presented first, in Section 4.1. The logging data obtained throughout the experiment was used to calculate the current density which are presented graphically. Further are the potential measurements of series 4 (OCP) and the potential measurements of the working electrode from the potentiostats presented. LPR was recorded twice during the experiment and was used to calculate the corrosion rate of all samples in the long-term experiment. Corrosion rate is presented both graphically and numerical. The polarization curves from samples in the long-term experiment are presented graphically for each series, in addition to a comparison of all samples. A polarization curve was recorded several times for one of the samples, and the result are presented in the end.

Section 4.3 will present the short-term results. Polarization curve of both polarized samples and samples exposed at OCP for all durations are presented. Potential measurements during the experiments are also presented.

The final section, Section 4.4 will present results from the SEM. One sample of each series was investigated, in addition to one sample that was not polarized anodically before inspection. One mapping analysis and three to four spot analyses are presented from each of the samples that was inspected. The rest of the SEM results can be found in Appendix A5.

4.1. LONG TERM EXPERIMENTS

As seen in the Figure 4.1, 4.2 and 4.3, the first days of the experiment have not been included in the results. This is because of logging problems where the values were obviously wrong and therefore not included. Similar errors happened throughout the experiment, where some recordings suddenly would show a very large increase in current, which most likely was an error. As the values returned to normal after some troubleshooting in the lab where connection problems were found, these loggings are removed from the graphs. There are 6 data logging points between day 22 and 24 that are missing as can be observed in the graphs, where the lab had a power outage which caused the logging device to stop. Samples in this

experiment was removed in three waves at three different times as explained previously, which is why the logging duration is not the same for all samples.

4.1.1 CURRENT DENSITY MEASUREMENTS

Most results from the long-term potentiostatic experiments shows a decrease in current density from the initiation of the experiment, see Figure 4.1, 4.2 and 4.3. For all series the change in current density seems to be larger in the beginning, and the individual trends flattens out after approximately one month. This is especially clear in series 2 (-30 mV), where the current density of most samples does not seem to change much after the initial month of exposure. The same trend of rapid decrease initially can be seen in series 1 (-10 mV) and series 3 (-80 mV) as well. However, after one month, the current density of several samples within series 1 (-10 mV) seems to show a opposite trend then what first observed. The current density of series 3 (-80 mV) is observed to continue its increasing trend, but at a much slower speed after 1 month. Sample 6 for series 3 (-80 mV) shows a much lower current density than the rest of the samples, but after approximately 120 days it jumps back to around the other sample's values. Based on this there is reason to believe that the logging from the first 120 days are incorrect.

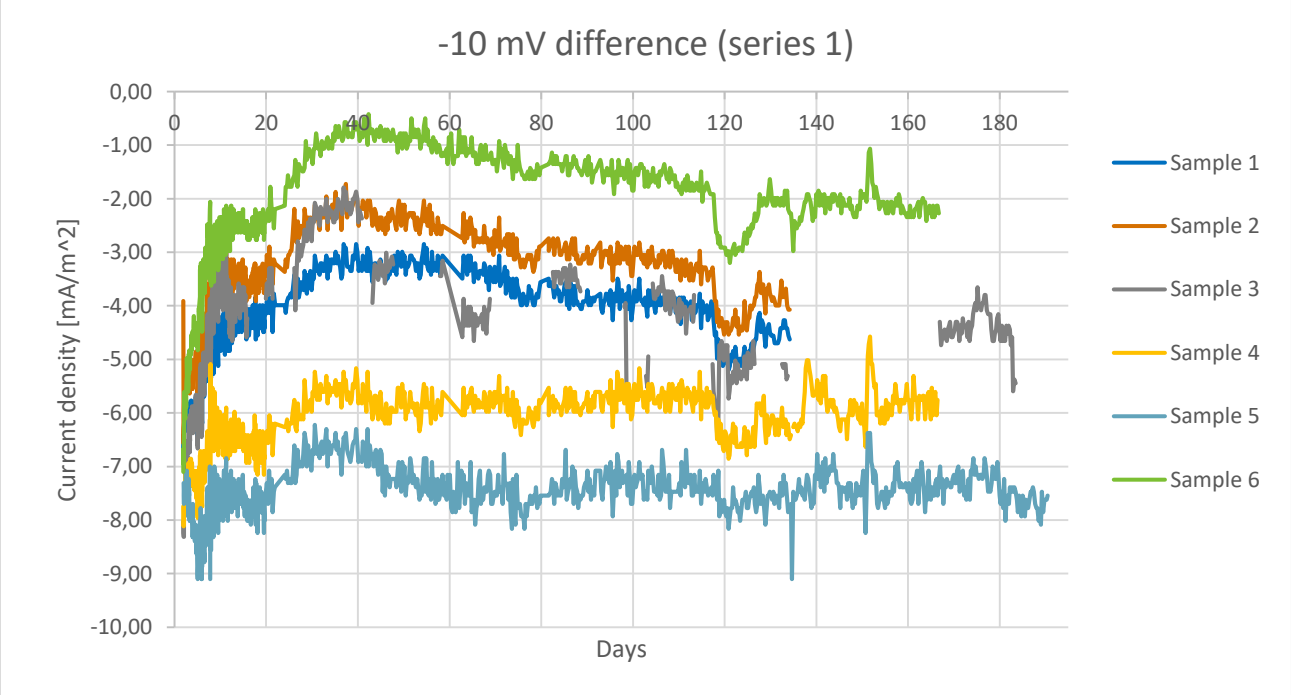

Figure 4.1: Current density versus time at -10 mV potential difference (Series 1) – test samples 1-6

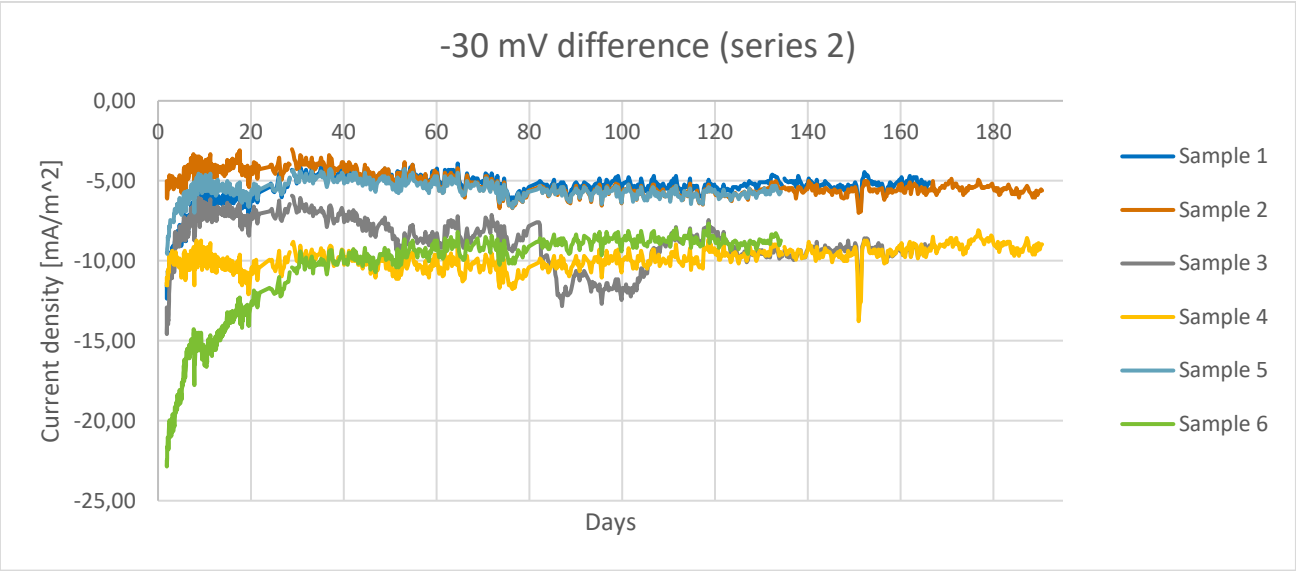

Figure 4.2: Current density versus time at -30 mV potential difference (Series 2) – test samples 1-6

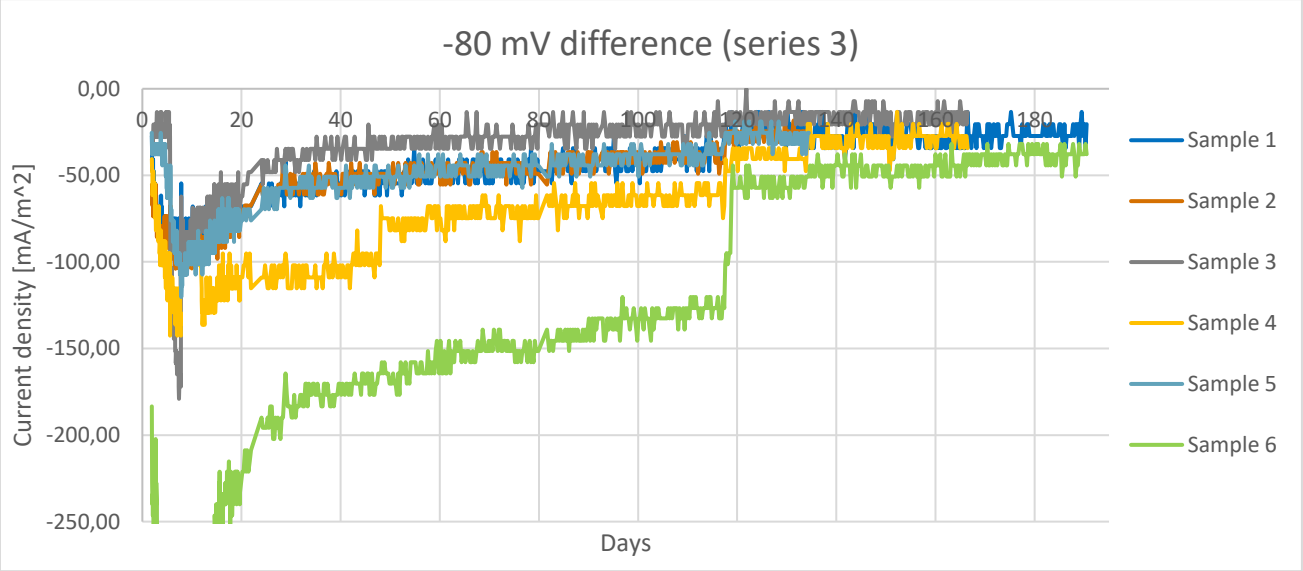

Figure 4.3: Current density versus time at -80 mV potential difference (Series 3) – test samples 1-6

4.1.2 POTENTIAL MEASUREMENTS FOR SAMPLES EXPOSED AT OCP (SERIES 4)

The potential measurements for series 4 which was exposed at OCP and set up as free running tests has experienced a small change throughout the experiment. As the results show in Figure 4.4, the potential fluctuates around 10 mV throughout the experiment, but a trend of decreasing potential can clearly be seen. The average potential changed from approximately -1080 $mV_{Ag/AgCl}$ in the beginning, to approximately -1100 $mV_{Ag/AgCl}$ in the end of the experiment. The change looks to be close to identical for all samples.

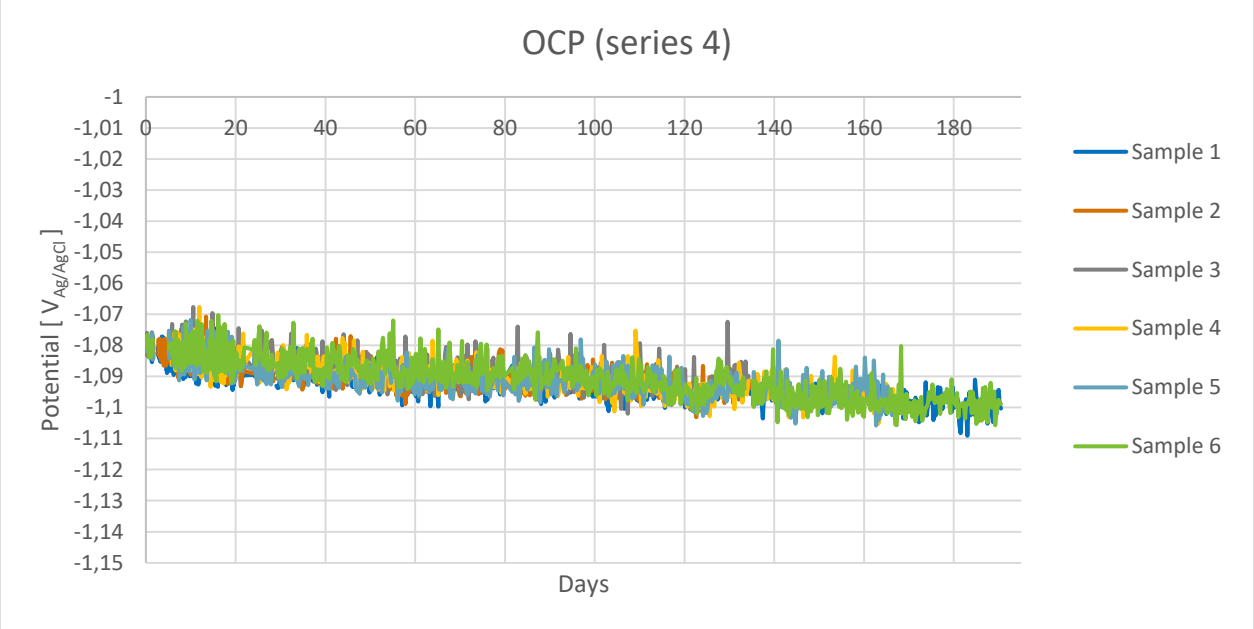

Figure 4.4: Potential versus time for series 4 (OCP)

4.1.3 POLARIZATION POTENTIAL

The working electrode potential used in Series 1-3 was measured throughout the experiment and presented in Figure 4.5. This was done to ensure that the potential difference for each series was stable. The change in the potentiostats potential throughout the experiment was approximately -20 mV, which is the same change that is observed in OCP samples. The change is also identical between the series. This is as expected because the reference material used for the three potentiostats are a combination of three anode material samples. Results in Figure 4.5 compared to the potential logging of OCP exposed samples in Figure 4.4 shows that the working electrode potential has been as planned throughout the whole experiment.

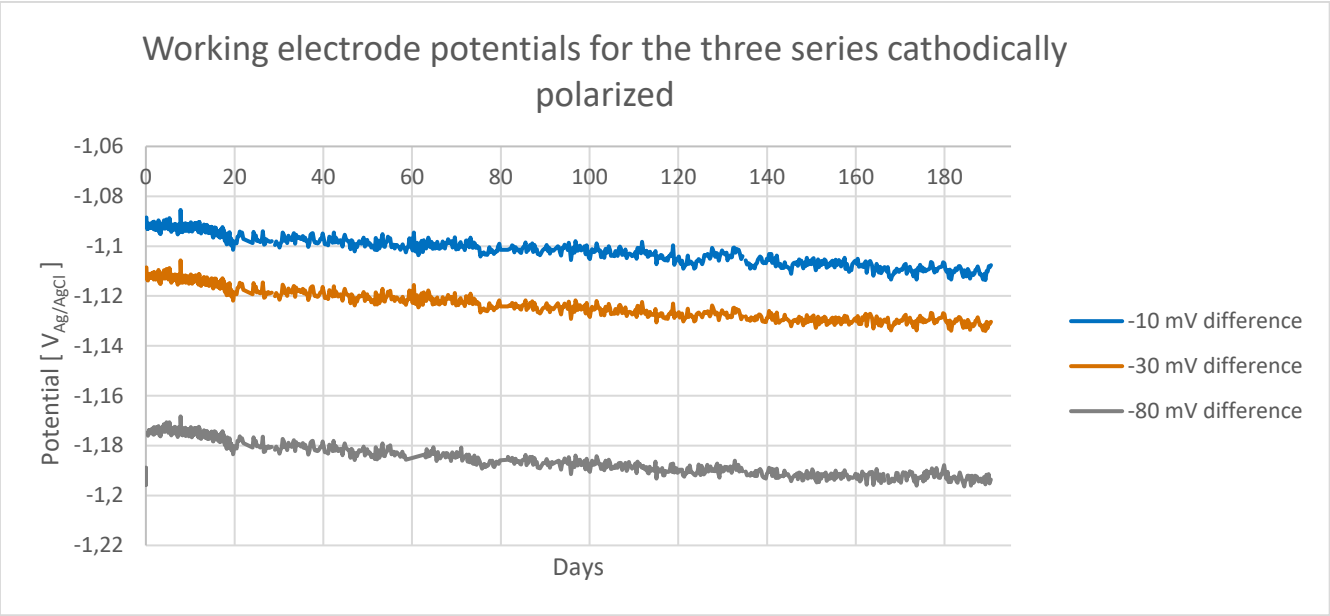

Figure 4.5: Potential versus time for the working electrode on the three series cathodically polarized

4.1.4 CORROSION RATES

LPR was performed after 27 and 120 days. The Tafel constant used for calculating the corrosion rates are from the polarization curve recorded of a non-exposed sample, and the process is described in Section 4.2. The individual corrosion rates for each sample from the LPR after 27 days are given in Table 4.1, and the corrosion rates from the LPR after 120 days are given in Table 4.2. LPR was performed on six non-exposed samples to compare with the results from the polarized samples, which are both included in Tables 4.1 and 4.2. In addition to individual rates being presented, the averages from each of the series corrosion rate calculations are presented graphically in Figure 4.6 as well as standard deviation, where both results from 27 days and 120 days are included.

Table 4.1: Corrosion rate after 27 days for different series and samples with average and standard deviation for each series included. Corrosion rate of non-exposed sample added for comparison.

	OCP (Series 4)	-10 mV (Series 1)	-30 mV (Series 2)	-80 mV (Series 3)	Non-exposed (Reference)
Sample 1	4.93 µm/year	3.42 µm/year	3.98 µm/year	6.37 µm/year	33.06 µm/year
Sample 2	3.29 µm/year	3.31 µm/year	3.55 µm/year	5.00 µm/year	25.66 µm/year
Sample 3	4.00 µm/year	3.28 µm/year	4.92 µm/year	3.65 µm/year	13.33 µm/year
Sample 4	3.29 µm/year	5.59 µm/year	6.82 µm/year	5.64 µm/year	18.01 µm/year
Sample 5	2.88 µm/year	6.33 µm/year	3.99 µm/year	5.16 µm/year	13.77 µm/year
Sample 6	3.77 µm/year	2.58 µm/year	9.06 µm/year	5.37 µm/year	25.03 µm/year
Average	3.69 µm/year	4.09 µm/year	5.38 µm/year	5.20 µm/year	21.47 µm/year
Standard deviation	0.72	1.50	2.15	0.9	10.46

Table 4.2: Corrosion rate after 120 for different series and samples with average and standard deviation for each series included. Corrosion rate of non-exposed samples added for reference.

	OCP (Series 4)	-10 mV (Series 1)	-30 mV (Series 2)	-80 mV (Series 3)	Non-exposed (Reference)
Sample 1	8.64 µm/year	2.34 µm/year	3.24 µm/year	3.18 µm/year	33.06 µm/year
Sample 2	6.90 µm/year	2.92 µm/year	3.56 µm/year	2.83 µm/year	25.66 µm/year
Sample 3	5.30 µm/year	7.68 µm/year	4.77 µm/year	2.10 µm/year	13.33 µm/year
Sample 4	4.44 µm/year	2.24 µm/year	5.07 µm/year	3.09 µm/year	18.01 µm/year
Sample 5	3.99 µm/year	4.25 µm/year	3.92 µm/year	3.18 µm/year	13.77 µm/year
Sample 6	5.16 µm/year	2.33 µm/year	5.17 µm/year	3.09 µm/year	25.03 µm/year
Average	5.74 µm/year	3.62 µm/year	4.29 µm/year	2.91 µm/year	21.47 µm/year
Standard deviation	1.74	2.12	0.83	0.42	10.46

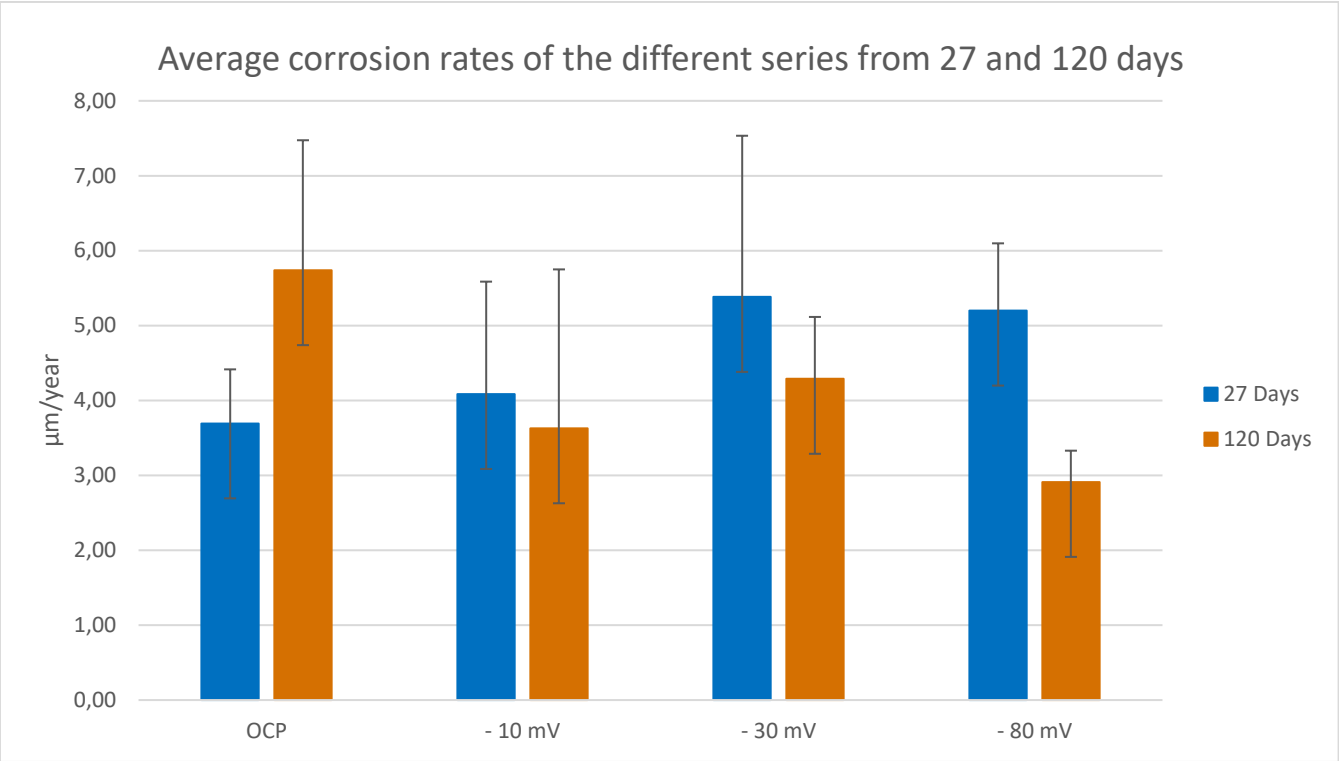

Figure 4.6: Average corrosion rate from the four different series from 27 and 120 days

From the averages shown in Table 4.1 and in Figure 4.6 it can be seen that the corrosion rates for series 1 (-10 mV) is a little higher than for series 4 (OCP), and that the corrosion rate for series 2 (-30 mV) and 3 (-80 mV) is approximately the same, but a little higher than for series 1 (-10 mV). However, the standard deviation is rather high for all series, which means that there are large variations in measurements in the individual series. This difference in each series is in some cases larger than the difference between series.

A different trend can be seen for corrosion rates after 120 days, ref. Table 4.2. The corrosion rates of series 4 (OCP) seem to be highest, and the corrosion rates of series 3 (-80 mV) are the lowest, which was most polarized. The corrosion rate of all samples cathodically polarized are lower than for samples exposed at OCP as can be seen in Figure 4.6. No clear trend other than that series 3 (-80 mV) has the lowest corrosion rate can be found between the polarized series. The same degree of variation as after 27 days of exposure applies for the measurements after 120 days.

Comparing corrosion rates recorded after 27 and 120 days could indicate that the corrosion rate has decreased for polarized samples, ref. Figure 4.6. However, since the difference is small, and the standard deviation is larger than the difference the comparison should be done with care. The corrosion rate of samples exposed at OCP has increased. The trend of higher corrosion rates for polarized to the lowest potential found after 27 days, changed to the opposite trend from the measurements performed after 120 days, where samples polarized the most had the lowest corrosion rate. Even though the measurements have a large degree of variations, the measurements clearly show that non exposed samples have a noticeably higher corrosion rate than samples that has been included in the long-term experiment, as can be seen in Table 4.1 and 4.2.

4.1.5 POLARIZATION CURVES

Polarization curves are presented for all samples from the potentiostatic experiment and presented in graphs for each series. The samples that were polarized with a slower scanning rate are included in the diagram, but they are marked with a S. Further are all polarization curves compared in the same graph in order to see differences more easily. Lastly are this comparison presented together with nine polarization curves from non-exposed samples in order to see how the polarization curves has changed compared to a non-exposed material.

As seen in Figure 4.7, 4.8 and 4.9, it seems that all series experience a slow increase in current density up to a given potential, where the current density suddenly rapidly increases. Results also show that polarization curves within each series vary, and for some samples the difference is as much as one decade. Polarization curves after exposure to OCP (series 4) is seen to have little variations, and the polarization curves of the polarized series does seem to vary more. All samples which have been polarized at a lower speed has a little higher current density than the rest in the same series. No clear correlation between differences in current density measurements during the polarization and polarization curves can be observed.

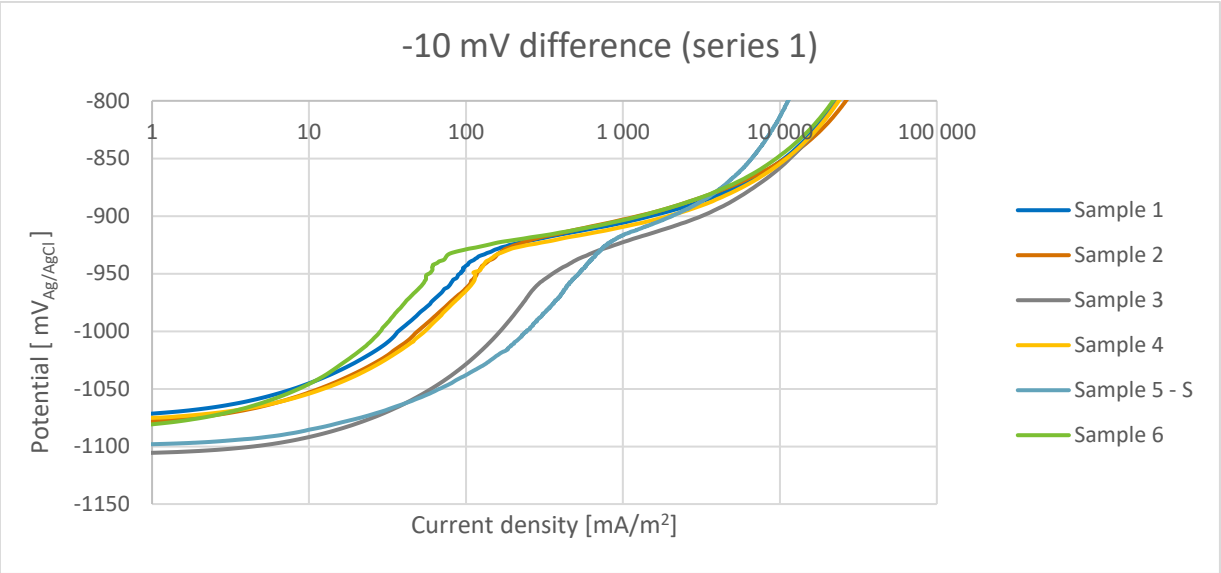

Figure 4.7: Polarization curves of samples subjected to a -10 mV potential difference (series 1) – test samples 1-6 ('S' denotes measurement with lower can rate)

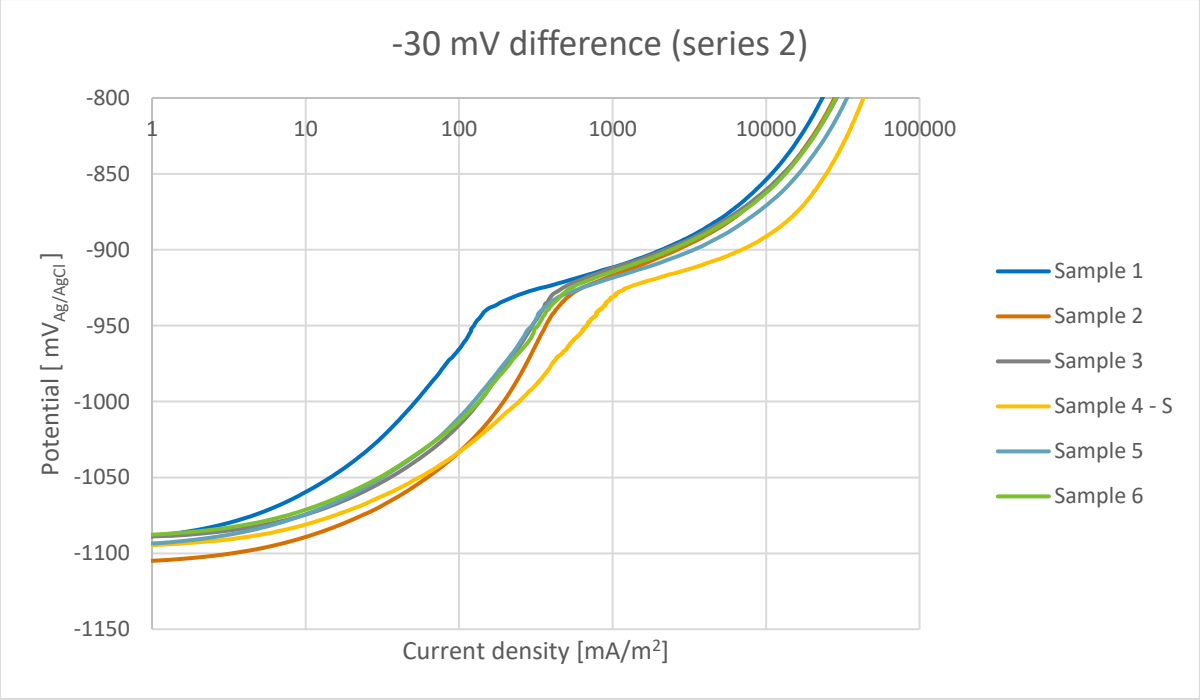

Figure 4.8: Polarization curves of samples subjected to a -30 mV potential difference (series 2) – test samples 1-6 ('S' denotes measurements with lower scan rate)

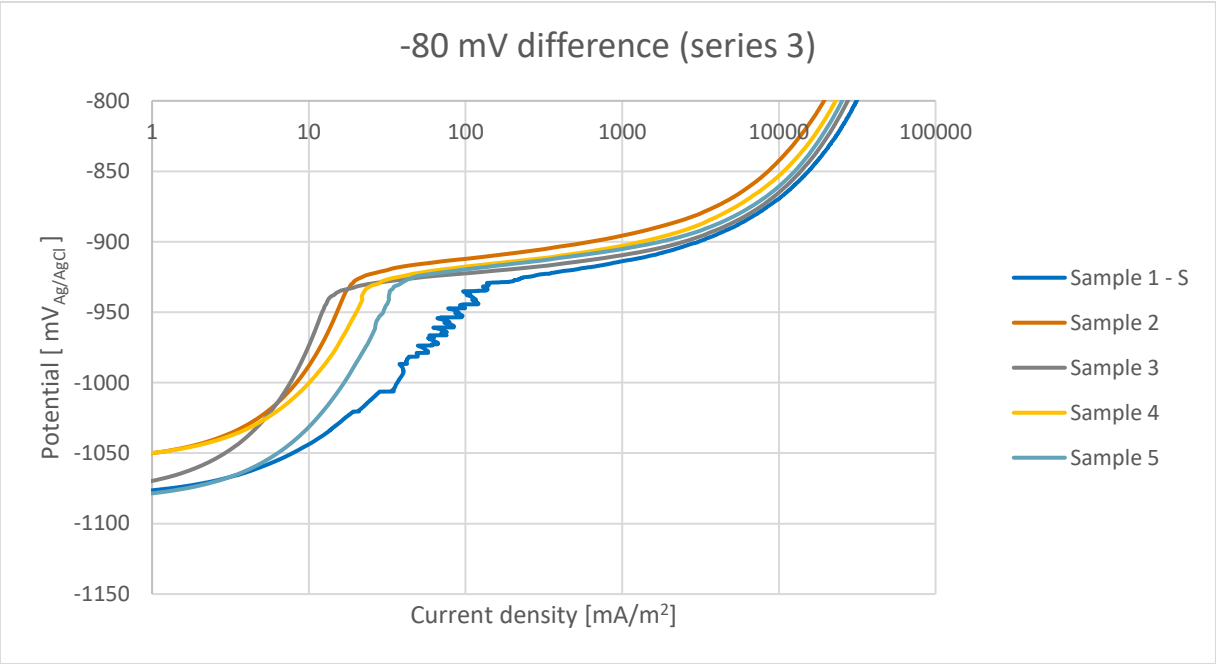

Figure 4.9: Polarization curves of samples subjected to a -80 mV potential difference (series 3) – test samples 1-6 ('S' denotes measurements with lower scan rate)

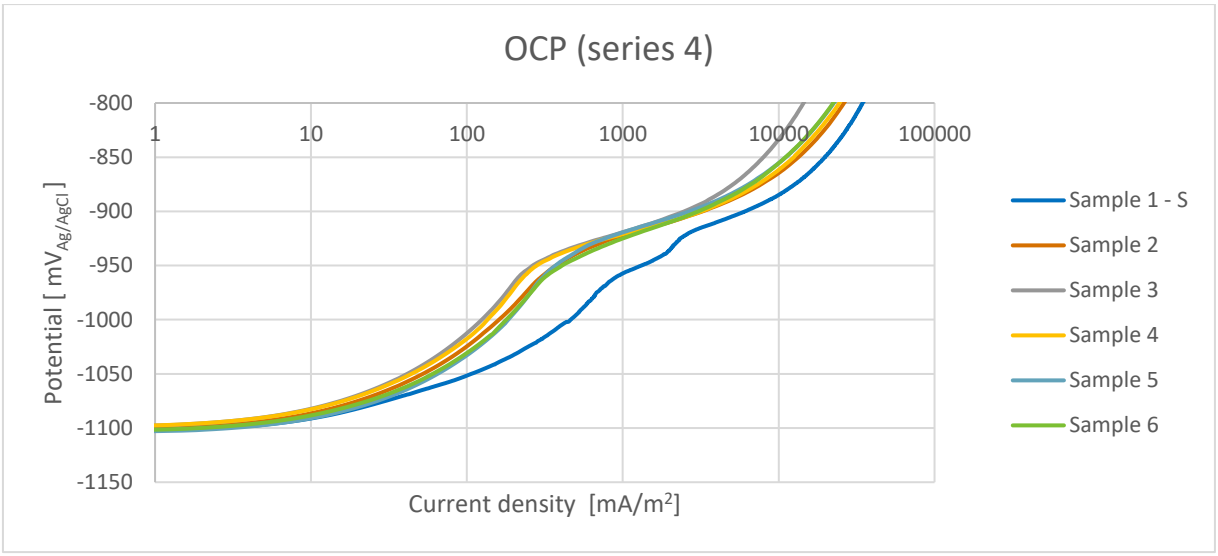

Figure 4.10: Polarization curves of samples exposed at OCP (series 4) – test samples 1-6 ('S' denotes measurements with lower scan rate)

Figure 4.11 compares the polarization curves from the long-term experiment. These curves will also be compared to the polarization curves of non-exposed samples in Figure 4.12. Two important parameters from these comparisons are further defined in order to better compare the different samples and series.

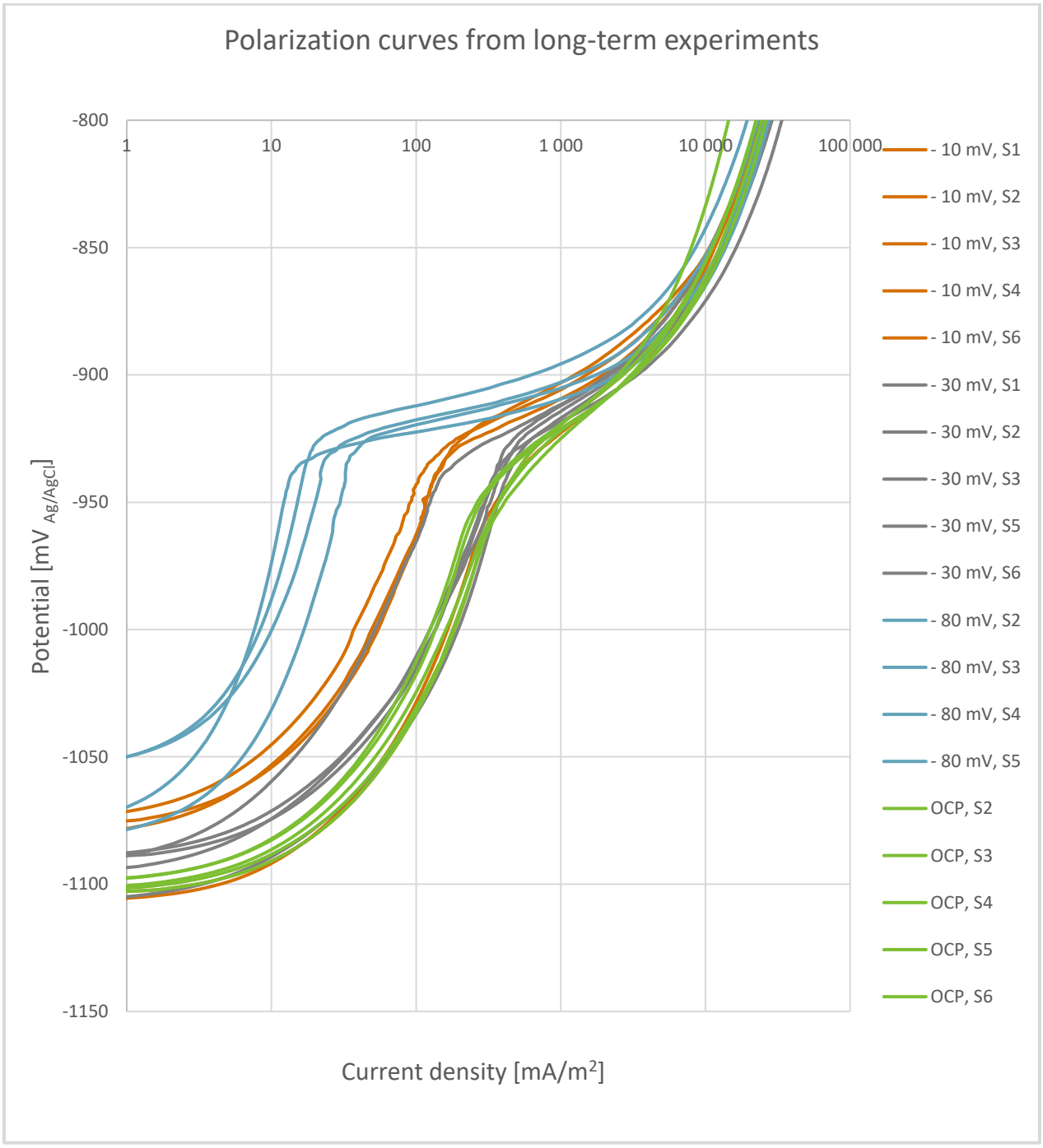

Figure 4.11: Polarization curves of samples from the long-term potentiostatic experiment

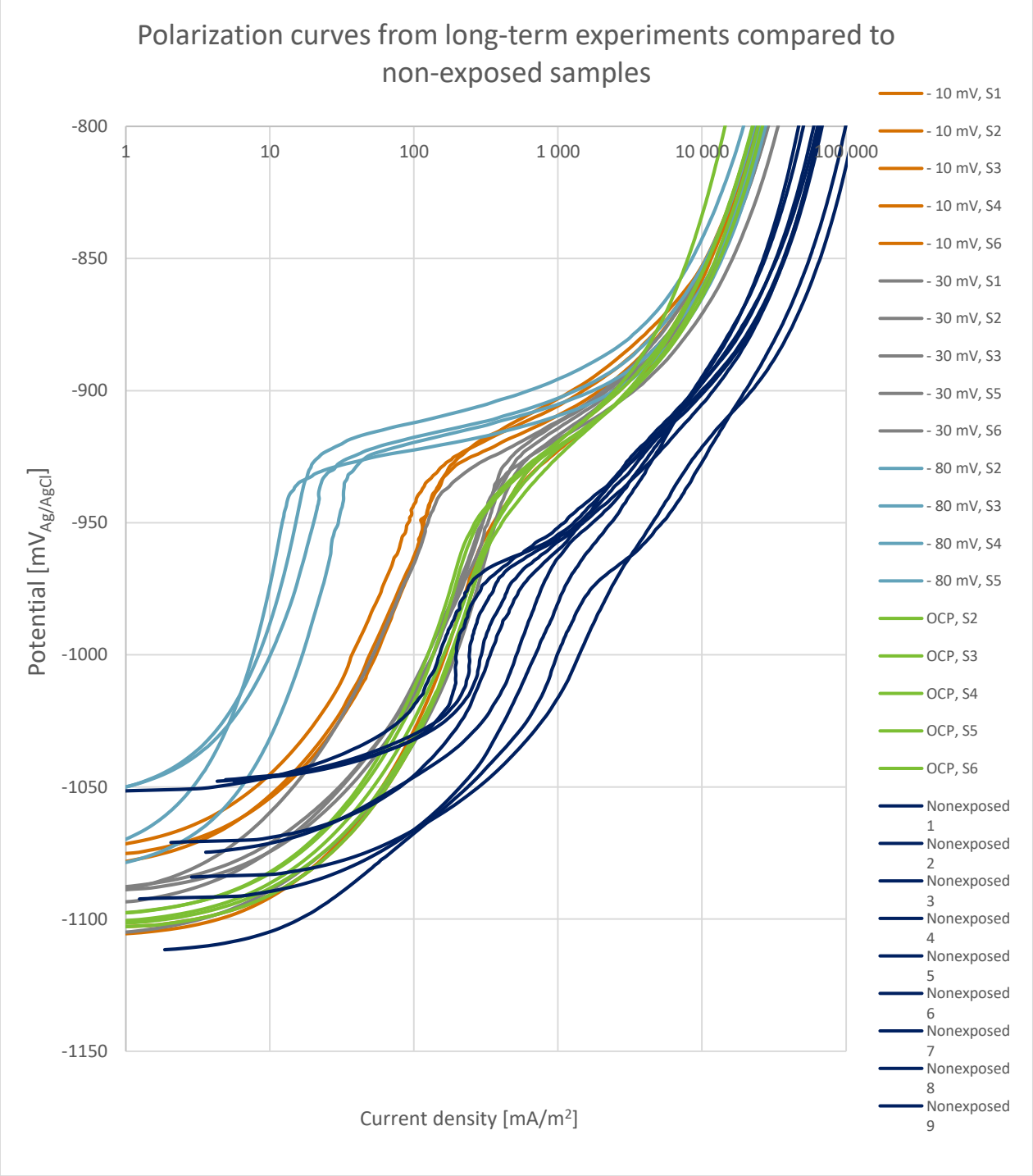

Figure 4.12: Polarization curves of all samples after the long-term potentiostatic experiment compared to polarization curves of non-exposed samples

The first parameter that will be defined is the potential of where anode samples will activate. As the polarization curves in Figure 4.11 show, the current density of the samples increases rather slow as the potential moves away from OCP, but rapidly increases when it reaches a specific potential. This potential is defined as the activation potential. Results in Figure 4.11 show that the activation potential is approximately the same for all polarized series and seem to be independent of the amount of cathodic polarization and current density. This activation potential is approximately -925 $mV_{Ag/AgCl}$ for all polarized samples, and approximately -940 mV $_{Ag/AgCl}$ for the samples only exposed at OCP. Figure 4.12 show that some of the non-exposed samples show signs of a potential where they become more active, but not to the same degree as the polarized samples, and at a more negative potential.

The second important parameter which will be defined is the current density given at the activation potential. As seen in Figure 4.11, this value varies between series, but also to some degree for samples within the same series. In order to better compare the degree of passivation between the series, the current density at the activation potential are presented for each of the samples in table 4.3, where the average and standard deviation also are presented. In these averages, the polarization curve recorded with lower scanning rate is not included. The averages are also graphically presented in Figure 4.14.

Table 4.3: Current density at the activation potential from the polarization curve of long-term experiment samples. The activation potential is approximately -925 mV for the polarized series, and -940 mV for the series exposed at OCP.

	OCP (Series 4)	-10 mV (Series 1)	-30 mV (Series 2)	-80 mV (Series 3)
Sample 1	-	150 mA/m^2	190 mA/m^2	-
Sample 2	550 mA/m^2	200 mA/m^2	500 mA/m^2	20 mA/m^2
Sample 3	350 mA/m^2	650 mA/m^2	460 mA/m^2	15 mA/m^2
Sample 4	350 mA/m^2	200 mA/m^2	-	30 mA/m^2
Sample 5	500 mA/m^2	-	460 mA/m^2	40 mA/m^2
Sample 6	550 mA/m^2	90 mA/m^2	450 mA/m^2	-
Average	460 mA/m^2	258 mA/m^2	412 mA/m^2	26 mA/m^2
Standard deviation	102	224	126	11

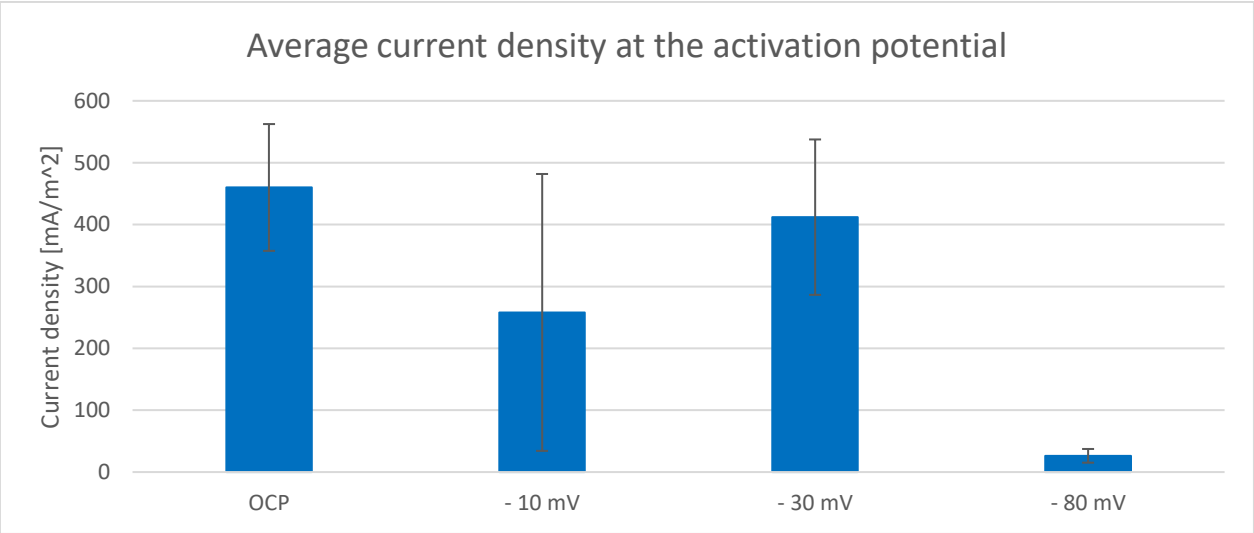

Figure 4.13: Average current density at the activation potential from the polarization curves of long-term experiment samples

Series 3, which was subjected to -80 mV potential difference clearly show most signs of passivation in Figure 4.11, and this is confirmed from the averages in Figure 4.13 and Table 4.3 where the series has an average of 26 mA/m^2 at the activation potential. In the graph in Figure 4.11, it looks like the series that are exposed at OCP shows the least sign of passivation, which is also confirmed in Figure 4.13 and Table 4.3, where the series has the higher average current density at the reactivation potential. This series also have a little more negative activation potential as previously mentioned.

The different curves of series 1 (-10 mV) and series 2 (-30 mV) seems to vary quite similarly when the graph in Figure 4.13 is visually inspected. However, the averages calculated in Table 4.3 and shown in Figure 4.14 show that the average current density of series 1 (-10 mV) are somewhat lower than series 2 (-30 mV). Even though the difference in average current density at the activation potential between series 1 (-10 mV) and series 2 (-30 mV) are larger than the difference between series 1 (-10 mV) and series 4 (OCP), it could appear as if series 1 (-10 mV) and series 2 (-30 mV) have reacted similarly to the polarization, and that they both have a lower current density than the series exposed at OCP. The reason for this is that the curves in series 1 (-10 mV) and series 2 (-30 mV) vary more similarly than for series 4 (OCP), where the latter series does not vary much.

Most of the polarization curves of samples from the long-term experiment have a generally lower current density than the polarization curves of non-exposed samples during the whole anodic polarization. The curves from the non-exposed samples seems to vary, so that some results look similar to the curves of series 1,2 and 4. However, at the activation potential of exposed samples, the non-exposed samples have approximately one decade higher current density than the samples from the long-term experiment. This indicates that all samples from the long-term experiment shows passivation to some degree compared to the non-exposed samples.

4.1.6 REACTIVATION

Several polarization curves were obtained on one sample from series 3 (-80 mV) with approximately 30 minutes in between, and the results are presented in Figure 4.14. The polarization curves of this sample are also compared to the polarization curve of a non-exposed sample. Results show that after the first polarization, the following polarization curves are similar to a non-exposed sample, indicating that the sample is permanently reactivated.

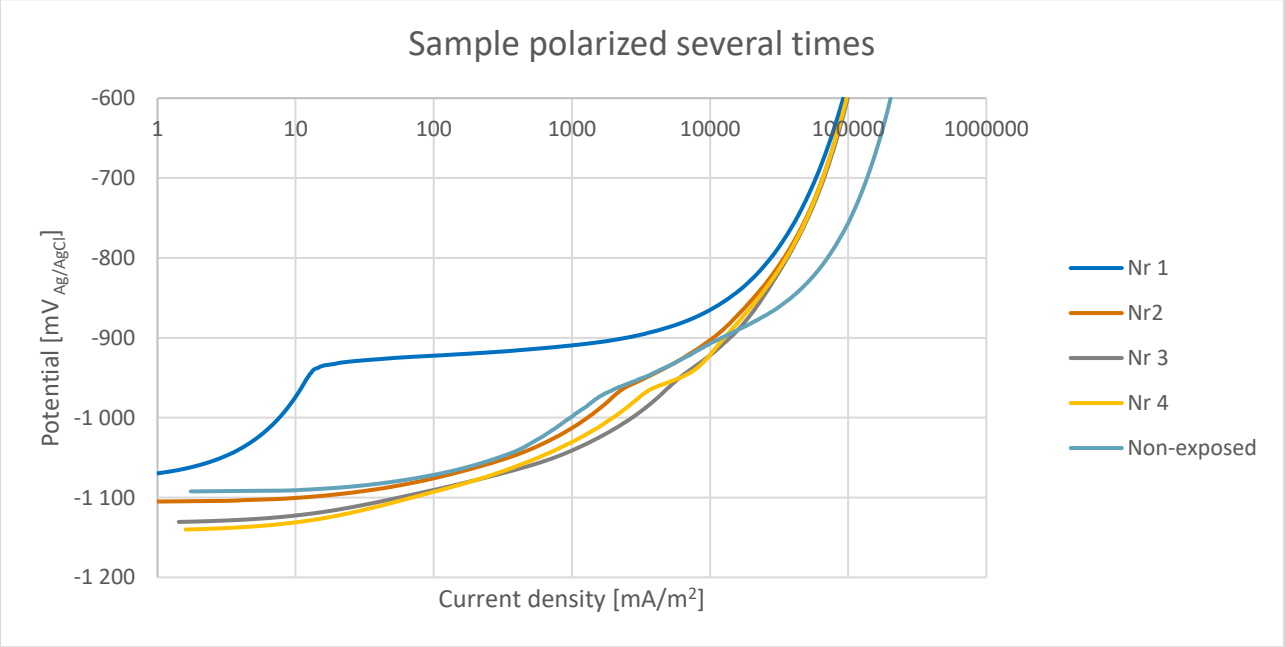

Figure 4.14: Polarization curve of sample 3 from series 3 (-80 mV) with three following polarization curve recordings. Polarization curve of a typical non-exposed sample included.

4.2 POLARIZATION CURVE OF NON-EXPOSED SAMPLE

The polarization curve of a non-exposed sample was recorded and is shown in Figure 4.15. The potential drop in the electrolyte was accounted for, where a resistance of 10 Ω was used. This curve was used to see what potential the current used in the galvanostatic experiment corresponded to. The Tafel constant used for calculating the corrosion rate in Section 4.1.4 were also estimated from this curve. Tafel constant B_a was estimated to be 0.04 V/decade, and B_c was estimated to be 0.4 V/decade.

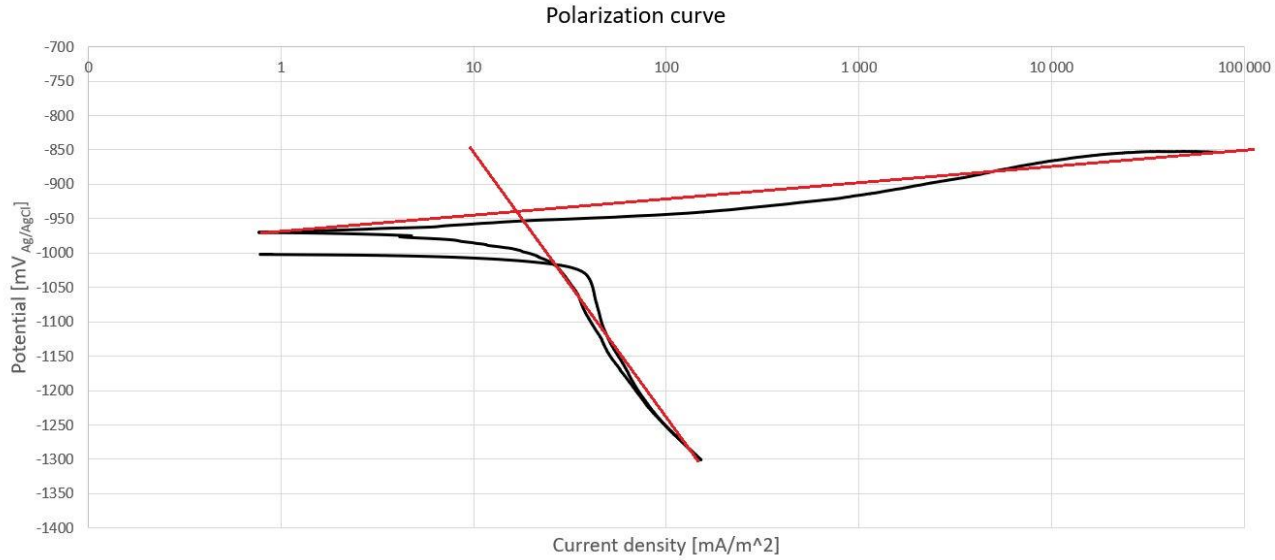

Figure 4.15: Polarization curve from a non-exposed anode material sample

4.3 SHORT-TERM GALVANOSTATIC EXPERIMENTS

Results from the short-term galvanostatic experiments with varying exposure duration is presented in this section. The section is divided into four sections, where the results from each experiment duration is presented in Section 4.3.1 (2 days), 4.3.2 (5 days) and 4.3.3 (10 days). In Section 4.3.4, some of the results are compared to each other as well as the polarization curves of non-exposed sample. The potential of the samples galvanostatically polarized with different durations were measured throughout all the experiments and are presented for each duration. Anodic polarization curves were recorded after each galvanostatic experiment for both the sample that was polarized, and the sample that was exposed at OCP. All samples were polarized to -800 $mV_{Ag/AgCl}$.

4.3.1 GALVANOSTATIC EXPERIMENT NO. 1 - 2 DAYS

The potential measurements show large variations, even though experiment conditions were identical, ref. Figure 4.16. The polarization curves of the galvanostatically polarized samples also seem to vary to a large degree, but the polarization curves of samples only exposed at OCP does not vary to the same degree, see Figure 4.17. It could be reason to believe that the variations in potential measurements is the reason for variations in polarization curves recorded after galvanostatic polarization, but no clear correlation between the two can be seen. The results from the shortest experiment duration shows that the polarization curve of samples cathodically polarized seem to be slightly different than samples exposed at OCP. The galvanostatically polarized samples seems to have slightly less current density at a given potential up to approximately -950 - -900 $mV_{Ag/AgCl}$. To polarize these samples to somewhere between -900 - -950 $mV_{Ag/AgCl}$ it requires around just below 100 mA/m^2, where the same polarization requires around 100 - 1000 mA/m^2 for the samples that are not galvanostatically polarized, see Figure 4.17.

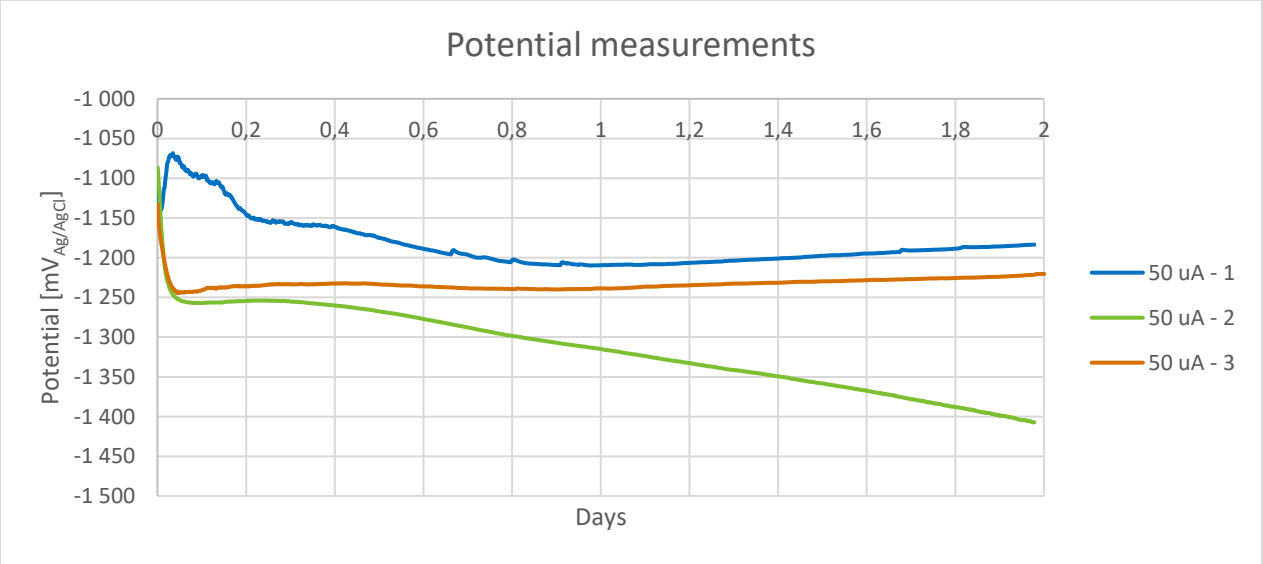

Figure 4.16: Potential versus time for the 2-day galvanostatic experiment at -50 µA

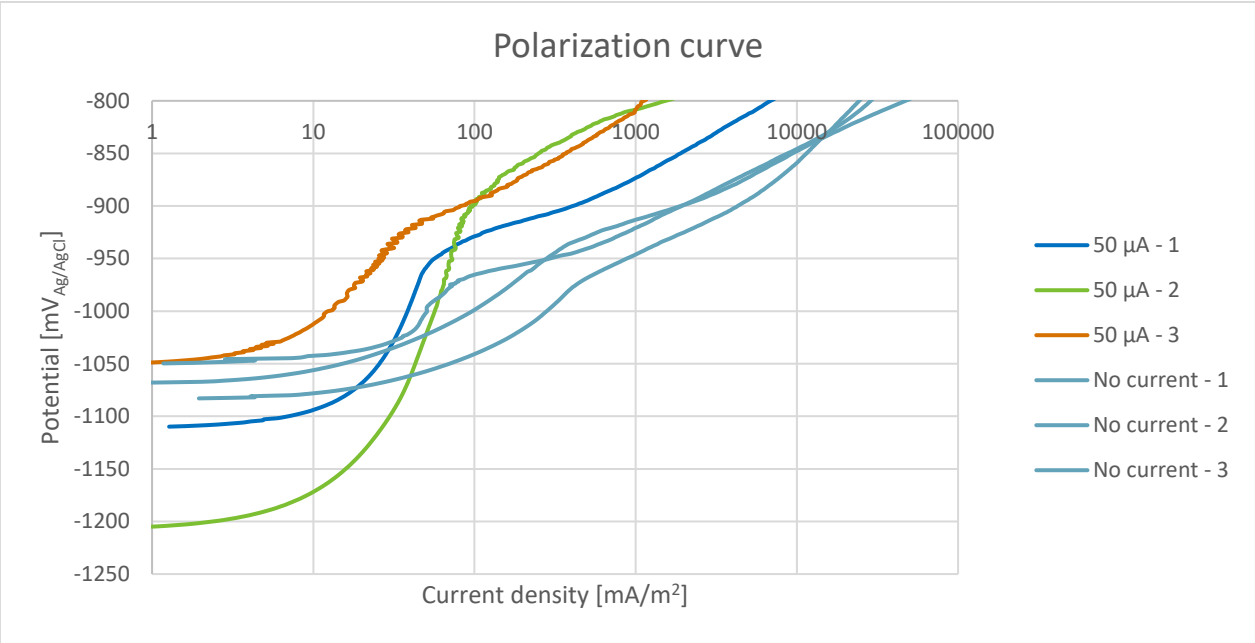

Figure 4.17: Polarization curves of all samples from the 2-day galvanostatic experiment at - 50 µA

4.3.2 GALVANOSTATIC EXPERIMENT NO. 2 - 5 DAYS

The potential measurements seem vary to the same degree as the first experiment, ref. Figure 4.18 vs Figure 4.16. Sample no. 3 have experienced a large potential drop after one day of exposure, where the potential is 200 - 250 mV lower than the other samples for a couple of days, but where the potential suddenly returned to a value comparable to those seen for the other two samples after 5 days.

Similar results as for the 2-day galvanostatic experiment can be seen for the 5-day experiment for the polarization curves as well, ref. Figure 4.19 vs Figure 4.17. Sample no. 2 and 3 of the current induced samples require somewhere between 10 and 100 mA/m^2 to polarize to approximately -950 $mV_{Ag/AgCl}$, where the samples exposed at OCP requires somewhere between 100 and 1000 mA/m^2, see Figure 4.19. However, variation can be seen in polarization curves of the polarized samples. Especially sample no. 1 behaves very different, and contrary to sample no. 2 and 3 it has a lower current density than the samples exposed at OCP until approximately -900 $mV_{Ag/AgCl}$. As can be seen in Figure 4.18 this sample is the one that has experienced the highest potential throughout the galvanostatic experiment. Polarization curves of samples exposed at OCP for 5 days shows very little sign of variations, similarly to the first experiment.

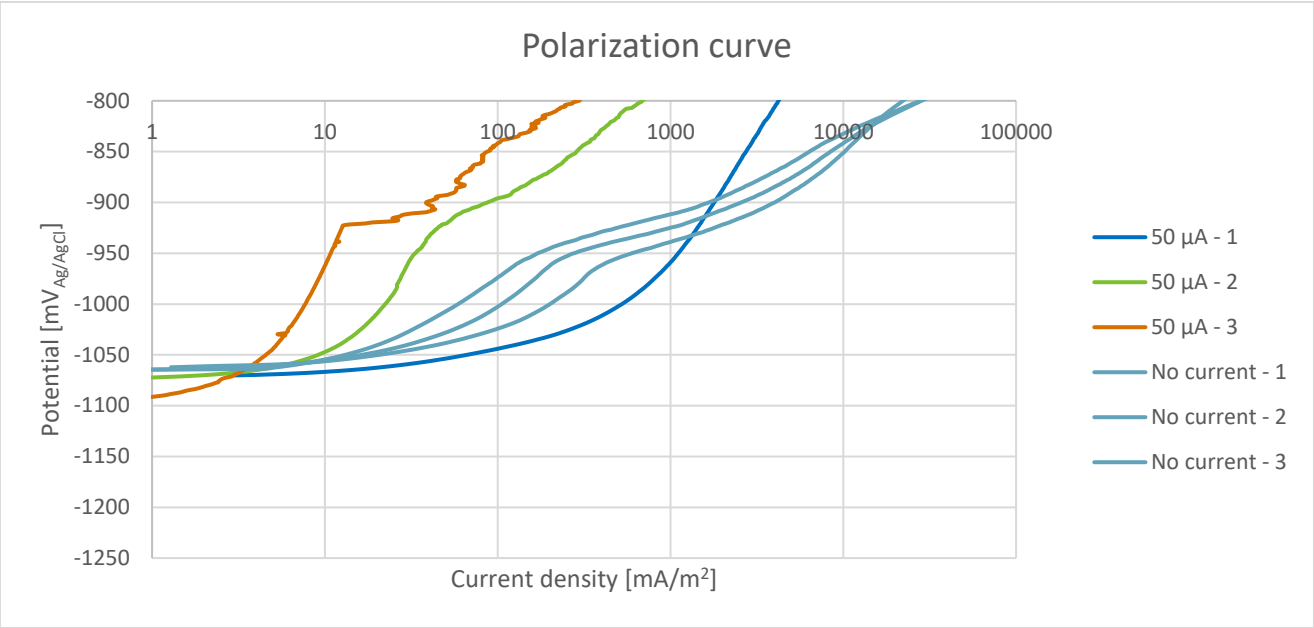

Figure 4.18: Potential versus time for the 5-day galvanostatic experiment at -50 µA

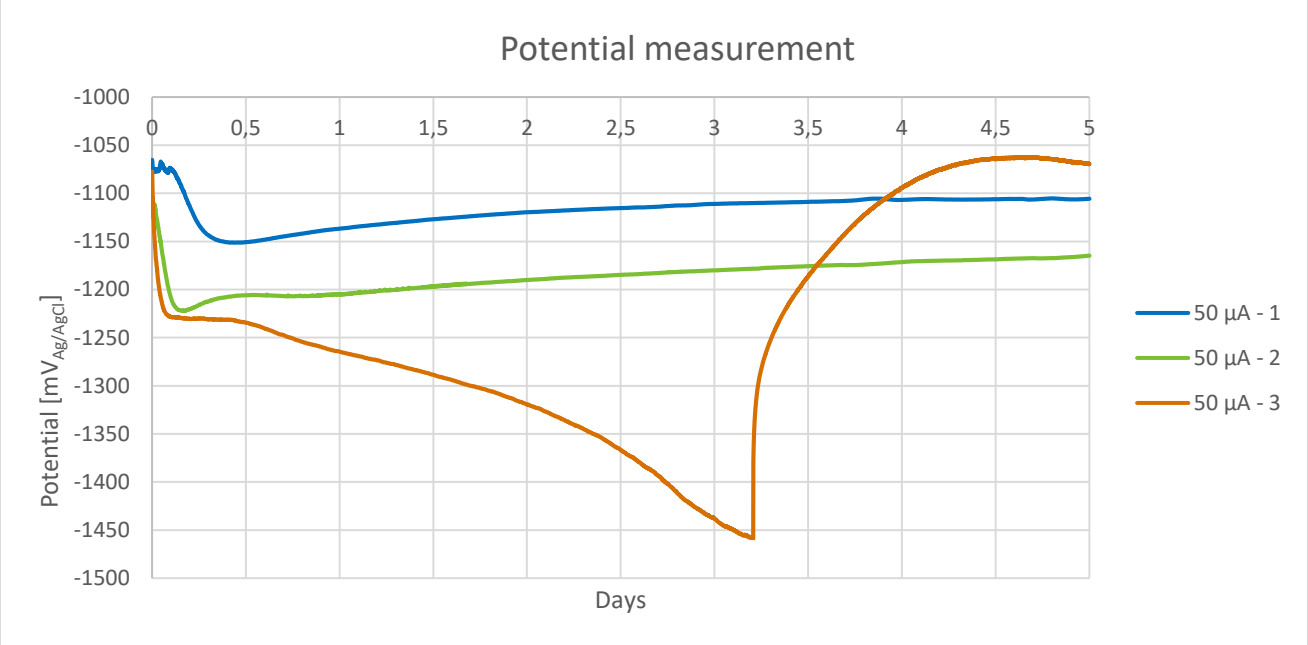

Figure 4.19: Polarization curves of all samples from the 5-day galvanostatic experiment -50 µA

4.3.3 GALVANOSTATIC EXPERIMENT NO. 3 - 10 DAYS

Varying potential measurements can be seen for the galvanostatic experiment with the longest duration as well, ref. Figure 4.20. None of the potential measurements of the three tests behaves similar in the beginning, but they seem to reach approximately the same value at the end of the experiment. Sample no. 1 and no. 2 from the 10-day galvanostatic experiment show a 50 - 100 mV higher open circuit potential than most of the other samples in the 10-day experiment, as well as the other experiment durations, ref Figure 4.21 vs Figure 4.17 and 4.19. The polarization curve of these two samples also shows a clear difference from the OCP exposed samples, where they reach a maximum current density of around 70 mA/m^2 until it reaches the activation potential at approximately -800 $mV_{Ag/AgCl}$. At this point, the current density increases fast. Similar as for the 5-day experiment (Figure 4.19), one of the samples in this experiment as well does not seem to be affected by the galvanostatic polarization, where the polarization curve behaves very similar to the samples exposed at OCP. This sample also has had the least variation in potential measurement throughout the experiment.

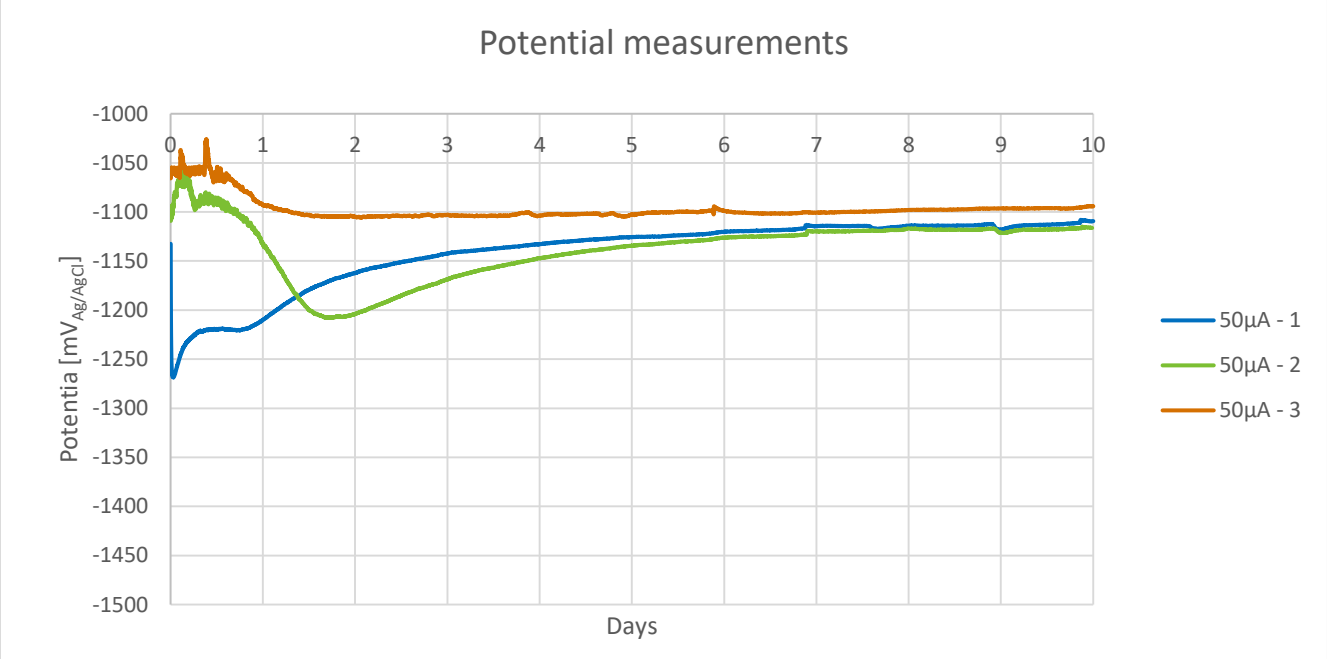

Figure 4.20: Potential versus time for the 10-day galvanostatic experiment -50 µA

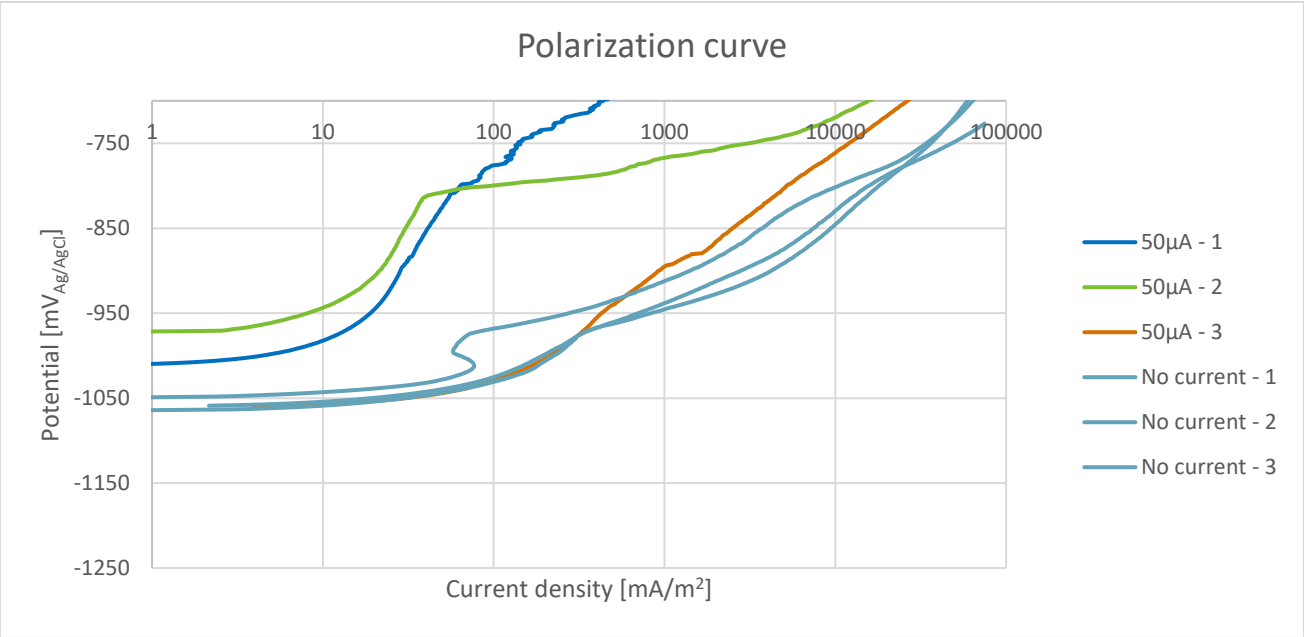

Figure 4.21: Polarization curves of all samples from the 10-day galvanostatic experiment -50 µA

4.3.4 GALVANOSTATIC RESULTS COMPARED

Figure 4.22 compares the polarization curves from the galvanostatic experiment with the polarization curves of non-exposed samples. In order to more easily compare the different experiment durations, the same parameters that were defined for the potentiostatic results will be used, ref. Section 4.1.5. Based on these definitions, the activation potential and the current density at this potential will be presented in Table 4.4. Samples which seemed to not have responded to the galvanostatic experiment are not included in the Table 4.4. Because of variations in activation potential for the different series, individual activation potentials are presented in Table 4.4. The average current densities are presented graphically in Figure 4.22.

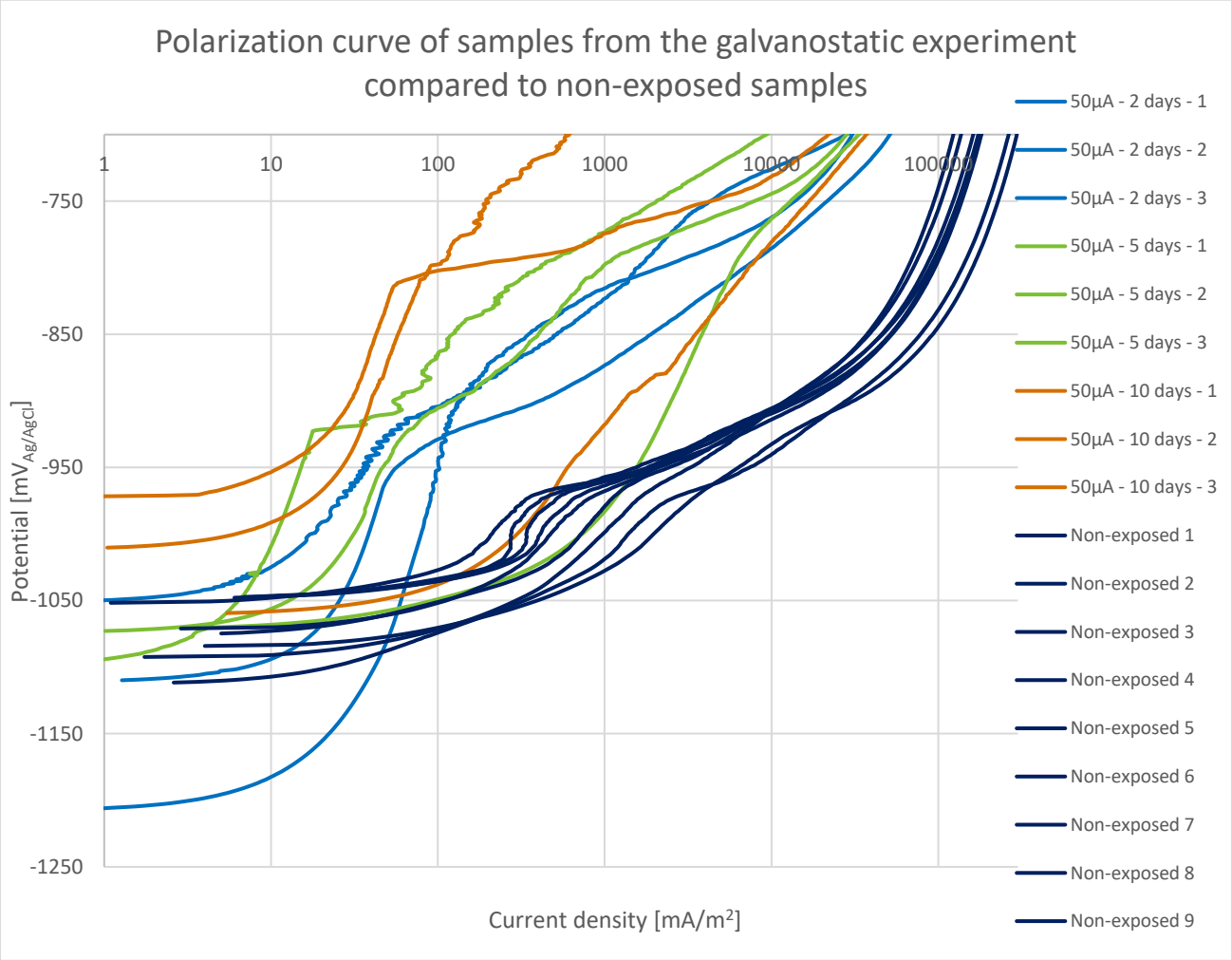

Figure 4.22: Polarization curves of all the polarized samples from the galvanostatic experiments compared to polarization curves of non-exposed samples

Table 4.4: Current density and activation potential from polarization curves after the galvanostatic experiment for the different experiment durations

	2 days		5 days		10 days	
	Activation potential	Current density	Activation potential	Current density	Activation potential	Current density
Sample 1	~ 940 mV	70 mA/m^2	-	-	~ 800 mV	70 mA/m^2
Sample 2	~ 880 mV	140 mA/m^2	~ 920 mV	55 mA/m^2	~ 810 mV	40 mA/m^2
Sample 3	~ 910 mV	50 mA/m^2	~ 920 mV	20 mA/m^2		
Average	910 mV	87 mA/m^2	920 mV	38 mA/m^2	805 mV	55 mA/m^2
Std.dev	30	47	0	25	7	21

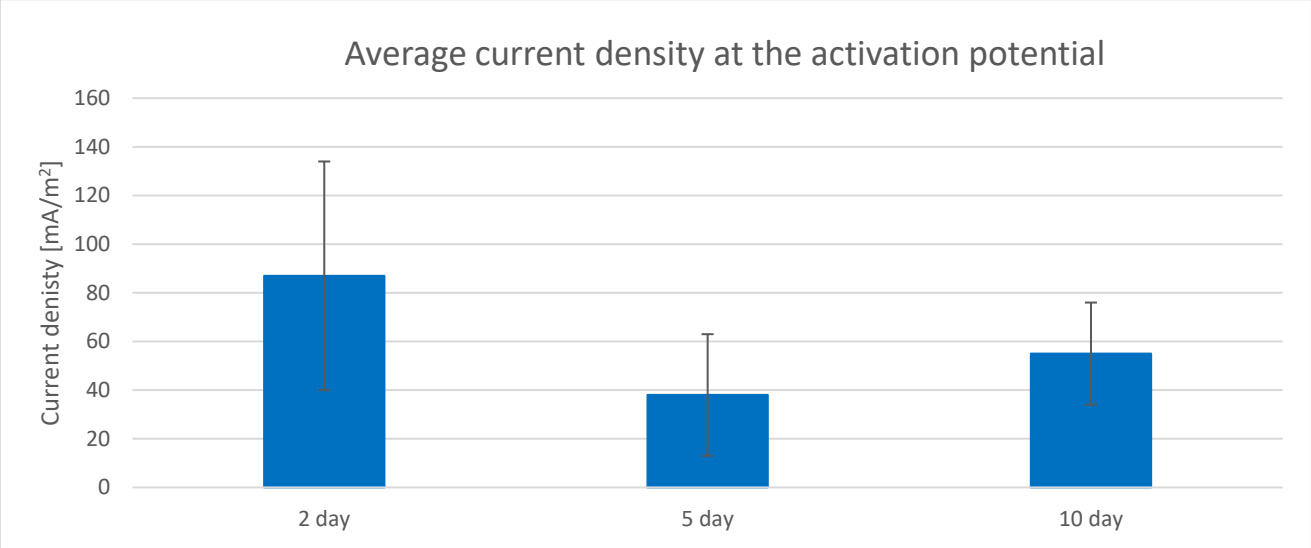

Figure 4.23: Average current densities at the activation potential from the polarization curves of the galvanostatic experiment for the different experiment durations

Compared to non-exposed samples the polarization curve of most samples polarized galvanostatically seemed to have passivated to some degree, i.e. the polarized samples have generally a lower current density, ref. Figure 4.24. Even though the results vary, a minor trend off increasing degree of passivation along with increasing experiment duration can be seen visually from Figure 4.22, as the current density required to polarize the samples to an activation potential is decreasing with increased experiment duration. This observation is confirmed to some degree from the current density averages shown in Table 4.4 and Figure 4.23, as the 2-day experiment shows the highest current density. However, the 5-day experiment has a somewhat lower current density than the 10-day experiment, but the difference is not significant. Table 4.4 show that the activation potential where current density suddenly increases is similarly between -910 mV $mV_{Ag/AgCl}$ and -920 $mV_{Ag/AgCl}$ for the polarized samples in the two experiments with the lowest duration (2 and 5 days), and that the potential is around 100 mV higher for the polarized samples with the longest experiment duration (10 days).

In Figure 4.24 the polarization curve of the samples exposed at OCP for reference in the galvanostatic experiments are compared to the polarization curves of non-exposed samples.

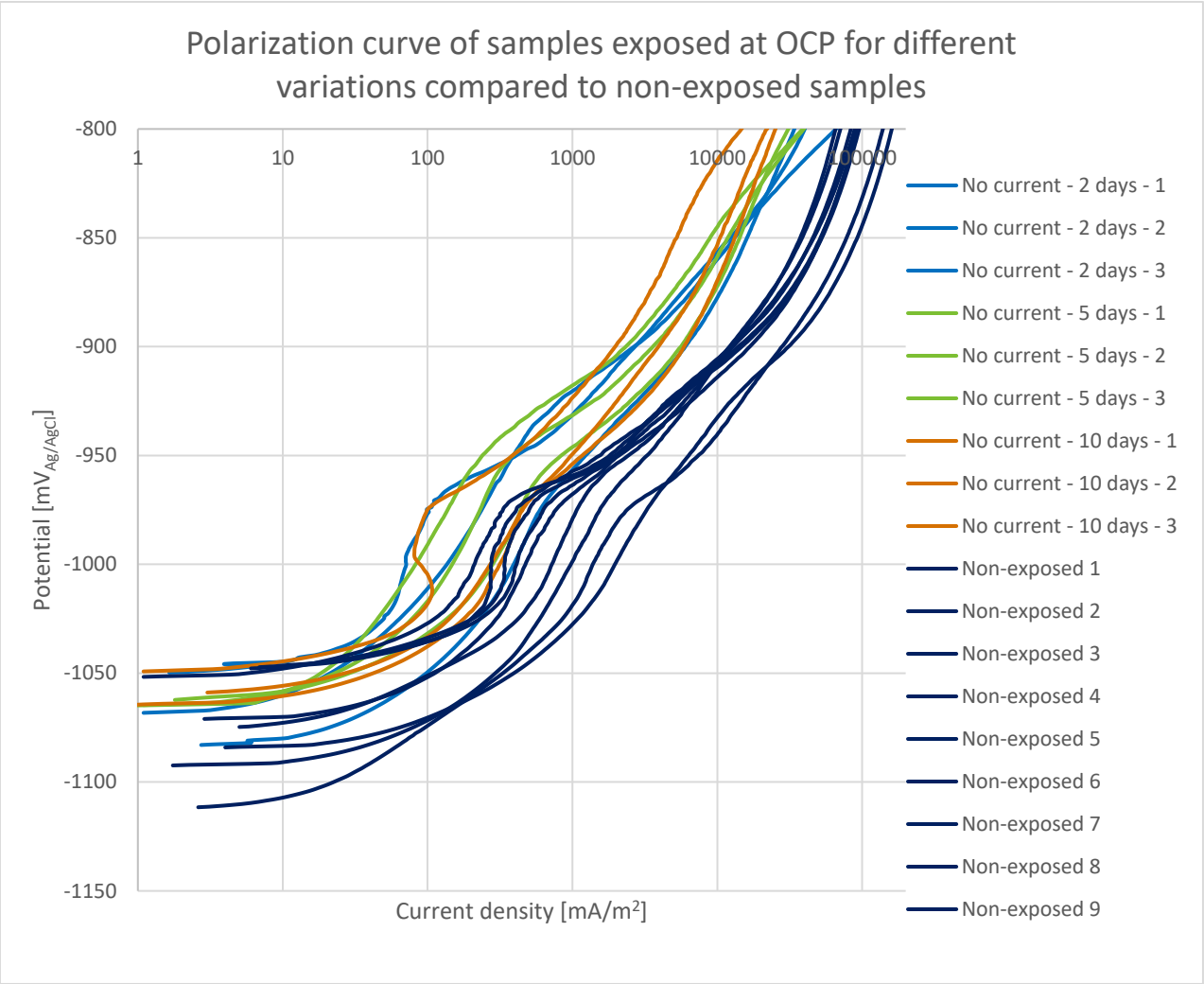

Figure 4.24: Polarization curves of all the OCP exposed samples from the galvanostatic experiment compared to polarization curves of non-exposed samples.

The comparison in Figure 4.24 shows that even though samples only have been exposed at OCP, the curves seem to show some degree of passivation compared to the curves of non-exposed. The polarization curves of samples exposed at OCP does show signs of an activation potential, where it seems that samples activate around -970 $mV_{Ag/AgCl}$, but the activation potential is not as clear as for the polarized samples. However, at this point, the current density is generally approximately half a decade higher for the non-exposed samples compared to the ones exposed at OCP for different durations. The polarization curves of samples exposed at OCP does not vary much, and the difference between the different durations is not significant.

4.4 SCANNING ELECTRON MICROSCOPE

Mapping and spot analysis were performed on three different areas of the sample in the SEM. Results from one of the inspected areas for each of the four series are included in this section, as well as the results from one area of a sample which was inspected without recording a polarization curve before examination. The section is divided into 5 sub-sections, one for each sample which was investigated. The rest of the results from the SEM is included in the Appendix A5.

Traces of other elements than presented were also found, but only aluminium, oxygen, calcium and magnesium is presented. Especially large amounts of carbon were found, but this was expected because of contamination between preparation and inspection, as well as the samples were coated with carbon.

Results from the mapping analysis are first presented with an image of all detected elements, in addition to the mapping results of magnesium and calcium individually. The secondary electron picture where the mapping was performed for each individual sample can be found in the Appendix A5. The mapping analysis presented was performed on the same area as the spot analysis, and the secondary electron image also be seen in the spot analysis section within each series.

Spot analysis was performed with 4 or 3 spots for each inspection area. Spots analysis was performed prior to mapping analysis, and the spot selection was done independently from the mapping result. The weight percent of aluminium, oxygen, magnesium and calcium are tabulated for each of the different test series, as well as the spot location is shown.

The result from different inspection areas and spots between the same series varied rather much, and it is therefore emphasized that comparison should be done with care. The spot measurements are not necessarily representative for the whole surface layer either. The main objective with the investigation in the SEM was to see what the surface deposit consists of, and if there would be any noticeable differences between the series.

4.4.1 SAMPLES POLARIZED -10 MV POTENTIOSTATICALLY

Mapping results from sample 2 in series 1 (-10 mV) shows clearly that a layer containing a lot of oxygen is formed on the surface, ref. Figure 4.25. The analysis also detected some content of magnesium and calcium as can be seen in Figure 4.26 and Figure 4.27, but a lot of this seems to be found on the aluminium matrix. However, some small areas of magnesium can be seen at the surface layer as the arrows in Figure 4.26 show. The analysis also shows that there are two areas with signs of calcium on the sample, as the arrows in Figure 4.27 show.

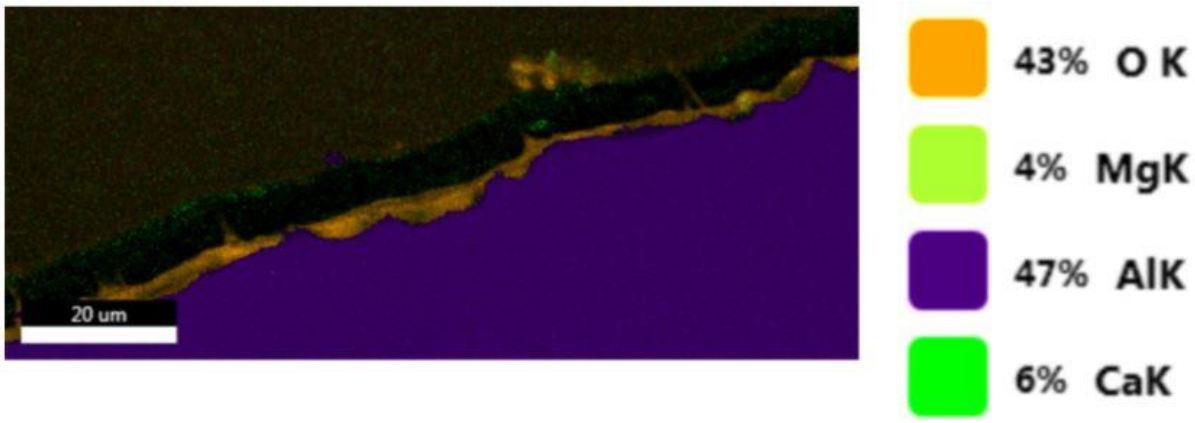

Figure 4.25: Element overlay from the cross section of sample 2 from series 1 (-10 mV, potentiostatically)

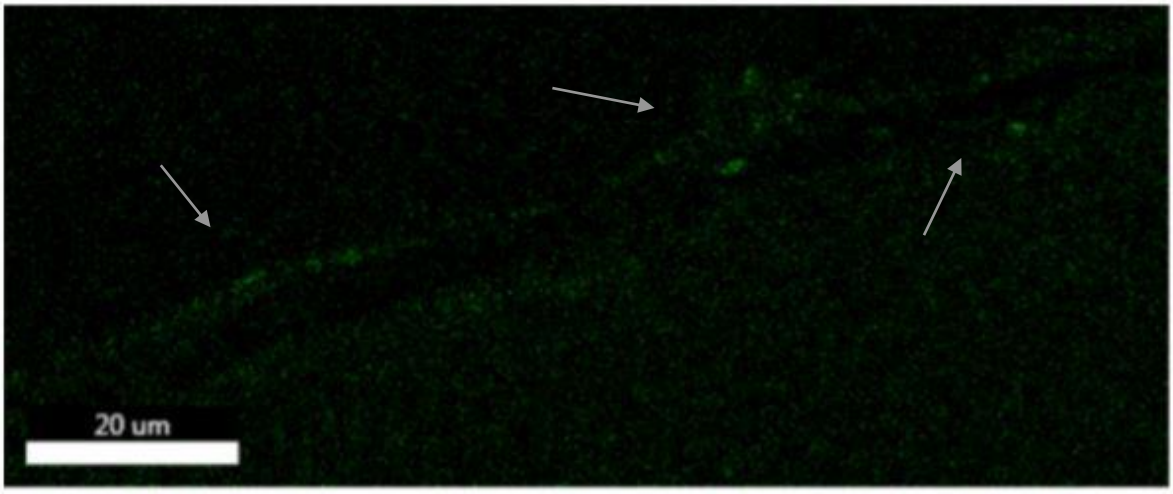

Figure 4.26: Mapping result showing the magnesium content of sample 2 from series 1 (-10 mV, potentiostatically)

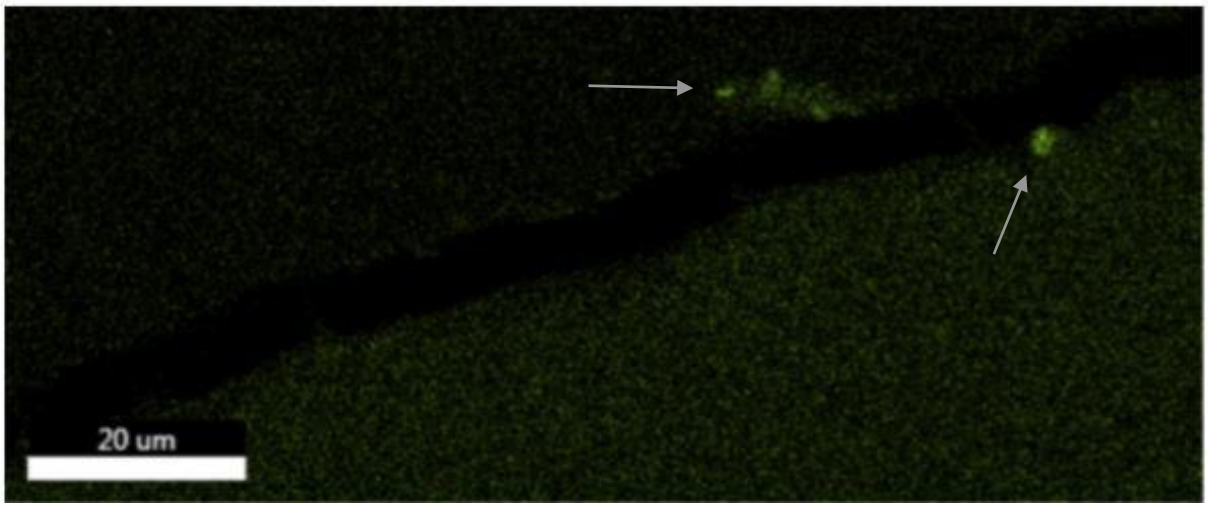

Figure 4.27: Mapping result showing the calcium content of sample 2 from series 1 (-10 mV, potentiostatically)

Results from the spot analysis show the readings vary to a large degree. As seen in Table 4.5, the results are inconsistent, but still shows that the layer that has formed on the anode surface consists of mainly aluminium and oxygen. No magnesium was found in the spot analysis, but traces of calcium can be seen. The spot locations are shown in Figure 4.28.

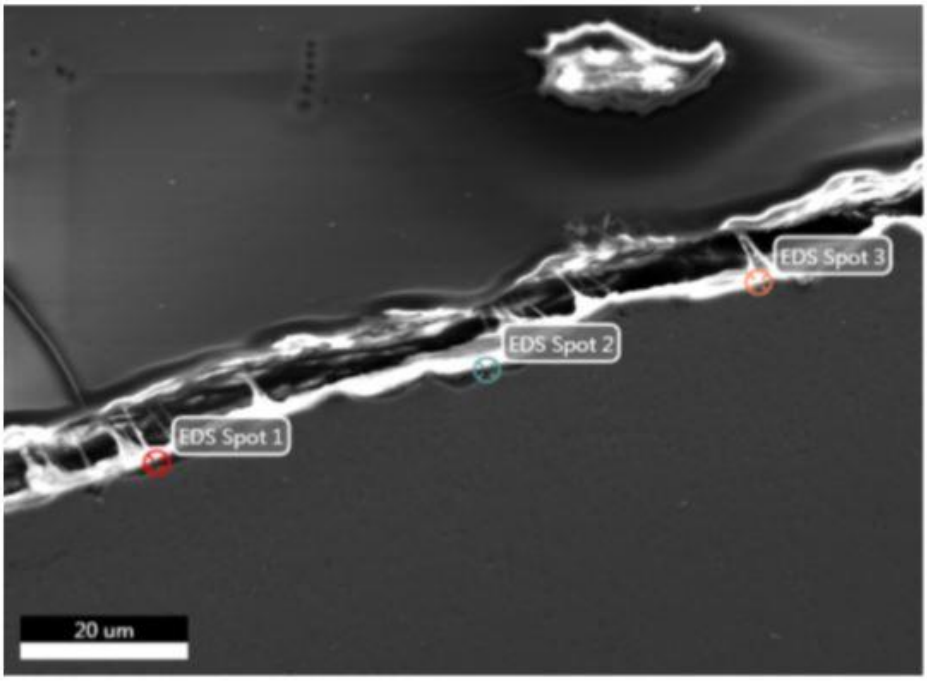

Figure 4.28: Placement of the spot analysis performed on sample 2 from series 1 (-10 mV, potentiostatically)

Table 4.5: Element weight percent of aluminium, oxygen, magnesium and calcium from the three different spot analysis

Element [wt%]	Spot 1	Spot 2	Spot 3
Aluminum	17.8	24.3	26.4
Oxygen	36.5	61.6	18.54
Magnesium	0	0	0
Calcium	1.1	2.1	0

4.4.2 SAMPLES POLARIZED -30 MV POTENTIOSTATICALLY

Clear signs of oxygen in the coating on the surface of the anode can be found for sample 5 in series 2 (-30 mV) as well, ref. Figure 4.29. Some magnesium and calcium are also present, but where these elements mainly detected in the aluminium matrix as seen in Figure 4.30 and Figure 4.31. Very little magnesium seems to be present in the coating layer, other than one area which seems to contain some magnesium which the arrow in Figure 4.30 shows. The calcium content seems to be a little more concentrated in the surface layer than rest of the aluminium matrix, ref. Figure 4.31.

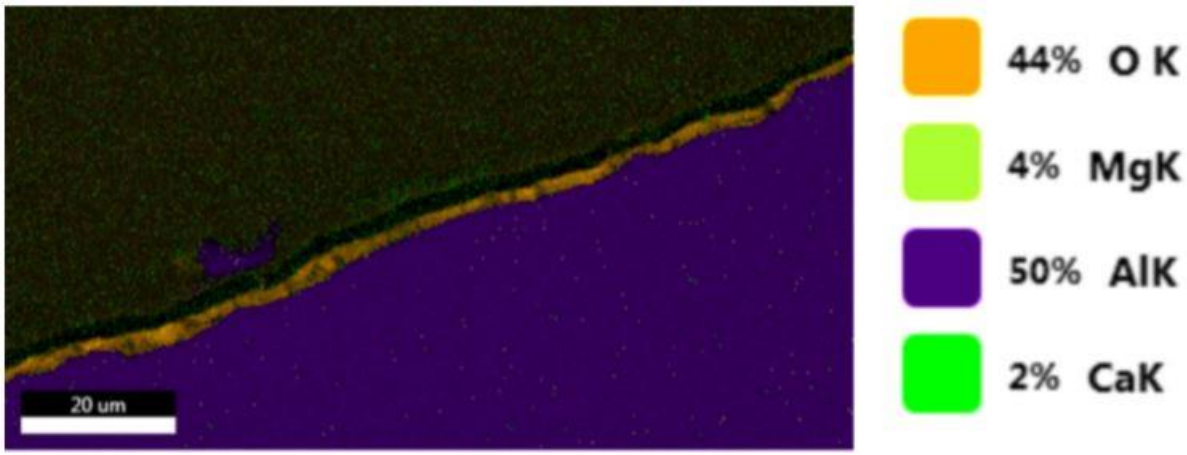

Figure 4.29: Element overlay from the cross section of sample 5 from series 2 (-30 mV, potentiostatically)

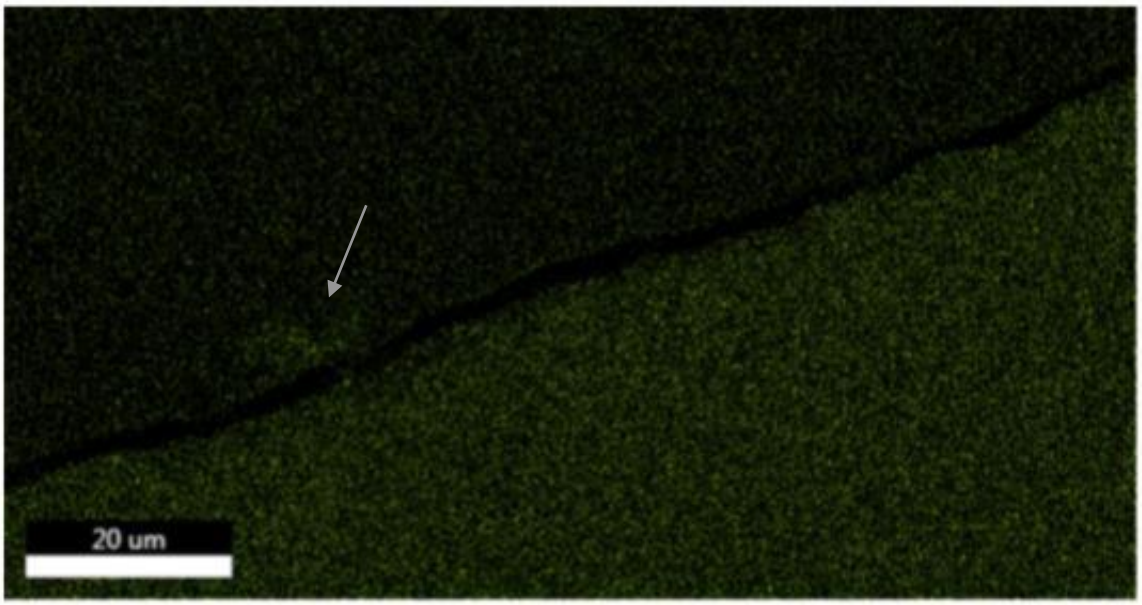

Figure 4.30: Mapping result showing the magnesium content of sample 5 from series 2 (-30 mV, potentiostatically)

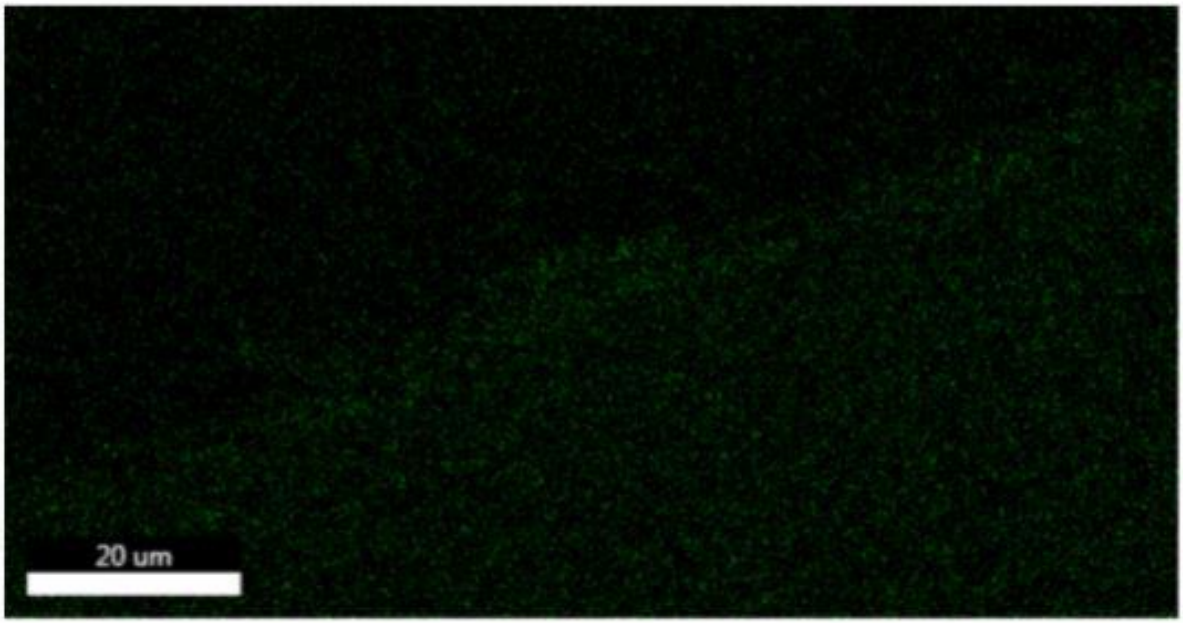

Figure 4.31: Mapping result showing the calcium content of sample 5 from series 2 (-30 mV, potentiostatically)

For series 2 (-30 mV), the spot analysis results are more uniform than for series 1 (-10 mV), ref Table 4.6 vs Table 4.5. The coating clearly consists mainly of aluminium and oxygen, but some minor content of both magnesium and calcium are found in a few of the spots, ref. Table 4.6. The spot locations are shown in Figure 4.32.

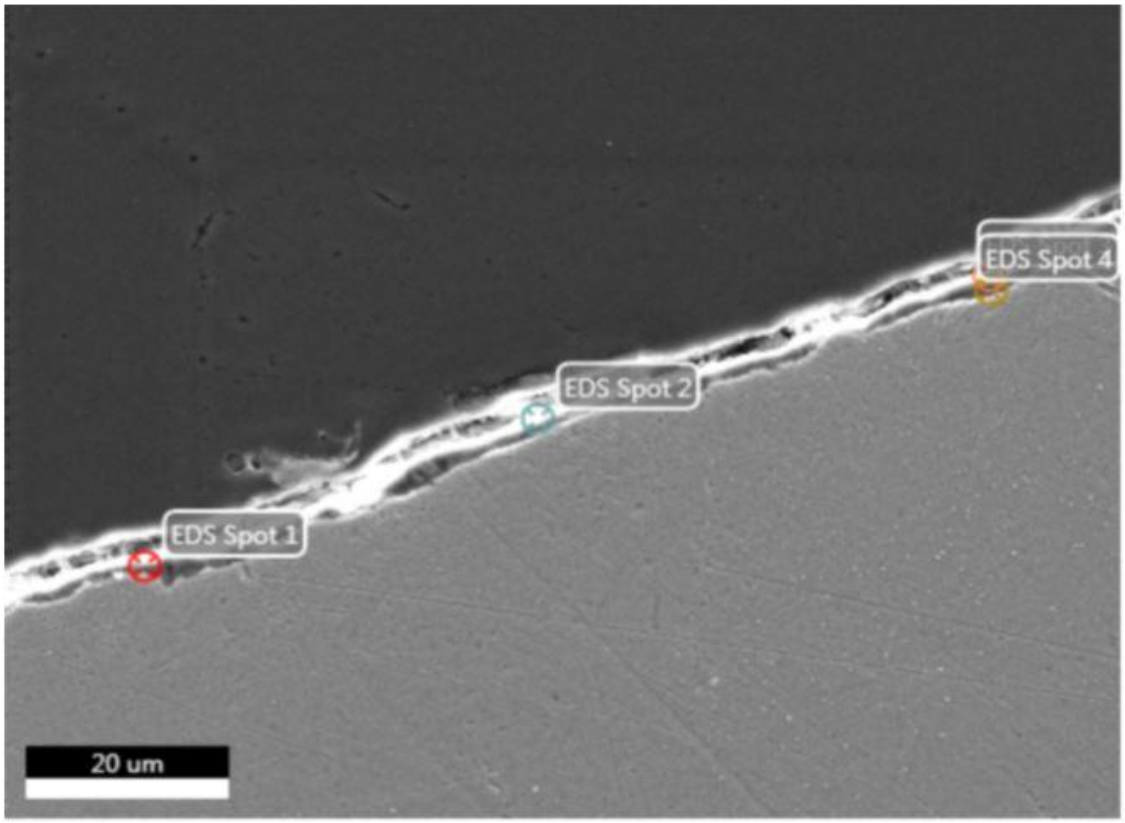

Figure 4.32: Placement of the spot analysis performed on sample 5 from series 2 (-30 mV, potentiostatically)

Table 4.6: Element weight percent of aluminium, oxygen, magnesium and calcium from the four different spot analysis

Element [wt%]	Spot 1	Spot 2	Spot 3	Spot 4
Aluminum	18.6	13.9	22.9	33.1
Oxygen	36.7	37.2	31.3	34.8
Magnesium	0	0	1.6	0
Calcium	0	0	1.5	1.7

4.4.3 SAMPLES POLARIZED -80 MV POTENTIOSTATICALLY

A thicker surface layer is observed for series 3 (-80 mV) compared to series 2 (-30 mV) and series 1 (-10 mV), ref. Figure 4.33 vs Figure 4.25 and Figure 4.29. The mapping analysis shows that the surface layer seems to mainly consist of oxygen, see Figure 4.33. The mapping analysis also shows signs of magnesium and calcium, where the findings is mainly located in the coating area as can be seen in Figure 4.34 and Figure 4.35.

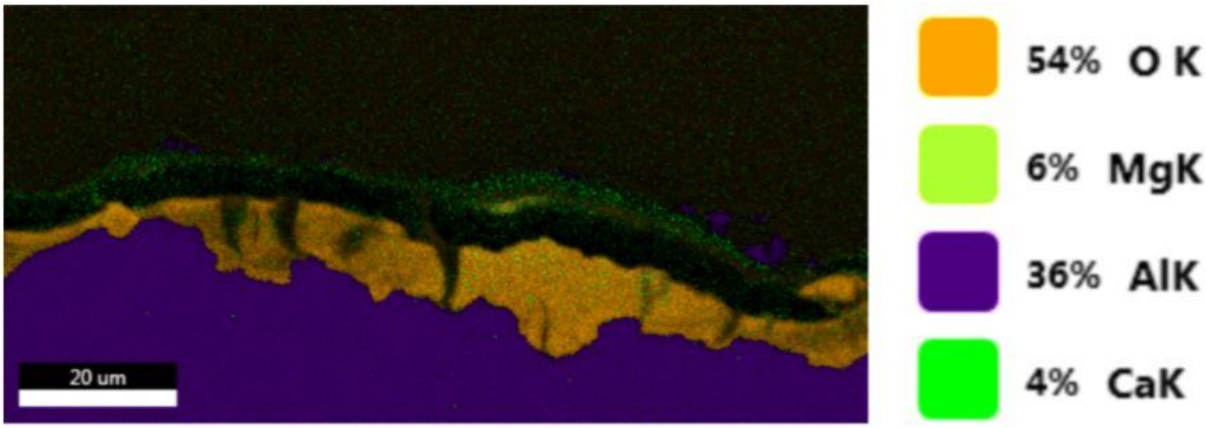

Figure 4.33: Element overlay from the cross section of sample 2 from series 3 (-80 mV, potentiostatically)

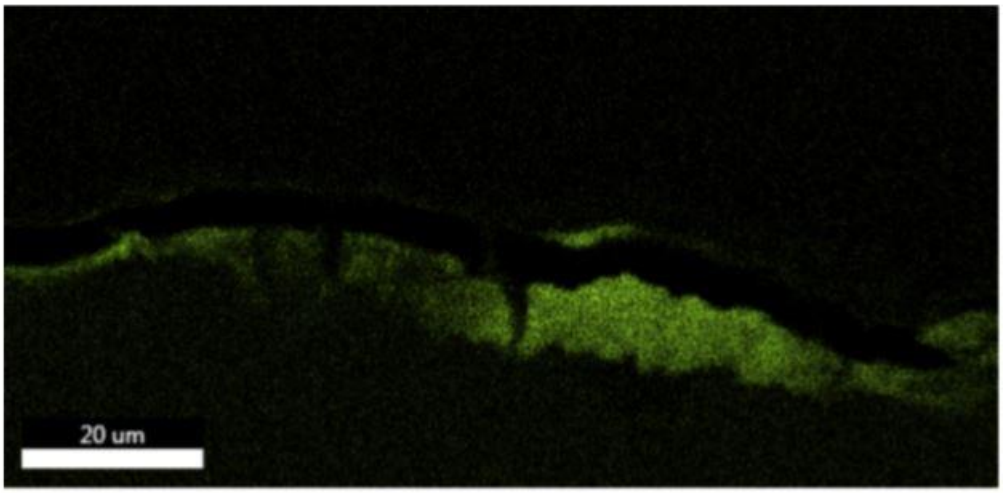

Figure 4.34: Mapping result showing the magnesium content of sample 2 from series 3 (-80 mV, potentiostatically)

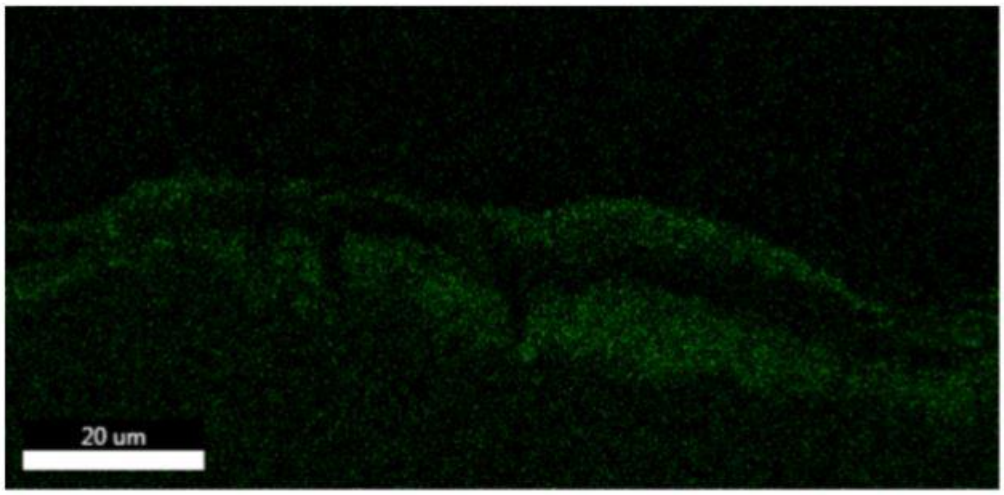

Figure 4.35: Mapping result showing the calcium content of sample 2 from series 3 (-80 mV, potentiostatically)

The results seem to vary rather much for all the elements, and it seems as if the placement of the spot analysis inside what seems to be the coating is very determinantal. Nevertheless, the spot analysis for series 3 (-80 mV) shown in Table 4.7 show that the surface layer mainly consists of oxygen and aluminium. The spot analysis also shows signs of magnesium and calcium, where the amount is larger than for the other samples, as well as the findings are more consistent, ref Table 4.7 vs Table 4.5 and 4.6. The spot locations can be seen in Figure 4.36.

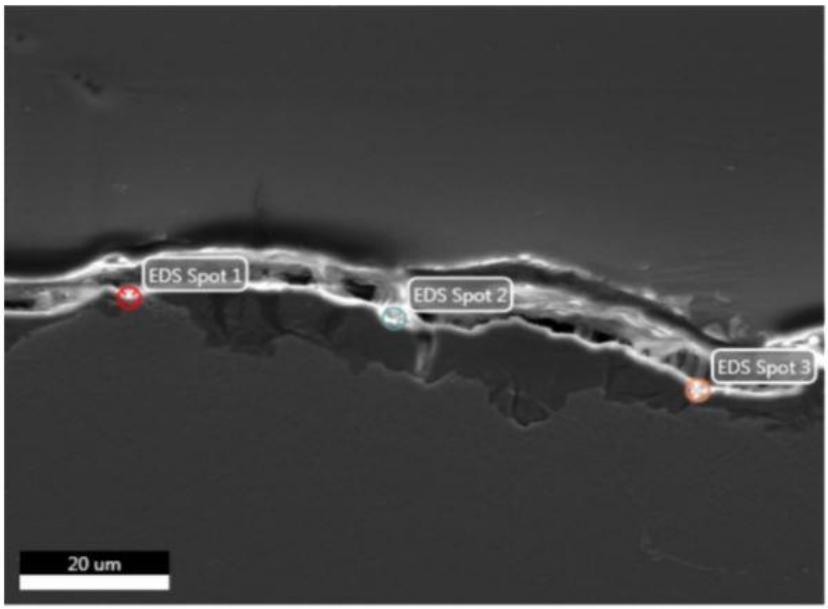

Figure 4.36: Placement of the spot analysis performed on sample 2 from series 3 (-80 mV, potentiostatically)

Table 4.7: Element weight percent of aluminium, oxygen, magnesium and calcium from the three different spot analysis

Element [wt%]	Spot 1	Spot 2	Spot 3
Aluminum	14.6	9.4	3.1
Oxygen	51.2	15.9	25.3
Magnesium	2.4	2.4	1.2
Calcium	1.3	3.9	0.4

4.4.4 SAMPLES EXPOSED AT OCP

Mapping analysis of sample 2 in series 4 (OCP) also clearly show some sort of oxide layer that has formed on the surface of the sample, ref Figure 4.37. There is some content of magnesium both in the aluminium matrix and the coating layer as shown in Figure 4.38, but it does not seem as if the amount of magnesium found on the sample matrix are more noticeable in the surface layer than rest of the sample, except for one small area where the content seem to be more concentrated which is located by an arrow in Figure 4.38. The calcium detected seems to be more concentrated around the coating layer than the rest of the sample, ref Figure 4.39.

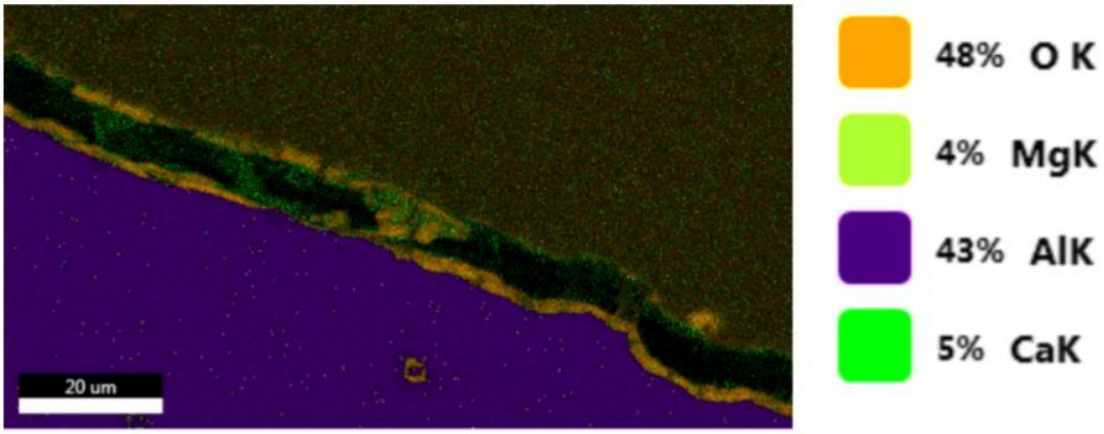

Figure 4.37: Element overlay from the cross section of sample 2 from series 4 (exposed at OCP)

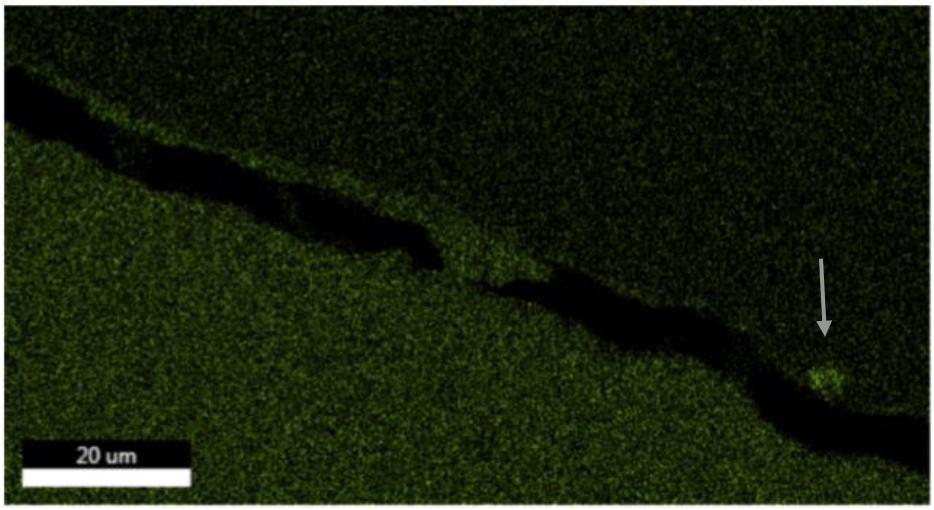

Figure 4.38: Mapping result showing the magnesium content of sample 2 from series 4 (exposed at OCP)

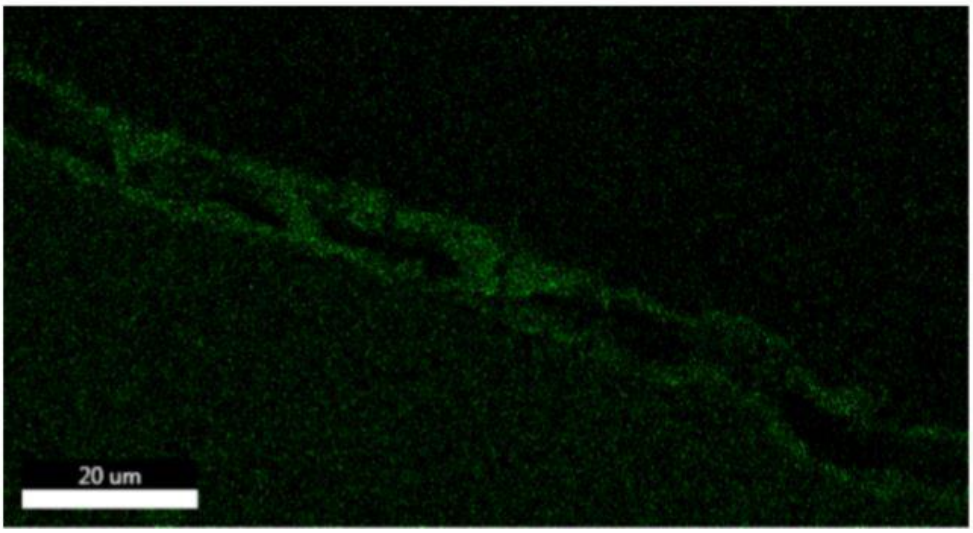

Figure 4.39: Mapping result showing the magnesium content of sample 2 from series 4 (exposed at OCP)

Two of the spots in the analysis shows zero oxygen content, ref. Table 8. This seems to be because one spots are placed between the aluminium and epoxy matrix, and the other in the aluminium matrix. The two other spot analysis shown in Table 8 reflects the mapping results (Figure 4.37), where a small detection of magnesium is found. Spot analysis also show that calcium can be found in the coating. The spot locations are shown in Figure 4.40.

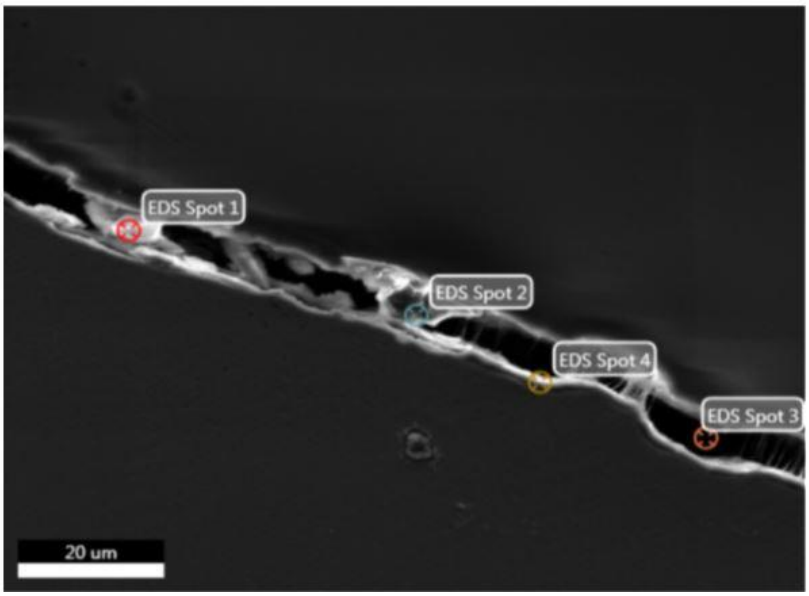

Figure 4.40: Placement of the spot analysis performed on sample 2 from series 4 (exposed at OCP)

Table 4.8: Element weight percent of aluminium, oxygen, magnesium and calcium from the four different spot analysis

Element [wt%]	Spot 1	Spot 2	Spot 3	Spot 4
Aluminum	20.5	10.3	100	14.5
Oxygen	38.5	0	0	21.9
Magnesium	0.7	0	0	0.4
Calcium	2.4	1.7	0	1.5

4.4.5 SAMPLES POLARIZED -80 MV POTENTIOSTATICALLY (NO POLARIZATION CURVE RECORDED BEFORE SEM)

Mapping analysis performed on one sample in series 3 (-80 mV), where a polarization curve was not recorded prior to inspection, gave similar results as for the sample which a polarization curve was recorded, ref. Figure 4.41 vs Figure 4.33. A clear layer of oxygen and aluminium can be seen in Figure 4.41, and a concentrated content of magnesium and calcium is also present in the coating layer, ref. Figure 4.42 and Figure 4.43. More cracks were observed in the coating layer, but this is expected to have occurred during SEM preparation.

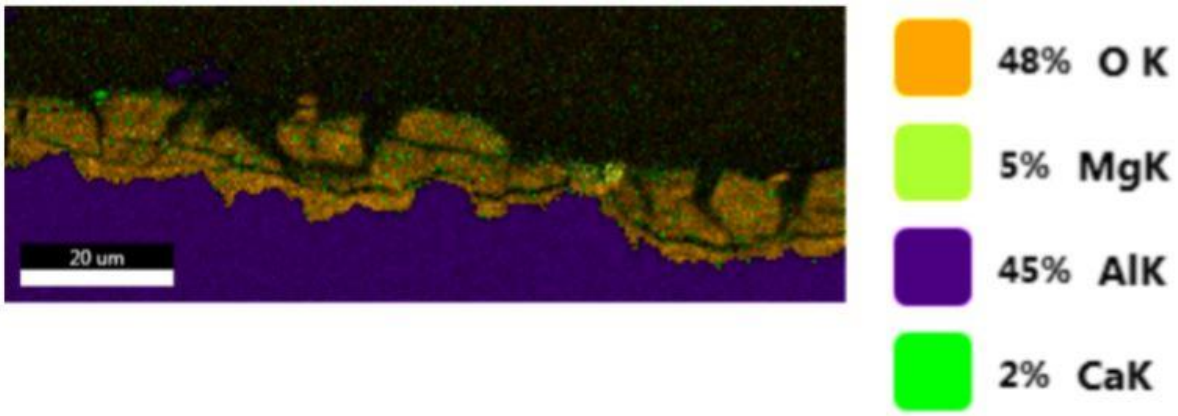

Figure 4.41: Element overlay from the cross section of sample 6 from series 3 (-80 mV, potentiostatically) – without polarization curve recorded before inspection

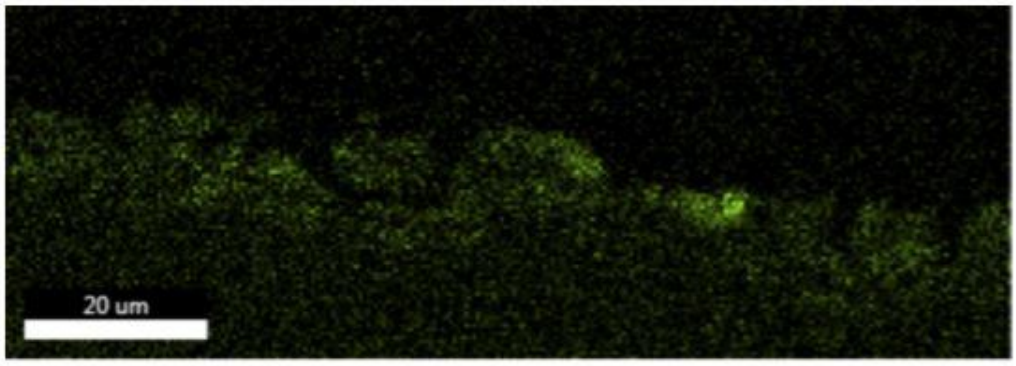

Figure 4.42: Mapping result showing the magnesium content of sample 6 from series 3 (-80 mV, potentiostatically) – without polarization curve recorded before inspection

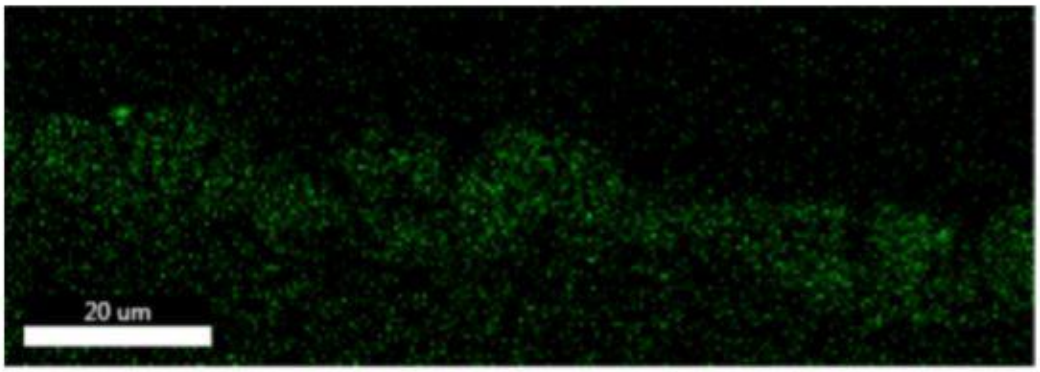

Figure 4.43: Mapping result showing the magnesium content of sample 6 from series 3 (-80 mV, potentiostatically) – without polarization curve recorded before inspection

The spot analysis results varied to a large degree, as can be seen in Table 4.9. The spot analysis results show that the calcium content is somewhat higher than for the sample that was polarized before inspection in SEM, ref. Table 4.9 vs Table 4.7. The magnesium content was approximately the same. The spot locations are shown in Figure 4.44.

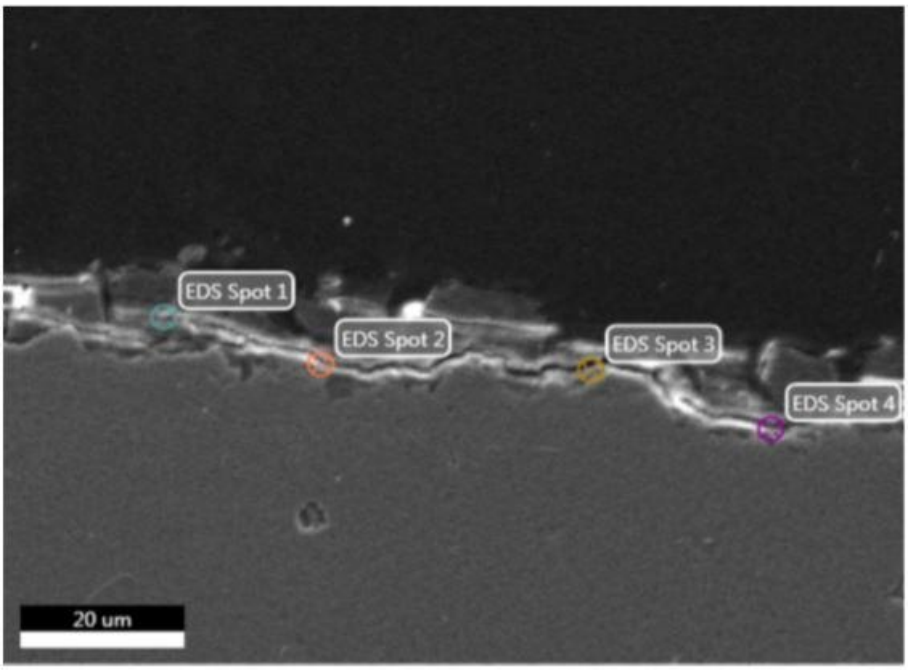

Figure 4.44: Placement of the spot analysis performed on sample 6 from series 3 (-80 mV, potentiostatically) – without polarization curve recorded before inspection

Table 4.9: Element weight percent of aluminium, oxygen, magnesium and calcium from the four different spot analysis

Element [wt%]	Spot 1	Spot 2	Spot 3	Spot 4
Aluminum	26.4	32.3	25.6	18.9
Oxygen	18.36	43.7	33.7	38.4
Magnesium	2.05	1.7	0.75	1.47
Calcium	12.48	5.1	1.82	3.5

5. DISCUSSION

5.1 CATHODICALLY POLARIZED ALUMINIUM ANODES

As the passivation of anodes is based on the possibility of a difference in operating potential between anodes, it is interesting to note from theory that very small differences in chemical composition could influence the operating potential. The requirements for the chemical composition in NORSOK M-503 also give room for variation. It is also worth noticing that the ISO 15589-2 recommended practice requires a maximum of -1050 mV_{SCE}, but no lower limit is given. The anode producer Skarpenord has stated that their quality testing has a minimum threshold of -1100 mV_{SCE}, making it theoretically possible with a potential difference of 50 mV and still satisfy the standard [8].

From the theory, other variables such as temperature, microstructure, salinity and current density can in some cases influence the operating potential, which also may result in potential differences. It should be mentioned that most of these effects most likely will never occur in reality, because the current densities are very low and variations in temperature and salinity are low. However, with these facts in mind, one could argue that it is plausible that an operating potential difference between anodes could occur on larger structures and pipelines offshore. Alloy composition differences due to variations between batches will in addition always occur at some level.

Both Lauvstad et al. and Jelinek found that the current demand design values for cathodic protection is higher than what are measured [25, 26]. Combined with Knudsen's findings, that coating breakdown also is much lower than given in the design codes, the current demand will probably be much lower than the design anticipates [2]. As cathodic protection is designed according to these very conservative anticipations, the number of anodes installed on structures and pipelines also will become very conservative. This could be why anodes without any activity were found, where the reason is that they do not have any steel to polarize. This could result in that some anodes will protect higher potential anodes on the same structure, which is the hypothesis behind this work. Hartt also concluded that partial anode passivation was the reason for an increasing steel potential in his experiments, where his conclusion substantiates this reports suspicion that very low current demand on structures could result in passivation of aluminium anodes [9].

5.2 EXPERIMENTAL METHODS FOR STUDYING PASSIVATION OF ANODES

Anodic polarization curves were recorded after all the electrochemical experiments were performed, and this method is found to give good information on passivation. The reason for this is that passive materials will have a typical anodic polarization curve. This typical passive curve will show a transition between passive and active potentials where the anodic current density rapidly increases, which is not seen in the polarization curve of active materials. By comparing the behaviour of a polarization curve of a non-exposed sample with polarization curves of exposed samples, passivation will be seen as a decrease in the current density at a given potential.

Both galvanostatic and potentiostatic experiments have been performed in this work. Experiments performed in potentiostatic mode is done by applying a constant potential difference from the reference electrode (in this case the sacrificial anode material), while the polarization current is measured. By using continuous logging, changes in current density of the anodes were observed throughout the potentiostatic experiment. A reduction in current density would mean that less current is needed to polarize the samples to the given potential difference and could indicate signs of passivation. It should also be emphasized that it is the potentiostatic experiments that are closest to realistic conditions, as this thesis' hypothesis is based on the possibility of a potential difference between anodes, and not a constant current.

It is difficult to conclude that passivation has occurred based on current density measurements during potentiostatic cathodic polarization alone. A decrease in current density at the beginning of the experiment can be observed, but it does not give any indication of the degree of passivation without further experimental evaluation. The decrease in current density that was seen at the beginning of the experiment could also probably be explained by the formation of oxides on the surface, as a result of sample surfaces being ground down and therefore the oxides removed prior to experiment exposure.

Galvanostatic experiments are carried out by applying a pre-defined constant current to the samples throughout the experiment duration and the experiment will provide potential logging during the polarization. It was difficult to find clear correlations between the potential measurements of samples during polarization and the degree of passivation. Some results indicated that samples that had a low potential drop during its galvanic polarization, experienced a larger degree of passivation, but this was not the case for all tests. As a result, polarization curves must be obtained after the galvanostatic polarization,

in order to investigate if the samples have passivated or not, and to which degree. Polarization curves after the galvanostatic experiments also showed that there were large variations in how the material reacted on the current, even though experiment conditions were identical. Some material samples did not seem to react to the cathodic polarization at all. Based on the results from the different experimental methods, it would seem as if long-term potentiostatic polarization will give better results than short-term galvanostatic polarization. It should be emphasized that the galvanostatic experiments performed were very short compared to the potentiostatic experiments and that there is no basis to exclude long-term galvanostatic experiments for further work.

Optionally, LPR measurements with fixed intervals throughout the experiment to observe trends in corrosion rate and comparing it with the corrosion rate of a non-exposed sample may also reveal passivation, by showing a decrease in corrosion rate. If passivation has occurred, a decrease in corrosion rate is expected because some kind of physical barrier most likely is involved in the passivation process, which will affect the corrosion rate. However, corrosion rate seems to not be largely affected by the different cathodic polarization performed in this thesis. Even though other results showed that less anodic current was needed to anodically polarize the samples up to a specific potential, and thereby appeared passive in this manner, the corrosion rate measurements seemed very little affected. LPR results performed on the long-term experiment also show that such measurements vary to a large degree and seems to be difficult to use for comparing, because the variations for the same series could be larger than the difference between series. A clear decrease in corrosion rate from non-exposed samples to all exposed samples could be seen, but this does not seem to provide any information regarding passivation. Based on the results, corrosion rate measurements do not seem to be a good method for investigating passivation in further work.

Polarization curves seem to give the most accurate indication of both passivation and the degree of passivation. These results showed differences between samples galvanostatically polarized with varying durations, as well as a difference compared to non-exposed samples. Polarization curves from the long-term experiment also gave clear results in comparison with non-exposed samples, as well as between the different series. Polarization curves will also provide information regarding the potential which the sample will reactivate. However, results showed that the polarization curves did vary to some degree, where the reason for this is not known. It is also difficult to say if these variations are caused by the potentiostatic/galvanostatic treatment or by the polarization curve recording itself. The polarization

curves from the potentiostatic experiment seemed to vary the least, indicating that long-term potentiostatic polarization will give results with less variations. It should be noted that as polarization curves are recorded, the sample has most likely been polarized to such a degree that the experiment can be terminated, and this kind of analysis can only be performed at the end of the experiment.

5.3 EFFECT OF CATHODIC POLARIZATION

Most of the current density measurements for Series 1-3 are all showing some indications of decreasing current density for the first 40 days. Compared to the initial current density, most of the current density measurements decreased, which could indicate that samples were passivated to some degree. Based on current density measurements it is difficult to say if the passivation process continues throughout the whole experiment, as the change in current density slows down after the 40 days, especially for series 1 (-10 mV) and 2 (-30 mV). Series 1 (-10 mV) shows a slightly reverse change in current density after 40 days, which also could mean that the series passivation process was reversed towards the end of the experiment, although this is hard to conclude. As series 3 (-80 mV) experienced a decrease in current density throughout the whole experiment, it could indicate that these samples were increasingly passivated for the entire experiment duration, which also could explain why these samples seem to be most passivated from the polarization curves. It should be mentioned that these samples are expected to be the most passivated because they were polarized to the lowest potential.

Results showed variation in the current density measurements in the same series during the long-term potentiostatic experiment. The reason for these current density variations could be that for aluminum, the cathodic reaction mainly occurs on noble intermetallic particles such as Fe and Cu. As a result, the cathodic current will be dependent on the concentration of these particles in the surface, which could cause the cathodic current to vary because of variations in the amount of noble intermetallic particles present in the surface. Even though current density measurements seemed to vary quite much, the individual measurements do not seem to correlate to how the polarization curves behave. The polarization curve of samples that logged a higher current density throughout the experiment did not directly behave differently than samples that logged a lower current density. It could, therefore, seem as it is the change in current density that determines the degree of passivation rather than the actual current transfer throughout the experiment.

The polarization curves obtained after the long-term experiment substantiates the observations from the current density logging. Series 3 (-80 mV), which experienced a decrease in current density the whole experiment clearly is the most passivated samples as they generally show the lowest anodic current density compared to the non-exposed samples. Results show that the reduction in anodic current density is dependent on the long-term cathodic polarization, where the current density decreases as cathodic polarization increases. However, the activation potential does not change between the series and appears to be independent of the degree of polarization.

Samples from series 1 (-10 mV) and series 2 (-30 mV) seem to be similarly passivated from the polarization curves. The current density at the activation potential was a little lower for series 1 (-10 mV) than for series 2 (-30 mV). This was not expected considering the lower polarization of series 1 (-10 mV), but the difference is not significant, and it could appear that the samples react approximately similar to polarization to -10 mV and -30 mV vs OCP, as the polarization curves vary similarly. This indicates that even small potential differences can passivate samples to some degree, where it seems as if realistic potential difference will give approximately the same degree of passivation. In realistic conditions, anodes could be subjected to this kind of polarization for a much longer duration than what tested in this experiment because of long lifetime on offshore structures or pipelines. This combined with results from the galvanostatic experiments where duration seems to be directly correlated to the degree of passivation, it could be reason to believe that substantial passivation could occur from small potential differences. The current density measurements for series 1 (-10 mV) could seem to have more variations than for series 2 (-30 mV), which possibly could have affected the unexpected order of current density at the activation potential from the polarization curves.

The polarization curves of samples only exposed at OCP did also show a typical passive-active transition, where an activation potential also could be seen. Samples also had a decrease in current density compared to the non-exposed samples, but both to a lesser degree than the cathodically polarized series. The signs were most clear for the OCP exposed samples from the long-term experiment, indicating that passivation for samples exposed at OCP is dependent on exposure duration. This points towards that all samples included in the experiment experience some degree of passivation, but that the cathodic polarization accelerates the process. Samples exposed at OCP has a little lower activation potential than the polarized samples.

Most of the polarization curves recorded after the galvanostatic experiments show signs of passivation compared to the reference samples included in the experiment. Some samples seem unaffected by the cathodic polarization, which was unexpected. Polarization curves from the two-day experiment showed that the anodic current density at the activation potential was highest for the samples exposed for the shortest duration. The current density at the activation potential was lower for the five-day experiment than for the ten-day experiment, but the difference was not significant. However, for the ten-day experiment, the galvanostatic polarization seems to have increased the open circuit potential around 100 mV, where the same change occurred for the reactivation potential. As polarization curves from the potentiostatic experiment indicate that the reactivation potential is constant, this increase in potential is unexpected. Nevertheless, the results tell us that the degree of passivation seems to increase as galvanostatic experiment duration increases, at least from the two-day experiment compared to the longer durations. Results show large variations, but it still seems as if the degree of passivation is directly correlated to experiment duration.

Some test from the galvanostatic experiments showed that samples with the lowest potential during the experiment showed the most sign of passivation. These results could indicate a correlation between the degree of passivation and potential variation during the galvanostatic polarization, where the degree of passivation is dependent on how far from OCP the potential drops. The samples which did not seem to react to the galvanostatic polarization was also observed to have the least change in potential during the experiment, supporting this theory. However, it should be mentioned that this was not the case for all results and that samples with similar potential measurements had very different polarization curves.

When comparing the polarization curves of samples exposed at OCP during the galvanostatic experiments with polarization curves of non-exposed samples, the small difference indicates that samples do not need to be cathodically polarized in order to show signs of passivation. The difference is very small, but all polarization curves show slightly less current density at a given potential compared to the non-exposed sample. This supports the findings from the potentiostatic experiment, where all samples seem to be passivated to some degree as a result of being exposed at OCP, but that the cathodic current accelerates the passivating process.

The LPR corrosion rates seem to be approximately similar for all the long-term samples at both 27 and 120 days but are all drastically decreased compared to the corrosion rate of a non-exposed sample. Corrosion rate results do not give any clear trend between the series. One difference that is seen if the small difference is considered, is that the corrosion rate in general decreases to some degree from 27 days to 120 days, but the different series does not decrease similarly. These results could indicate that the samples have increased the degree of passivation from 27 days to 120 days. However, the variations between the series are rather large, which makes this difference is less reliable.

Variations in LPR corrosion rate measurements within the series that only were exposed at OCP are close to the same magnitude as variations between the four series. This could indicate that these kinds of variations should be expected and that differences of a few µm/year not necessarily are of significance. It could also mean that corrosion rate measurements are not suited for evaluation of passivation, as previously mentioned. The results indicate that the same degree of reduction in corrosion rate occurs for both samples cathodically polarized and exposed at OCP. As the polarization curves indicate differences between the series, LPR results indicate that the degree of cathodic polarization seems to have very little impact on corrosion rate and that this method does not give information regarding the degree of passivation. The corrosion rates for the non-exposed samples also vary to a large degree, but the general difference between corrosion rate of these samples compared to the samples from the long-term experiment are at a much larger magnitude than the variations between the series. This tells us that the corrosion rate decreases for all samples after exposure to the long-term experiment, but without giving any information across the series.

The lowest potential used in the long-term experiment is not realistic. These samples clearly gave the highest degree of passivation, as expected. The results from the two other series polarized to realistic cathodic potentials were as previously mentioned more similar, where it could appear as if both potential differences gave approximately the same degree of passivation. This indicates that the degree of passivation is independent of the potential difference as long as it does not exceed -30 mV, which is realistic. This could mean that very low potential differences could give the same results as maximum realistic potential differences. Results did show that the degree of passivation increases when the cathodic polarization is performed with unrealistically high potential differences.

5.4 PASSIVATION MECHANISM

Experiment results show that cathodic polarization seems to result in varying degree of passivation. For aluminium, passivation is generally caused by Al_2O_3, but the aluminium anodes tested are alloyed in order to prevent this passivation layer. The previously mentioned hypothesis is that cathodic polarization will cause passivation as a result of either the formation of Al_2O_3, or because of calcareous deposit formation. Traces of calcareous deposits are found on sample surfaces, but the amount of aluminium and oxide found are substantially higher, which indicates that it is the formation of Al_2O_3 that is causing the passivation. The same has previously been found by Knudsen in one of his papers, where he concluded that very little calcareous deposits were formed on the surface of cathodically polarized TSA. He also found that a layer of aluminium oxide was formed on the surface, which supports the findings in this thesis [31].

The reason why it is belived that calcareous deposits will form on the surface of the aluminium anodes is that this occurs for cathodically polarized steel structures. The typical current density for steel where calcareous deposits are formed is around 100 mA/m^2, which are somewhat higher than for the current densities that the samples in this thesis will experience. Series 1 (-10 mV) and 2 (-30 mV) experiences a lot lower current density, where it is below 10 mA/m^2 during the whole experiment for most samples. Series 3, which is subjected to a -80 mV potential differences shows a current density around 50 mA/m^2 during most of the experiment. One source also states that calcareous deposits will form on all metals that are cathodically polarized and exposed to seawater, no matter the degree of protection [28]. Based on this is it reason to believe that a calcareous layer could be formed on the aluminium surface and possibly contribute to passivating the sample, especially for experiments subjected to the highest polarization. This should mean that the corrosion rate would decrease as the degree of cathodic polarization was increased. If the small differences in the corrosion measurements could be trusted, the results from the first LPR measurement showed the opposite. Results from the second LPR gave results which were more as expected, where the OCP samples had the highest corrosion rate and the samples induces with the largest potential difference had the lowest.

Additionally, literature states that cathodic polarization can promote cathodic corrosion and it could be this phenomenon that explains the unexpected development in corrosion rate after 27 days [4]. Even though calcareous deposits or some kind of passivating layer may have been formed, the increased corrosion rate caused by cathodic corrosion may be larger than the possible reduction in corrosion rate

caused by the passivating layer. The difference in corrosion rate between series is as mentioned very small. However, the polarized samples showed after 27 days, a minor trend of higher corrosion rate than samples exposed at OCP, where it could seem as if increased cathodic corrosion is a possible explanation. Mapping from the SEM also shows that some small traces of calcareous deposits can be found at samples exposed at OCP as well, which could explain the reduction in corrosion rate on this series. Calcareous deposit formation on a sample which was not cathodically polarized was not expected, but the amounts are very small.

The first 27 days, the current density measurement of the long-term experiment was in general higher than for the rest of the exposure. This could possibly have caused cathodic corrosion to be more severe in the experiment beginning, while it decreases throughout the experiment as the current density decreased. This would also explain why the corrosion rate measurements are reduced after 120 days and are more as expected in the last corrosion rate measurement.

Results from the SEM shows some traces of calcareous deposit formation on all samples which was investigated, but that the surface layer mainly consists of aluminium and oxygen. The difference between the series does not seem to be significant, other than for the samples subjected to -80 mV vs OCP. The layer which is formed on the samples subjected to the highest potential difference is clearly thicker than for the rest of the samples. Results seem to vary quite much between different areas on the same sample, indicating that precise comparison between series should be performed with caution.

The spot analysis supports the mappings results and shows that the calcium and magnesium content are in general rather low and that the coating layer mainly consists of oxygen and aluminium for all series, which substantiates Egtvedt's, Knudsens and Gundersen and Nisanciogli's studies [29-31]. This indicates that it is a layer of aluminium oxide that causes the passivation, and not a calcareous layer. As mentioned, the aluminium oxide layer that can be seen on the series exposed at the lowest potential is also clearly thicker than for the rest of the samples. Since this series was the one that was most passivated, it supports the theory that it is the aluminium oxide that mainly causes the passivation.

Unexpectedly it would appear that series 4 (OCP) has grown close the same surface layer as series 1 (-10 mV) and 2 (-30 mV), where it actually seems as if there is more calcium present on the series which was exposed at OCP. Based on literature regarding calcareous deposit formation, this was unexpected as it is

believed that calcareous deposits are formed as a result of cathodic protection. Polarization to - 80 mV vs OCP is clearly found to have the most amount of both calcium and magnesium, which matches the expectations since this sample has been subjected to the highest cathodic polarization. However, the amounts are as previously mentioned rather small, indicating that these deposits do not contribute much to passivating the samples. Results show that some sort of layer mainly consisting of oxygen and aluminium is grown on all samples, where the formation process seems to be accelerated by the high cathodic polarization on series 3 (-80 mV). The high amount of magnesium found in series 3 (-80 mV) compared to the other series, indicates that the other series has not been in a pH range which allows precipitation of magnesium hydroxide.

The oxide layer that is formed on samples does not seem to change noticeably from obtaining anodic polarization curves. Since the comparison method is based on visual differences, it is difficult to conclude how much impact anodic polarization has. It could seem as if there is slightly more calcium present prior to anodic polarization, indicating that some calcareous deposit will dissolve during the polarization. However, the visual differences of the oxide layer between the two mapping results before and after anodic polarization does not seem to be significant, even though the sample appears to be reactivated after the anodic polarization. This indicates that the SEM analysis performed on samples that have been anodically polarized will give similar results as for the analysis performed on samples which have not been used for recording polarization curves prior to inspection.

5.5 REACTIVATION

Since the anodic current of the polarization curves increases rapidly after reaching a certain potential, it seems as if the passivated samples will reactivate at a certain level of anodic polarization. The potential where samples appear to reactivate seems not to be greatly dependent on the degree of passivation, as the interval of reactivation is around -900 $mV_{Ag/AgCl}$ and -950 $mV_{Ag/AgCl}$ for most of the samples, both in the potentistatic and the galvanostatic experiment. At this potential, the current density increases rapidly. The exception is the galvanostatic experiment with the longest duration, where both the open circuit potential and the reactivation potential has been increased approximately by 100 mV for two of the samples. There is no obvious explanation for this, and the results contradict the results from the potentiostatic experiment, as these results indicate that the reactivation potential is approximately the same for all potential differences.

In general, the reactivation potential does not seem to change considerably across the series, even though the degree of passivation seemed to increase. This would imply that the reactivation potential always will be more negative than the typical protection potential of bare steel, at least for the experiment duration and degree of passivation in this experiment. This will most likely mean that if anodes are passivated to a certain degree and some steel starts requiring cathodic protection, the steel potential will reactivate the anode causing it to start protecting the steel before the steel reaches an actively corroding potential. The explanation for this is that if the anode is passivated, it will not manage to polarize the steel. The potential between the two metals will then be decided by the steel because there is no current density from the anode, and if the steel potential becomes more positive, the anode will be polarized anodically until it reactivates.

The samples which were polarized at a slower rate indicates that slower polarization speed makes the samples reactivate at a more negative potential. In general, samples most likely reactivate because the anodic polarization breaks down the coating layer that was formed as a result of the cathodic polarization. The samples subjected to a slower polarization speed showed less sign of passivation compared to the normal polarization speed. The reason for this is probably that the slowed down polarization speed will decrease the pH more than the rapid anodic polarization. An increase in anodic current will increase formation of the Al^{3+} ions which will react with water and cause acidification [35]. As the pH is decreased, it will affect the breakdown mechanism of the passivation layer. When the samples were polarized at a slower speed, the formation of Al^{3+} ions was probably increased at a given potential compared to the normal speed. This will cause a larger decrease in pH, and thereby breaking down the coating layer at a higher speed. These results could indicate that anodes will reactivate at a lower potential if exposed to a higher potential for a longer duration.

The sample which was polarized several times showed that sample 3 from series 3 (-80 mV) seems to be reactivated after one polarization to -600 $mV_{Ag/AgCl}$. After the first polarization curve was recorded, the rest of the polarization curves look similar to the polarization curve of a non-exposed sample. This indicates that the passivation obtained after the potentiostatic experiment is reversed after one reactivation and that the sample is permanently reactivated.

5.6 FURTHER WORK

The galvanostatic experiment, as well as one of the potentiostatic series, were performed with current corresponding to unrealistically high cathodic polarization, where this was done in an attempt to accelerate the passivation process. Results indicated that these samples were more passivated than samples exposed to a realistic potential difference. However, these results do not give any indications regarding if samples subjected to a lower potential will become passivated to the same degree if the exposure duration is long enough. It would be of interest to perform experiments with less polarization for a longer duration and compare these to the experiments done at higher galvanostatic current or polarization for a shorter duration. If results were similar, it confirms that accelerated experiments with higher galvanostatic current would give an accurate result for realistic potential differences at longer durations.

As galvanostatic experiments only were performed at short durations, it would be interesting to perform long-term experiments with small amounts of galvanostatic current in order to compare the results of potentiation and galvanostatic experiments more directly.

It would be interesting to know if the passivation of samples converged against a maximum degree of passivation and if the degree was dependent on the amount of cathodic polarization. One way to further investigate this would be to systematically perform several experiments with realistic values at different variations. One option could be to perform cathodic polarization with a potential difference of e.g. -10 mV for 1 day, 2 days, 3 days and so on up to e.g. 20 days. The polarization curves from these results could then be combined, where the results hopefully could show a maximum degree of passivation that the samples were converging against.

Experiments performed in this thesis is based on the hypothesis of cathodic polarization, and the difference is held constant throughout the experiment. It would be interesting to connect one or several anodes to another anode which is known to have a lower potential while observing how the anodes will behave. If such an experiment is performed, it would investigate the theory of the thesis more practically, more than only in theory.

6. CONCLUSION

It has been attempted to passivate aluminium anodes by performing potentiostatic experiments with different cathodic potentials and galvanostatic experiments with varying experiment duration. Passivation has been evaluated by current density measurements, corrosion rate measurements and polarization curves. Some exposed samples have been further investigated in the SEM in order to inspect what causes the passivation. The following conclusions have been drawn from the results:

- Long-term potentiostatic experiments seem to be the best methods to study passivation, where polarization curves seem to be the best method for evaluating whether passivation has occurred, the degree of passivation and at what potential the anode will reactivate. Short-term galvanostatic experiments also are found to be a useful polarization method but give results with more variations.
- The potentiostatic experiments indicate that small amounts of anodic current are required to polarize samples up to potential between -900 $mV_{Ag/AgCl}$ and -950 $mV_{Ag/AgCl}$, which indicate partial passivation. The samples subjected to the highest cathodic polarization gave the lowest current density when polarized anodically, i.e. the most passive behaviour.
- Based on the polarization curves obtained after galvanostatic polarization, an indication of anode passivation was found, where the degree of passivation increases with longer experiment duration.
- LPR corrosion rate measurements were independent of cathodic polarization in the potentiostatic experiments but showed a decrease compared to non-exposed samples. LPR does not seem to be a good method for further investigating of passivation.
- Traces of magnesium and calcium were found on the anode surface, but the amounts were very low. The layer that is formed on the sample surface mainly consisted of oxygen and aluminium, indicating that it is aluminium oxide or hydroxide that is causing the passivation.
- Most of the partly passivated samples seemed to reactivate between -900 $mV_{Ag/AgCl}$ and -$950_{Ag/AgCl}$ mV, all well above the actively corroding potential of steel. The material is permanently activated after polarization once more positive than this potential.

REFERENCES

1. NORSOK, *M-503*, in *Cathodic Protection*. 1994.

2. Knudsen, O. and U. Steinsmo, *Current Demand for Cathodic Protection of Coated Steel - 5 Years Data*. 2018.

3. Gibson, G., *Behavior of Al-Zn-In anodes at elevated temperature*, in *CORROSION 2010*. 2010, NACE International: San Antonio, Texas. p. 31.

4. Moon, S.M. and S.I. Pyun, *The corrosion of pure aluminium during cathodic polarization in aqueous solutions.* Corrosion Science, 1997. **39**(2): p. 399-408.

5. Werenskiold, J.C. and H. Osvoll, *New tool for CP inspection*, in *Eurocorr*. 2014. paper no. 7746.

6. Gro Lauvstad, *FORCE Technology, Personal communication*. 2018.

7. ISO, *ISO 15589-2*, in *Petroleum, petrochemical and natural gas industries -- Cathodic protection of pipeline transportation systems -- Part 2: Offshore pipelines*. 2012.

8. Ulf A. Aspaas, *Skarpenord, Mail communication*. 2018.

9. Hartt, W.H., *2012 Frank Newman Speller Award: Cathodic Protection of Offshore Structures—History and Current Status.* CORROSION, 2012. **68**(12): p. 1063-1075.

10. Heggseth, A., *Passivation of aluminium sacrificial anodes*. 2018, NTNU.

11. Ferdian, D., et al., *Development of Al-Zn-Cu Alloy for Low Voltage Aluminum Sacrificial Anode.* Procedia Engineering, 2017. **184**: p. 418-422.

12. Shibli, S.M.A. and V.S. Gireesh, *Activation of aluminium alloy sacrificial anodes by selenium.* Corrosion Science, 2005. **47**(8): p. 2091-2097.

13. Asmara, Y.P., et al., *Improving Efficiency of Aluminium Sacrificial Anode Using Cold Work Process.* IOP Conference Series: Materials Science and Engineering, 2016. **114**(1).

14. Attanasio, S.A., J.N. Murray, and R.A. Hays, *Non-Uniform Electrochemical Behavior of Indium-Activated Aluminum Alloy Anodes*, in *CORROSION 96*. 1996, NACE International: Denver, Colorado. p. 18.

15. Idusuyi, N. and L. Oluwole, *Aluminium Sacrificial Anode Activation – A Review*. Vol. 2. 2012. 561-566.

16. Zazoua, A. and N. Azzouz, *An investigation on the use of indium to increase dissolution of AlZn anodes in sea water*. Vol. 29. 2008. 806-810.

17. Bessone, J.B., *The activation of aluminium by mercury ions in non-agressive media.* Corrosion Science, 2006. **48**(12): p. 4243-4256.

18. B.M. Ponchel, R.L.H., Jr, *Performance of Al-Zn-Sn Alloy Anodes in Seawater Service.* 1968.

19. Ponchel, B.M.a.H., L., *Materials Protection.* 1968. **7**: p. 33.

20. Francis, P., *Cathodic Protection.* National Physical Laboratory, disponível em: http://www. npl. co. uk/lmm/corrosion_control, acedido em Abril de, 2007.

21. Svartdal, T., *Performance Testing of Sacrificial Aluminum Anode Alloys - What Can be Concluded*. 2000.

22. Salinas, D.R., S.G. García, and J.B. Bessone, *Influence of alloying elements and microstructure on aluminium sacrificial anode performance: case of Al–Zn.* Journal of Applied Electrochemistry, 1999. **29**(9): p. 1063-1071.

23. Murai, T., Tamura, Y., and Miura, C., *Chemsa, 5 , p 11.* 1978.

24. Scrieber, C.F.a.M., R.W, *Materials Performance, 20, page 19.* 1981.

25. Jelinek, J., et al., *Current density surveys for optimizing offshore anode retrofit design*. Vol. 35. 1996.

26. Lauvstad. G.Ø, O.H., Werenskiold. J, Helgesen.L, *Field Graient Survey of Offshore Pipeline Bundles affected by Trawling.* 2016.

27. Solis, J.L. and J. Genesca, *Effect of calcareous deposit formation on galvanic anode cathodic protection of steel in seawater*. 2009.

28. Yang, Y., J. David Scantlebury, and E. Victorovna Koroleva, *A Study of Calcareous Deposits on Cathodically Protected Mild Steel in Artificial Seawater*. Vol. 5. 2015. 439-456.

29. Gundersen, R. and K. Nisancioglu, *Cathodic Protection of Aluminum in Seawater.* Corrosion, 1990. **46**(4): p. 279-285.

30. Egtvedt, S., *Thermally Sprayed Aluminum (TSA) with Cathodic Protection as Corrosion Protection for Steel in Natural Seawater: Characterization of Properties on TSA and Calcareous Deposit*, in *Department of Materials Science and Engineering*. 2011, Norwegian University of Science and Technology.

31. Knudsen, O., et al., *Corrosion of Cathodically Polarized TSA in Subsea Mud at High Temperature*. Vol. 72. 2014.

32. van de Ven, E.P.G.T. and H. Koelmans, *The Cathodic Corrosion of Aluminum.* Journal of The Electrochemical Society, 1976. **123**(1): p. 143-144.

33. Scully, J.R., *Polarization Resistance Method for Determination of Instantaneous Corrosion Rates.* CORROSION, 2000. **56**(2): p. 199-218.

34. Gamry, *Calculation of corrosion rate, https://www.gamry.com/Framework%20Help/HTML5%20-%20Tripane%20-%20Audience%20A/Content/EFM/Introduction/Calculation%20of%20Corrosion%20Rate.htm.*

35. Saukkoriipi, J. and K. Laasonen, *Theoretical Study of the Hydrolysis of Pentameric Aluminum Complexes*. Vol. 6. 2010.

APPENDIX

A1 CALCULATED SURFACE AREA FOR SERIES 1-5.

As surface area was calculated, the top surface that was isolated with silicone was withdrawn from the calculations.

Table 1: Surface area series 1

Series 1	
Sample	Area
1	15.1 cm^2
2	13.7 cm^2
3	15.0 cm^2
4	14.5 cm^2
5	13.8 cm^2
6	15.1 cm^2

Table 2: Surface area series 2

Series 2	
Sample	Area
1	13.7 cm^2
2	14.5 cm^2
3	14.1 cm^2
4	13.4 cm^2
5	14.1 cm^2
6	14.1 cm^2

Table 3: Surface area series 3

Series 3	
Sample	Area
1	15.7 cm^2
2	17.5 cm^2
3	15.6 cm^2
4	15.8 cm^2
5	17.0 cm^2
6	17.0 cm^2

Table 4: Surface area series 4

Series 4	
Sample	Area
1	13.7 cm^2
2	15.4 cm^2
3	15.5 cm^2
4	15.7 cm^2
5	15.7 cm^2
6	13.8 cm^2

Table 5: Surface of non-exposed samples

Non-exposed	
Sample	Area
1	16.0 cm^2
2	13.0 cm^2
3	14.8 cm^2
4	14.2 cm^2
5	14.2 cm^2
6	13.0 cm^2

A2 VALUES USED FOR CALCULATING CORROSION RATES

Table 2: Values for corrosion rate calculation

Property	**Value**	**Unit**
Molar weight of AlZnIn, M_{AlZnIn}	26.98	g/mol
Density of AlZnIn, ρ_{AlZnIn}	2.78	g/cm^3
Constant for mm/year, K	3268	
Electrons exchanged, η	3	

A3 TECHNICAL DATA FOR THE AL-IN-AN ALLOY USED IN THE EXPERIMENT

SKARPENORD
CORROSION A.S

TECHNICAL DATA

CORAL® 'A'
HIGH GRADE

Al-In-Zn alloy

Chemical composition according to NORSOK specification no. M-503, rev. 2 and certified according to DNV Type Approval program, IOD-90-TAI, November 1982.

The chemical composition and performance data of CORAL® 'A' High Grade alloy are as follows:

Elements	**Analysis (% by weight)**
Zn	3,5 – 5,0
In	0,015 – 0,025
Cu	max. 0,003
Fe	max. 0,09
Si	max. 0,10
Others (each)	max. 0,020
Al	Remainder

Specific gravity 2,78 kg/dm^3 (theoretically)

Performance data in ambient sea water

Capacity	2585 Ah/kg
Consumption rate	3,39 kg/A.yr
Closed circuit potential	-1,09 volt v.s. Ag/AgCl/sea water

Performance data in sea bottom sediments (mud)

	0-20°C	40°C	60°C	80°C
Capacity (Ah/kg)	2400	1750	1150	600
Consumption rate (kg/A.yr)	3,65	5,00	7,62	14,6
Closed circuit potential (volt v.s. Ag/AgCl/sea water	-1,05	-1,03	-1,01	-1,00

VERSION 1/03 – SKARPENORD CORROSION a.s, NORWAY

A4 RISK ASSESSMENT

RISIKOANALYSE

Enhet/Institutt:	Institutt for materialteknologi	**Dato opprettet:**	01.10.2018
Ansvarlig linjeleder (navn):		**Sist revidert:**	01.02.2019
Ansvarlig for aktiviteten som risikovurderes (navn):	Anders Heggseth		
Deltakere (navn):			

Beskrivelse av den aktuelle aktiviteten, området mv.:

Risikoanalysen omfattar labarbeid gjort i forbindelse med prosjektoppgåve og masteroppgåve.

Aktivitet/arbeidsoppgave	**Mulig uønsket hendelse**	**Eksisterende risikoreduserende tiltak**	**Vurdering av sannsynlighet (S)**	**Vurdering av konsekvens (K)** *Vurder en konsevenskategori om gangen. Menneske skal alltid vurderes*				**Risikoverdi (S x K)**	**Forslag til forebyggende og/eller korrigendene tiltak** *Prioriter tiltak som kan forhindre at hendelsen inntreffer (sannsynlighetsreduserende tiltak) foran skjerpet beredskap*	**Restrisiko etter tiltak (S x K)**
			(1-5)	Menneske (1-5)	Økt materiell (1-5)	Ytre miljø (1-5)	Omdømme (1-5)			
Kapping av anodeprøve	*Ødeleggelse av kutteskiver*	*Opplæring og vernebriller*	*4*		*1*			*4*	*Riktig val av kutteskiver og varsomheit*	3 (S = 3)
	Kuttskader	*Opplæring og vernebriller*	*2*	*3*				*6*	*Riktig bruk av utstyr og varsomheit*	3 (S = 1)
Grovsliping av forsøksprøve	Skade på fingrar		2	1				2	Varsomheit	2 (S = 2)
Borring av forsøksprøve	Skade på hender		2	2				4	Varsomheit og riktig bruk av utstyr	2 (S = 1)
Lekasje på kontainer med sjøvann	Materielle skader på omgivelsar		2		3			6	Undersøke at kontainer er tett og tilsyn	3 (S = 1)
Avslutte langtidsforsøk på Sealab	Ødelegge prøvar eksponert i mange måndar		2		3			6	Varsomheit i avvikling av forsøk	3 (S = 1)
Undersøke tverrsnitt i SEM	Skade på SEM	Opplæring	2		4			8		4 (S = 1)

Sannsynlighet vurderes etter følgende kriterier:

1 - Svært liten	2 - Liten	3 - Middels	4 - Stor	5 - Svært stor
1 gang pr. 50 år eller sjeldnere. Ergonomi/psykososialt: Ingen tilfeller.	1 gang pr. 10 år eller sjeldnere. Ergonomi/psykososialt: Ett enkelt tilfelle.	1 gang pr. år eller sjeldnere. Ergonomi/psykososialt: Enkelttilfeller	1 gang pr. måned eller sjeldnere. Ergonomi/psykososialt: Periodevis	Daglig - hver uke. Ergonomi/psykososialt: Kontinuerlig

Konsekvens vurderes etter følgende kriterier:

Gradering	Menneske	Ytre miljø Vann, jord og luft	Øk/materiell	Omdømme
5 - Svært Alvorlig	Død eller uførhet/varig nedsatt funksjonsevne	Svært langvarig og ikke reversibel skade	Drifts- eller aktivitetsstans >1 år.	Troverdighet og respekt betydelig og varig svekket
4 - Alvorlig	Alvorlig skade/belastning som krever medisinsk behandling. Mulig uførhet/varig nedsatt funksjonsevne	Langvarig skade. Lang restitusjonstid	Driftsstans > ½ år Aktivitetsstans i opp til 1 år	Troverdighet og respekt betydelig svekket
3 - Moderat	Alvorlig skade/belastning som krever medisinsk behandling. Lang restitusjonstid.	Mindre skade og lang restitusjonstid	Drifts- eller aktivitetsstans < 1 mnd	Troverdighet og respekt svekket
2 - Liten	Skade /belastning som krever medisinsk behandling. Reversibel skade. Kort restitusjonstid.	Mindre skade og kort restitusjonstid	Drifts- eller aktivitetsstans < 1uke	Negativ påvirkning på troverdighet og respekt
1 - Svært liten	Mindre skade/belastning som krever enkel behandling. Reversibel skade/belastning. Kort restitusjonstid.	Ubetydelig skade og kort restitusjonstid	Drifts- eller aktivitetsstans < 1dag	Liten påvirkning på troverdighet og respekt

Risikoverdi = Sannsynlighet x Konsekvens:

KONSEKVENS	5. Svært alvorlig	5	10	15	20	25
	4. Alvorlig	4	8	12	16	20
	3. Moderat	3	6	9	12	15
	2. Liten	2	4	6	8	10
	1. Svært liten	1	2	3	4	5
		1. Svært liten	2. Liten	3. Middels	4. Stor	5. Svært stor
		SANNSYNLIGHET				

Fargene angir grad av risiko:

Rød		Uakseptabel risiko. Tiltak skal gjennomføres.
Gul		Middels risiko. Tiltak skal vurderes.
Grønn		Akseptabel risiko. Tiltak kan vurderes.

A5 SEM MAPPING ANALYSIS RESULTS WHICH WAS NOT INCLUDED IN RESULTS

SERIES 1, SAMPLE 2

AREA 1

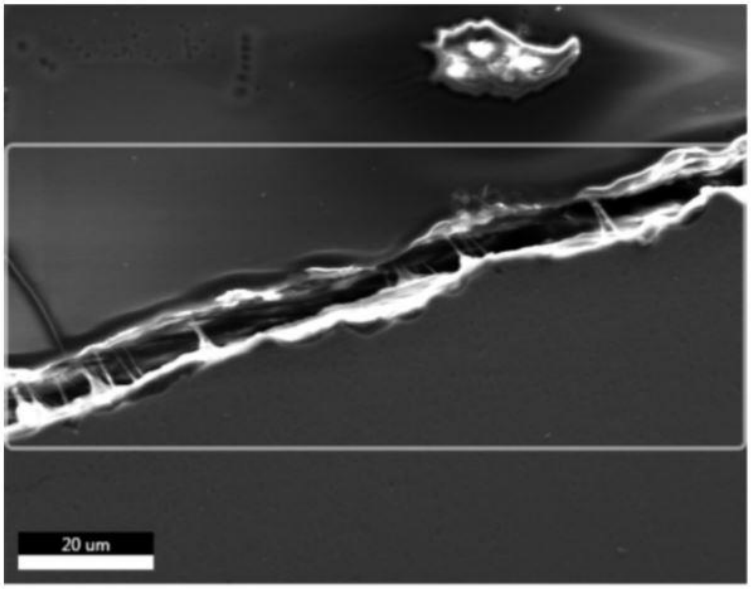

Figure A5.1: Secondary electron image of sample 2 in series 1 from area 1

AREA 2

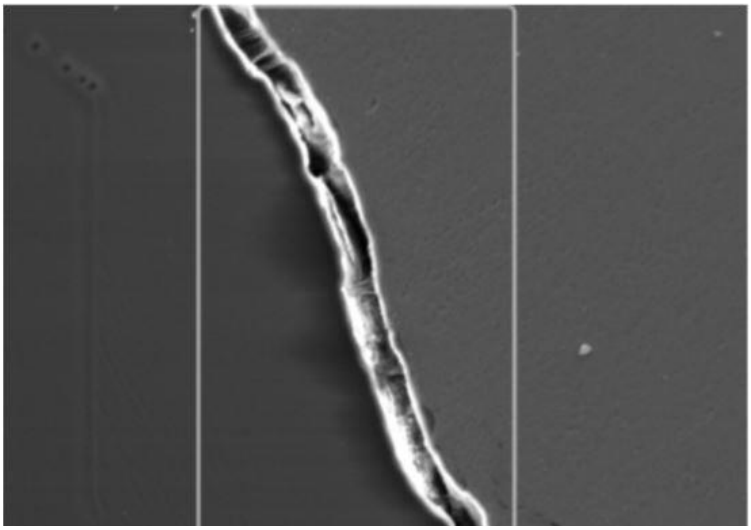

Figure A5.2: Secondary electron image of sample 2 in series 1 from area 2

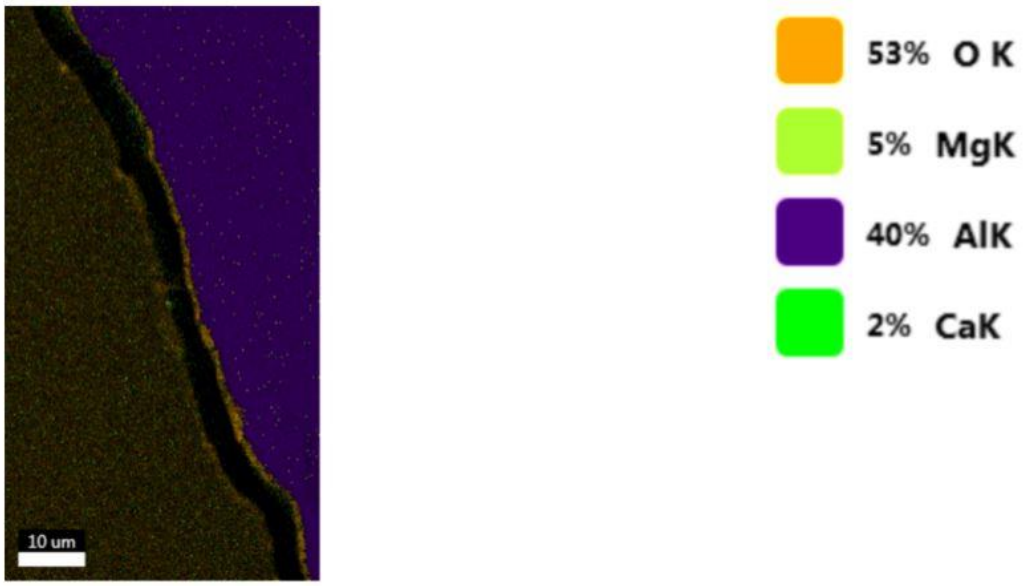

Figure A5.3: Element overlay from the cross section of sample 2 from series 1 from area 2

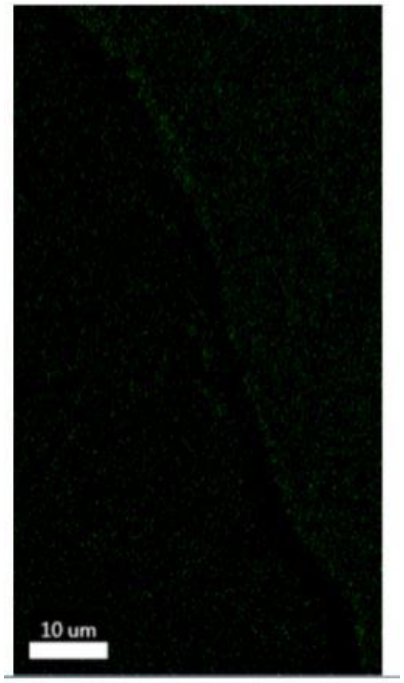

Figure A5.4: Mapping result showing the calcium content of sample 2 from series 1 in area 2

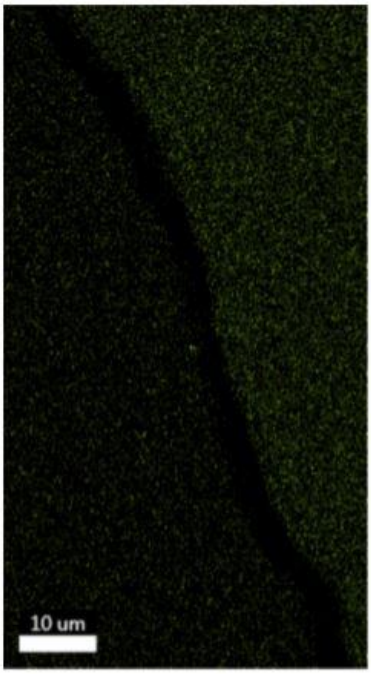

Figure A5.5: Mapping result showing the magnesium content of sample 2 from series 1 in area 2

AREA 3

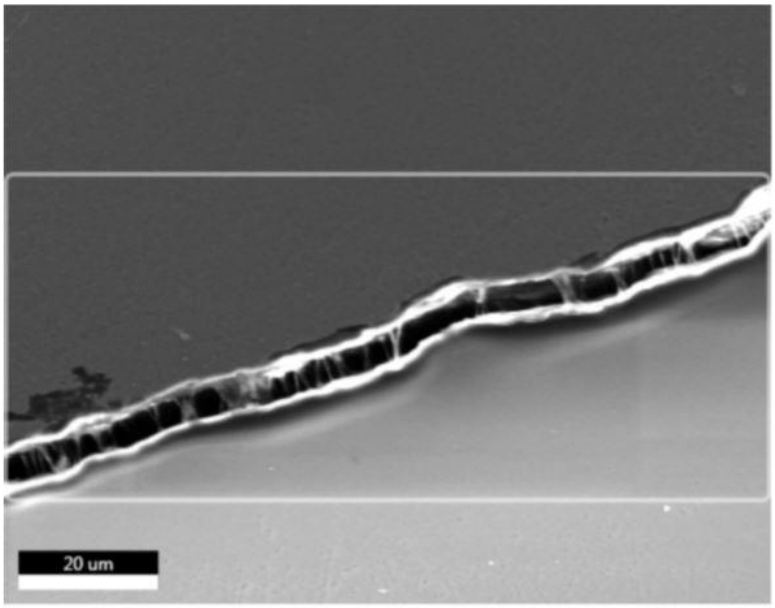

Figure A5.6: Secondary electron image of sample 2 in series 1 from area 3

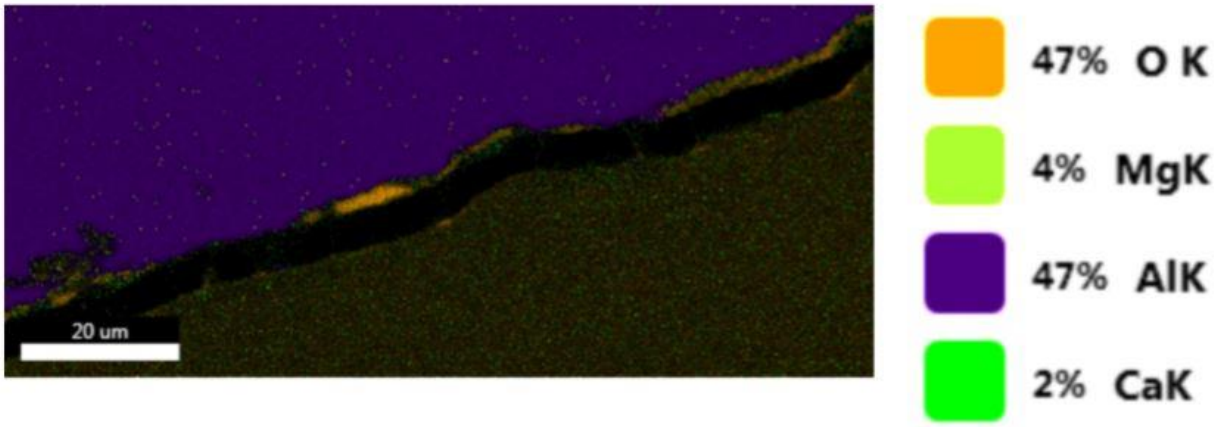

Figure A5.7: Element overlay from the cross section of sample 2 from series 1 in area 3

Figure A5.8: Mapping result showing the magnesium content of sample 2 from series 1 in area 3

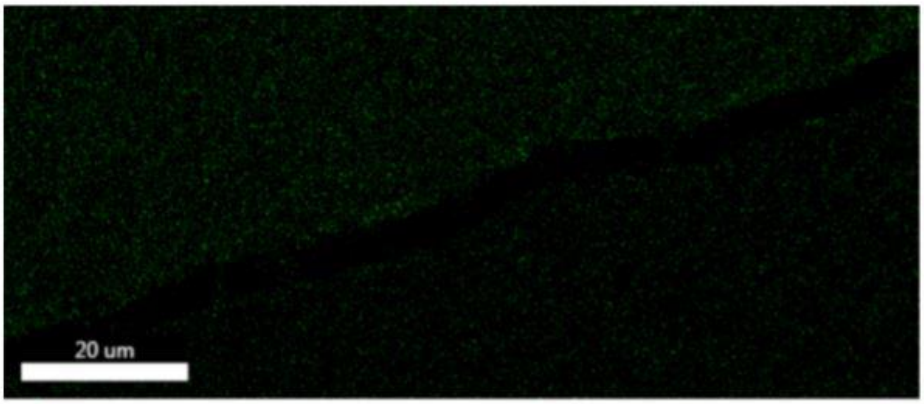

Figure A5.9: Mapping result showing the calcium content of sample 2 from series 1 in area 3

SERIES 2, SAMPLE 5

AREA 1

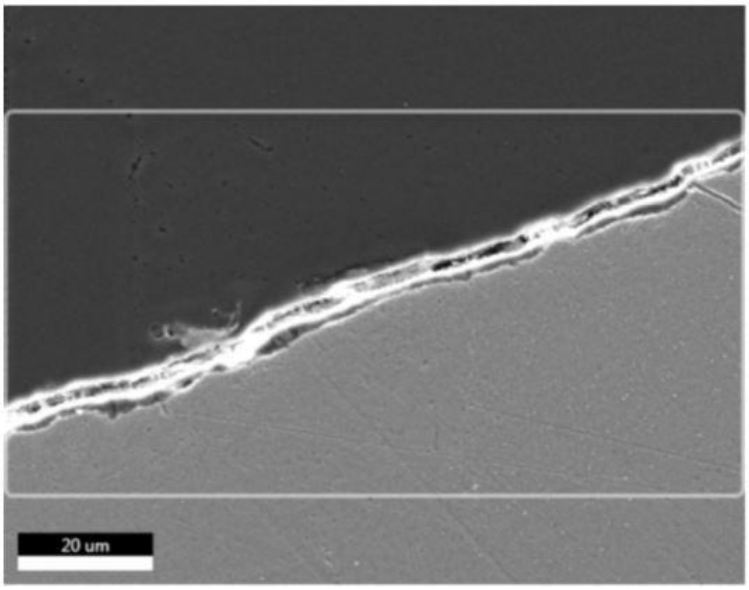

Figure A5.10: Secondary electron image of sample 5 in series 2 from area 1

AREA 2

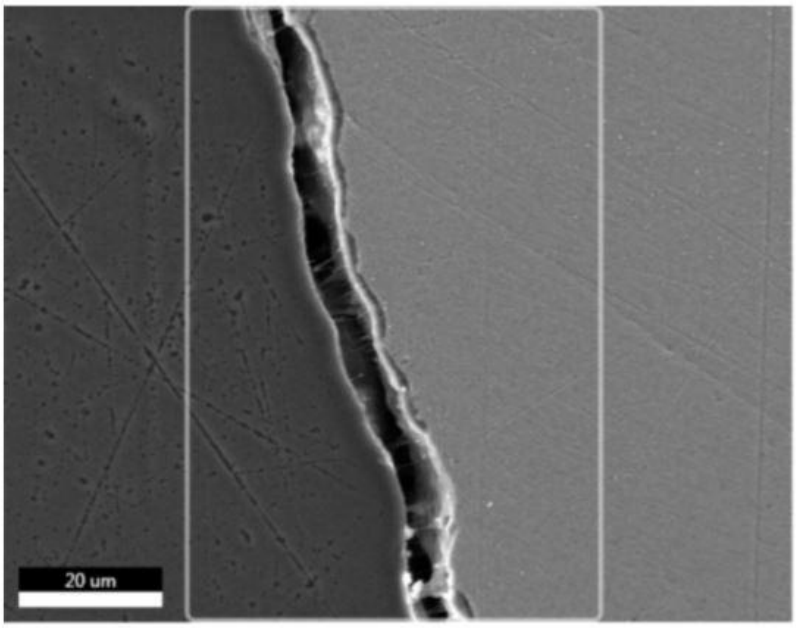

Figure A5.11: Secondary electron image of sample 5 in series 2 from area 2

Figure A5.12: Element overlay from the cross section of sample 5 from series 2 in area 2

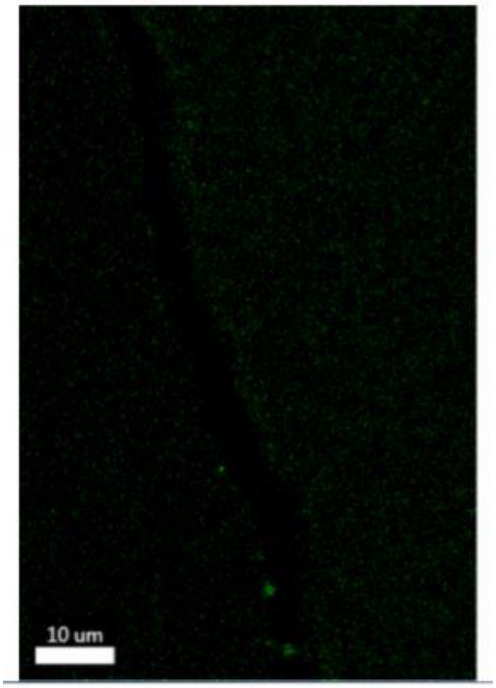

Figure A5.13: Mapping result showing the calcium content of sample 5 from series 2 in area 2

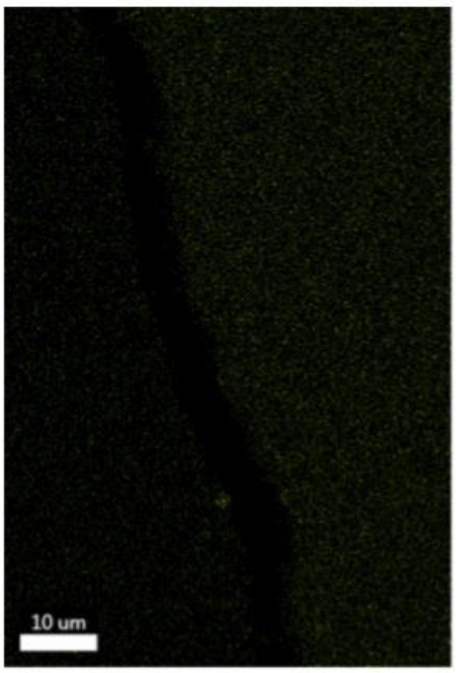

Figure A5.14: Mapping result showing the magnesium content of sample 5 from series 2 in area 2

AREA 3

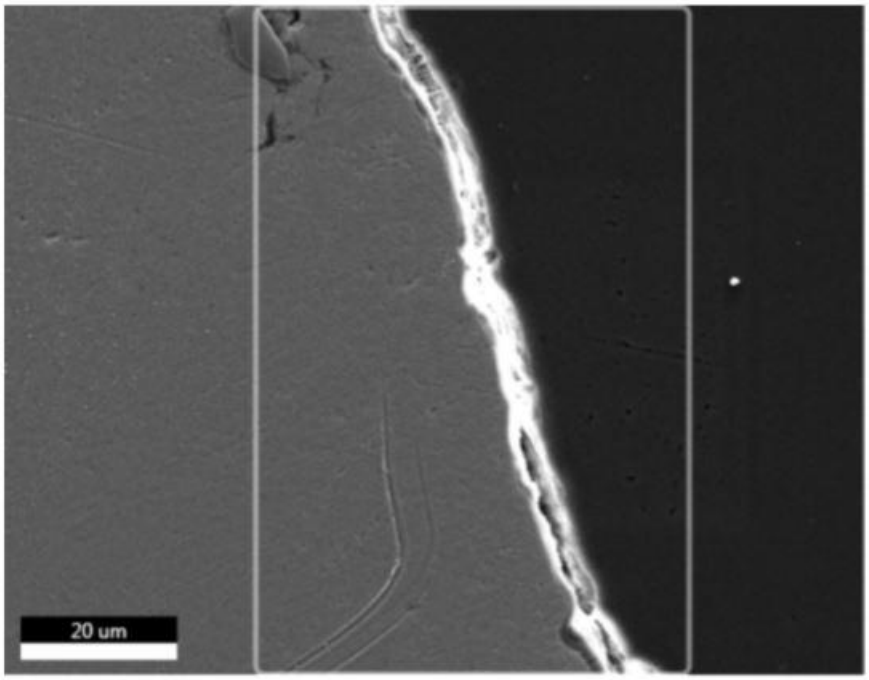

Figure A5.15: Secondary electron image of sample 5 in series 2 from area 3

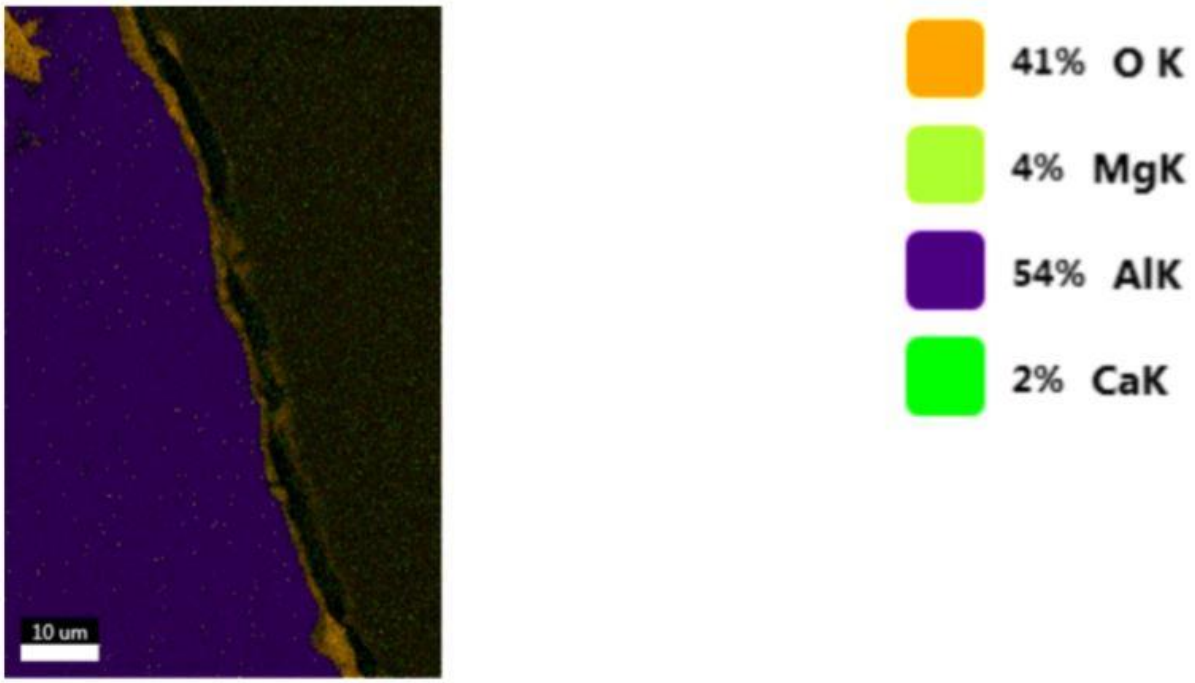

Figure A5.16: Element overlay from the cross section of sample 5 from series 2 in area 3

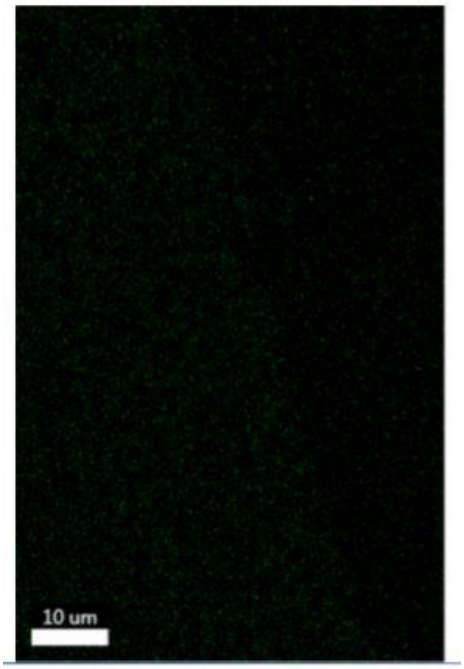

Figure A5.17: Mapping result showing the calcium content of sample 5 from series 2 in area 3

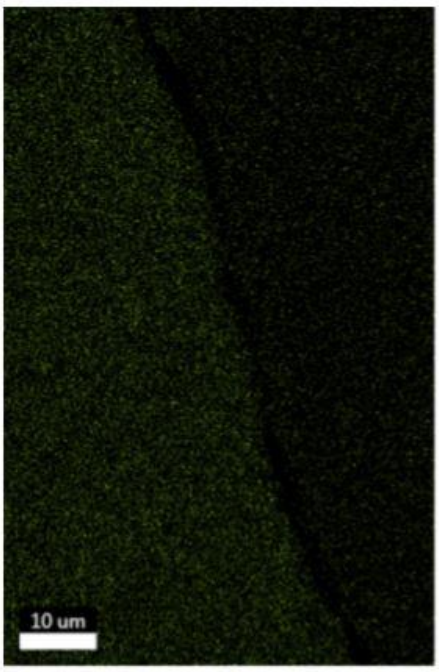

Figure A5.18: Mapping result showing the magnesium content of sample 5 from series 2 in area 3

SERIES 3, SAMPLE 2

AREA 1

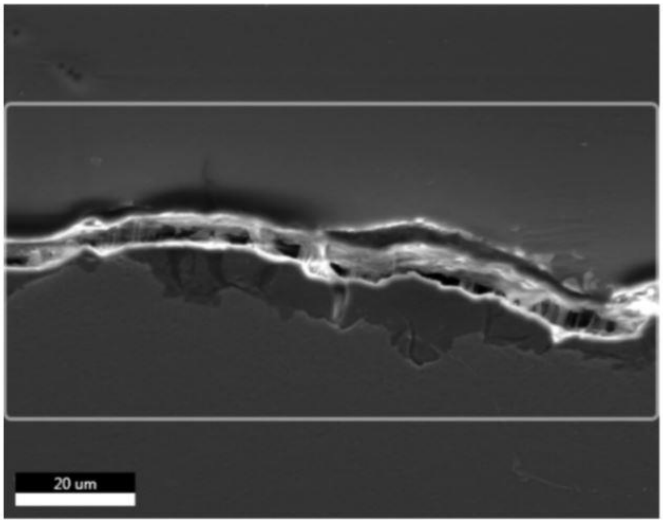

Figure A5.19: Secondary electron image of sample 2 in series 3 from area 1

AREA 2

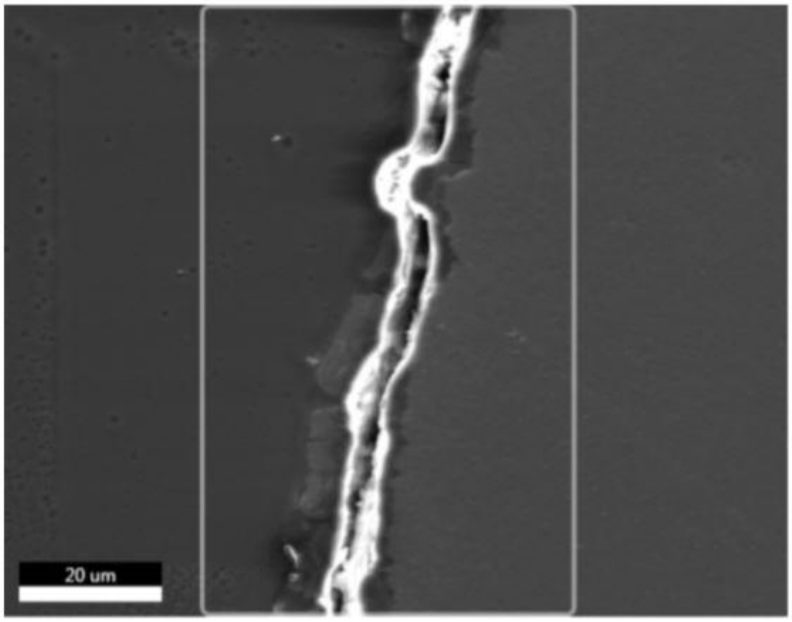

Figure A5.20: Secondary electron image of sample 2 in series 3 from area 2

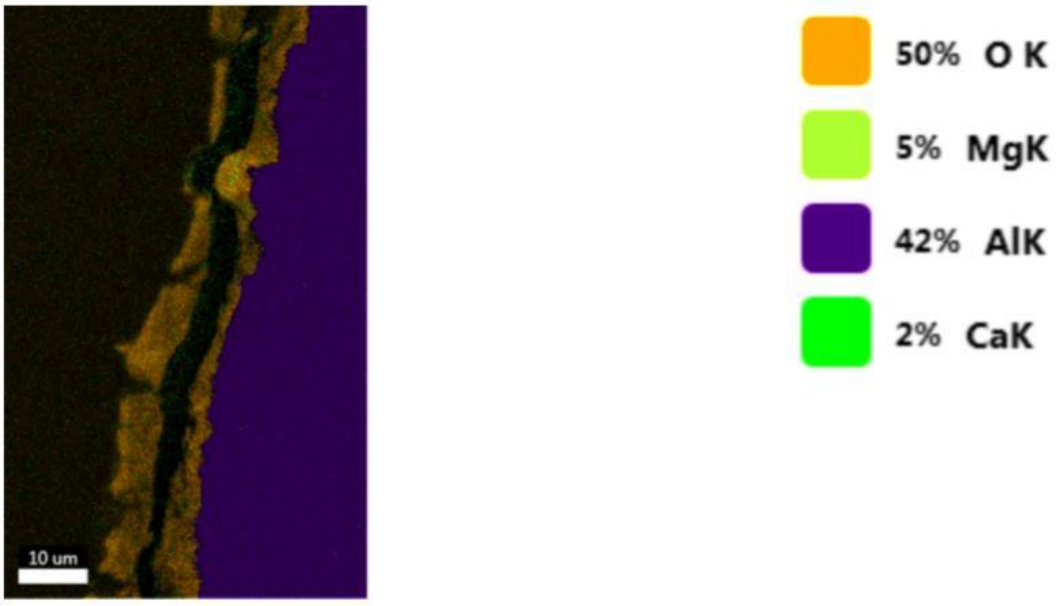

Figure A5.21: Element overlay from the cross section of sample 2 from series 3 in area 2

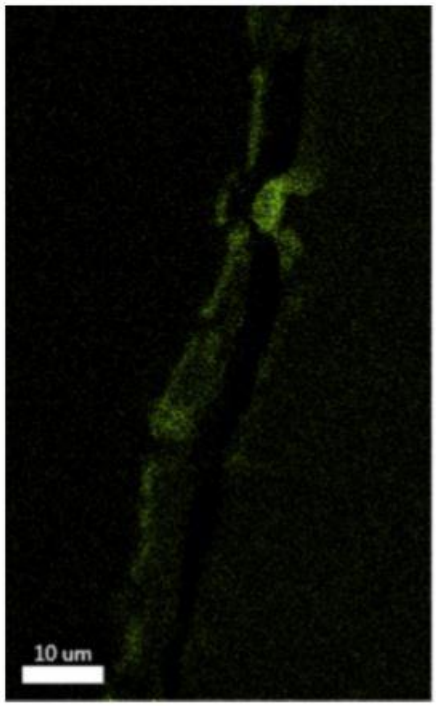

Figure A5.22: Mapping result showing the calcium content of sample 2 from series 3 in area 2

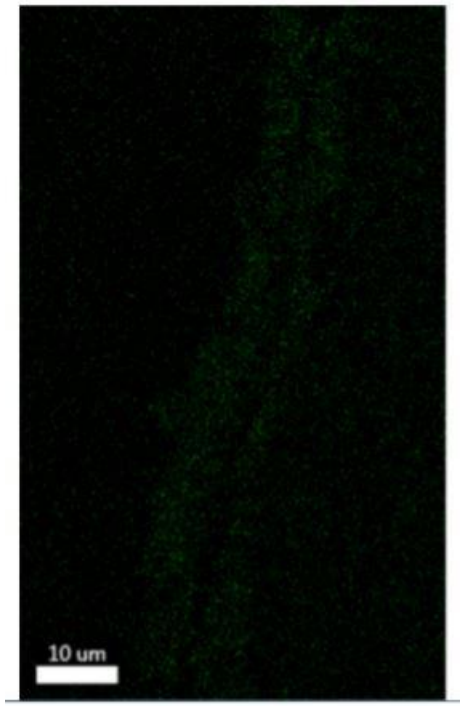

Figure A5.23: Mapping result showing the magnesium content of sample 2 from series 3 in area 2

AREA 3

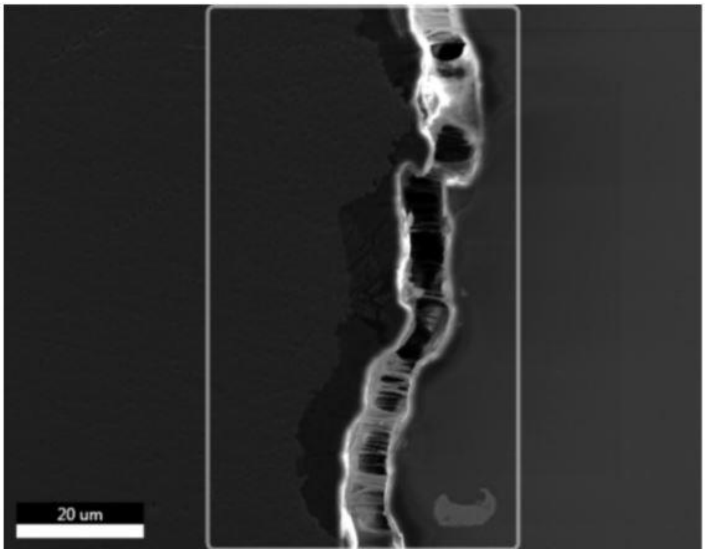

Figure A5.24: Secondary electron image of sample 2 in series 3 from area 3

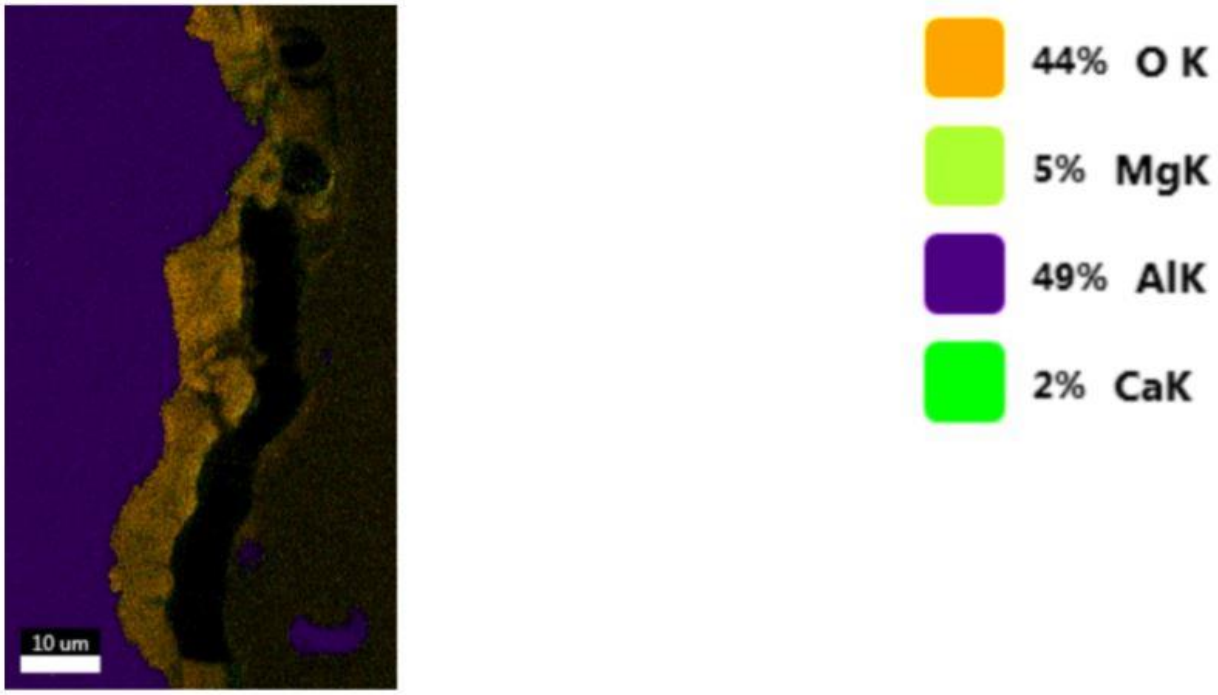

Figure A5.25: Element overlay from the cross section of sample 2 from series 3 in area 3

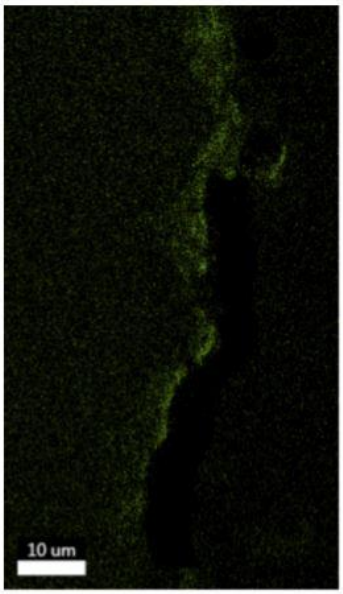

Figure A5.26: Mapping result showing the calcium content of sample 2 from series 3 in area 3

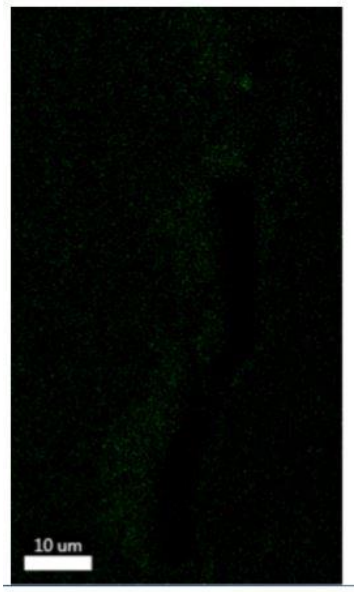

Figure A5.27: Mapping result showing the magnesium content of sample 2 from series 3 in area 3

SERIES 4, SAMPLE 2

AREA 1

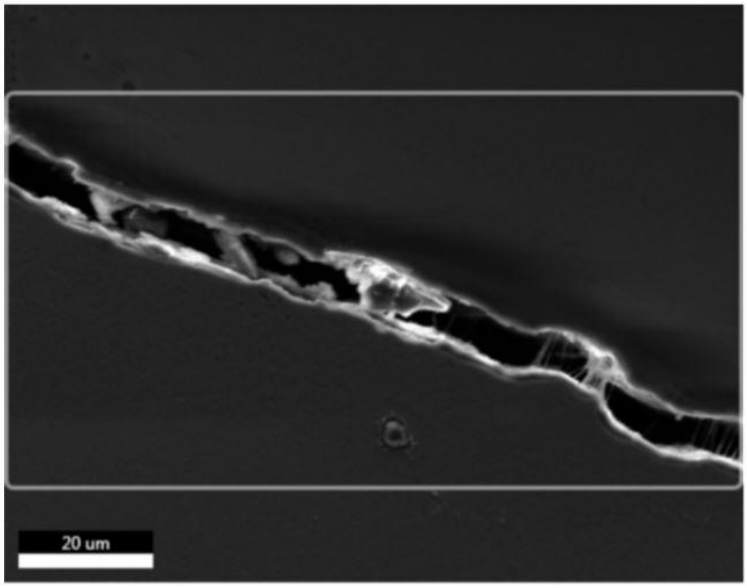

Figure A5.28: Secondary electron image of sample 2 in series 4 from area 1

AREA 2

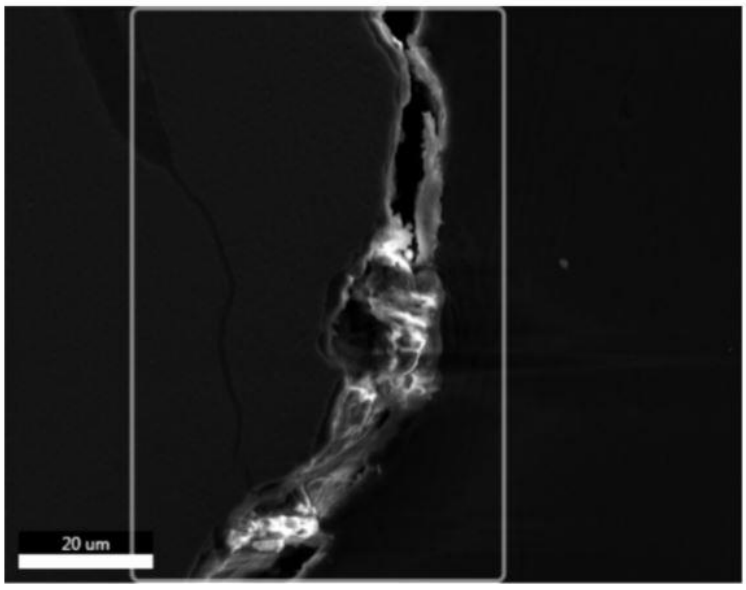

Figure A5.29: Secondary electron image of sample 2 in series 4 from area 2

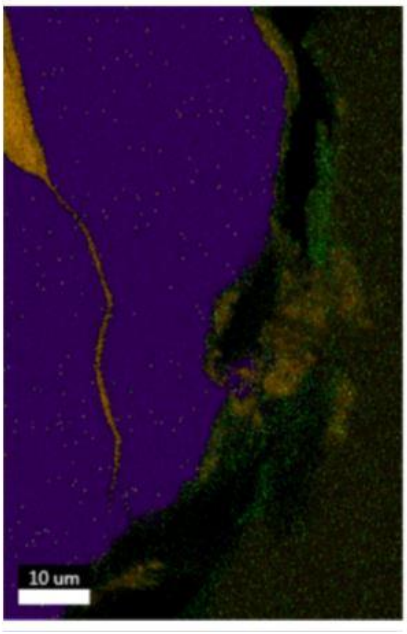

Figure A5.30: Element overlay from the cross section of sample 2 from series 4 in area 2

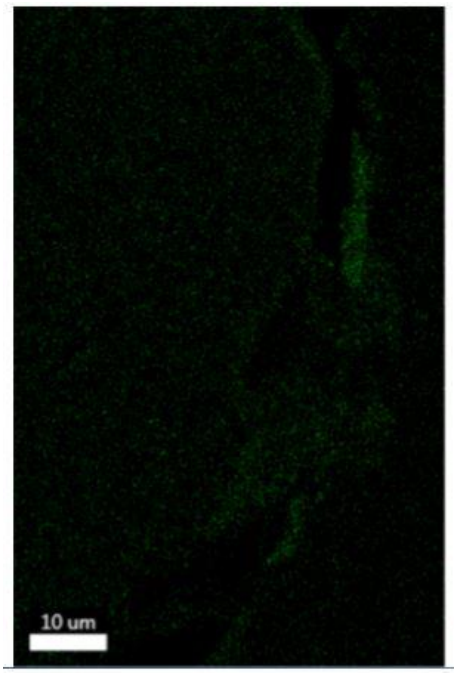

Figure A5.31: Mapping result showing the calcium content of sample 2 from series 4 in area 2

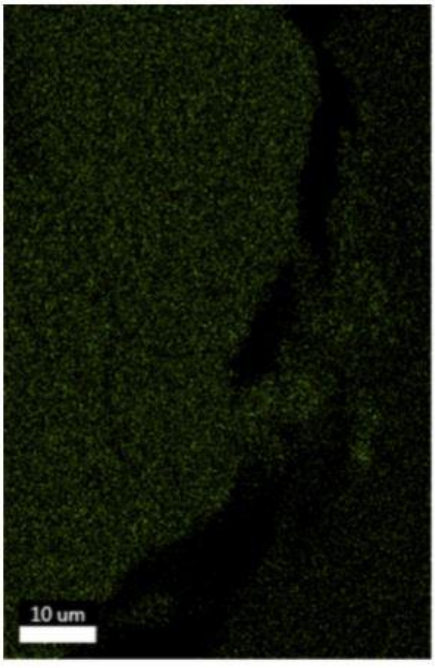

Figure A5.32: Mapping result showing the magnesium content of sample 2 from series 4 in area 2

AREA 3

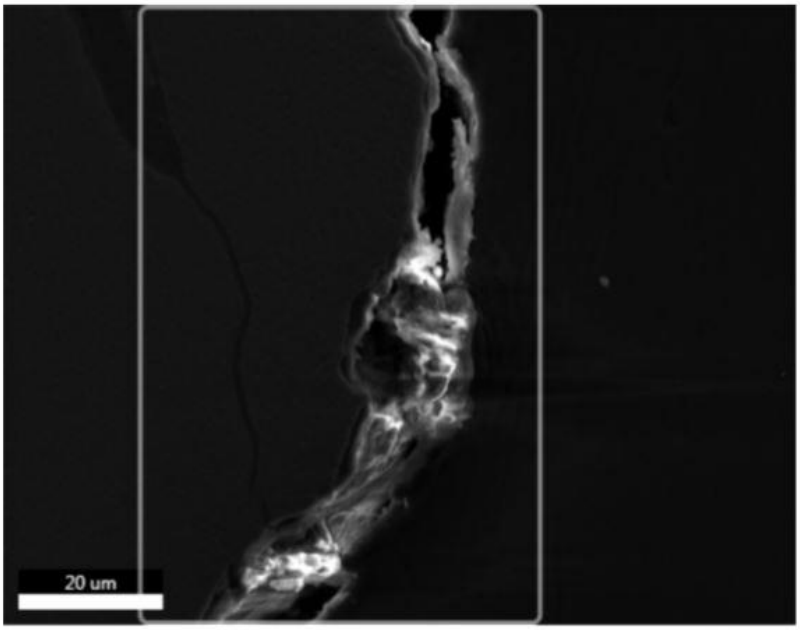

Figure A5.33: Secondary electron image of sample 2 in series 4 from area 3

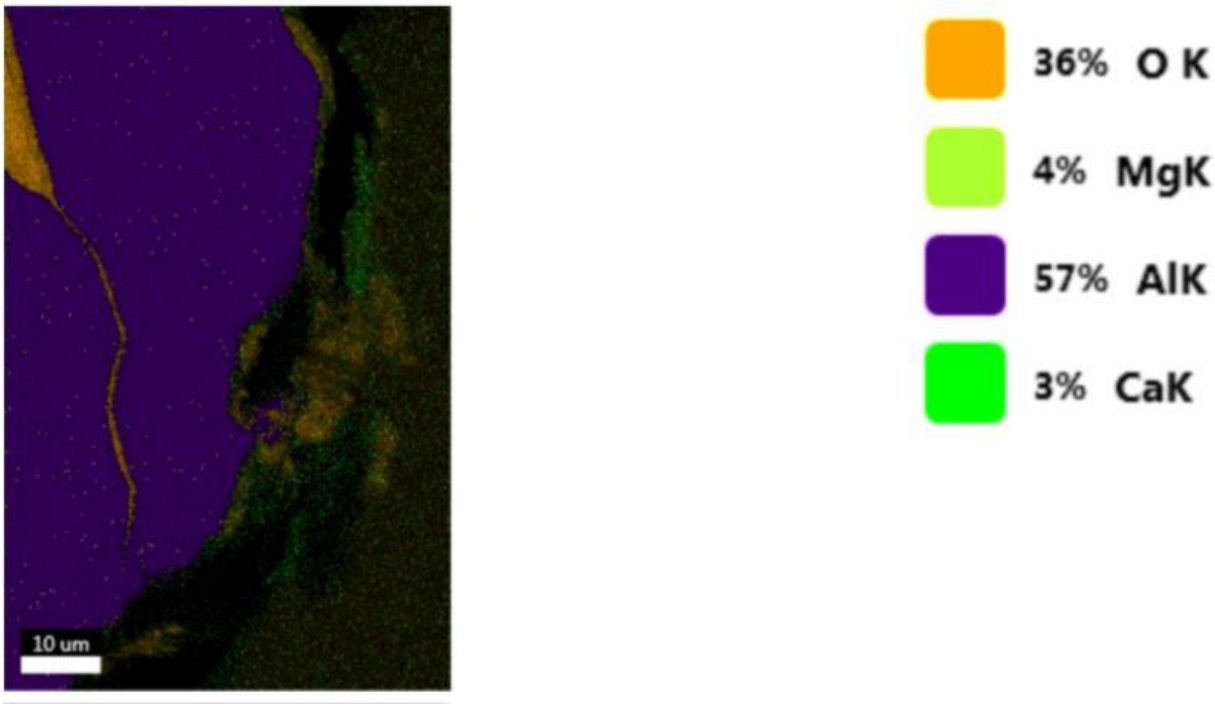

Figure A5.34: Element overlay from the cross section of sample 2 from series 4 in area 3

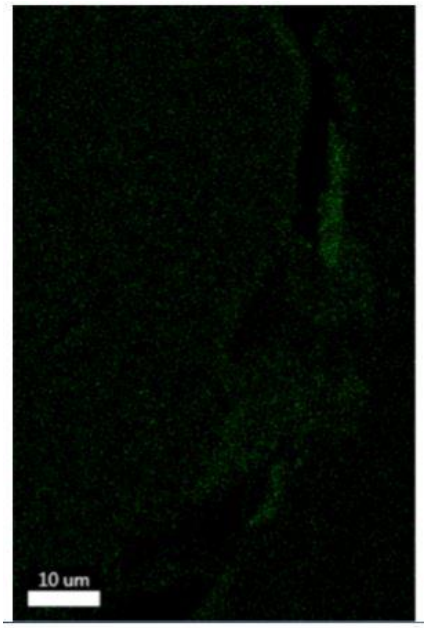

Figure A5.35: Mapping result showing the calcium content of sample 2 from series 4 in area 3

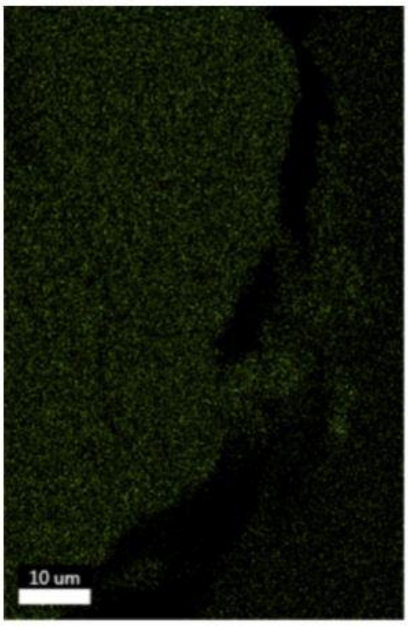

Figure A5.36: Mapping result showing the magnesium content of sample 2 from series 4 in area 3

SERIES 3, SAMPLE 6 (NO POLARIZATION CURVE RECORDED BEFORE INSPECTION)

AREA 1

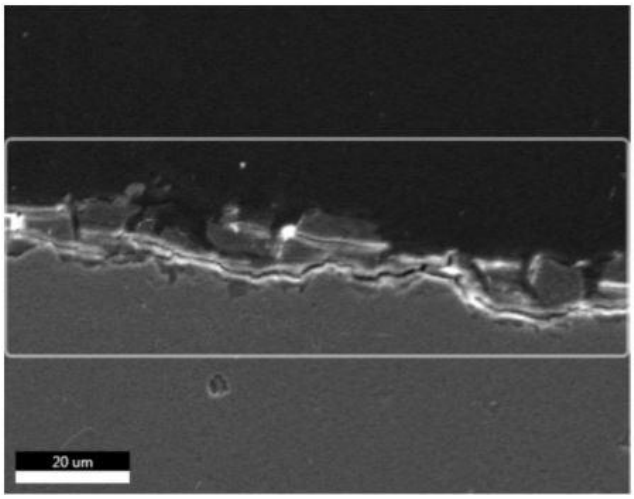

Figure A5.37: Secondary electron image of sample 6 in series 3 from area 1. Sample not anodically polarized prior to inspection

AREA 2

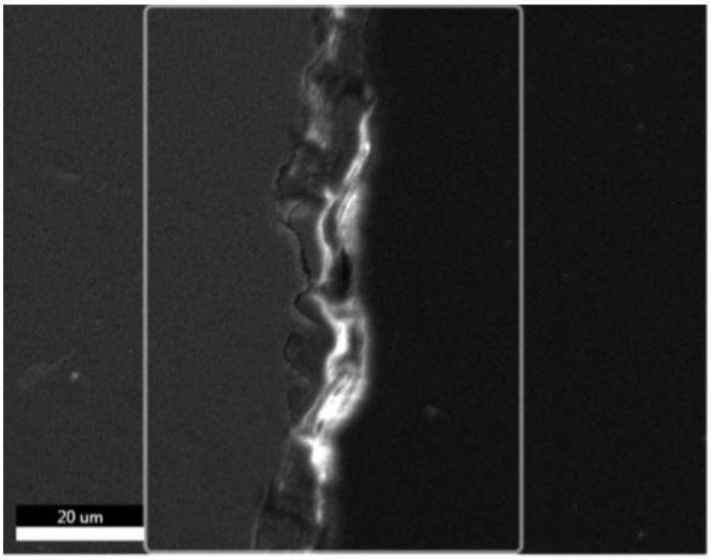

Figure A5.38: Secondary electron image of sample 6 in series 3 from area 2. Sample not anodically polarized prior to inspection

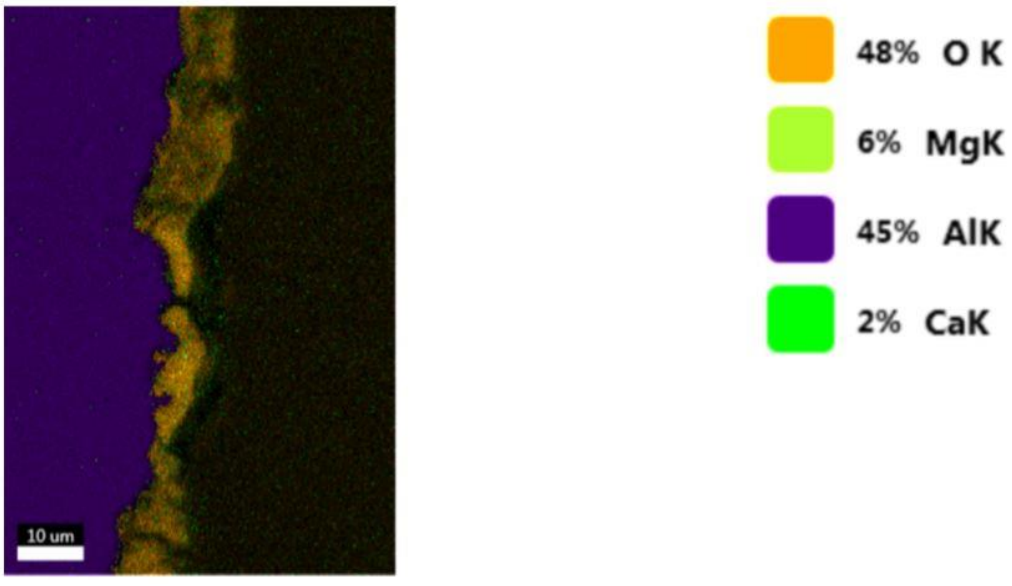

Figure A5.39: Element overlay from the cross section of sample 6 from series 3 in area 2. Sample not anodically polarized prior to inspection

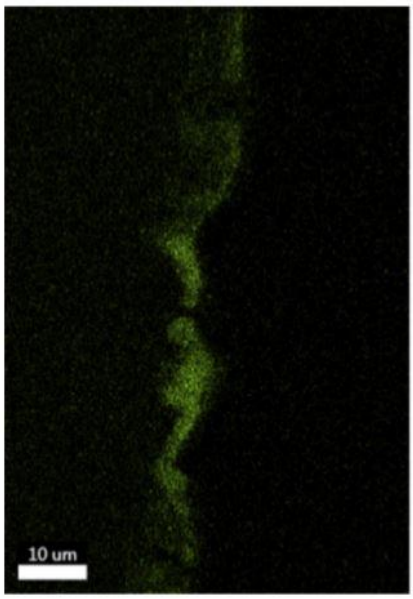

Figure A5.40: Mapping result showing the magnesium content of sample 6 from series 3 in area 2. Sample not anodically polarized prior to inspection

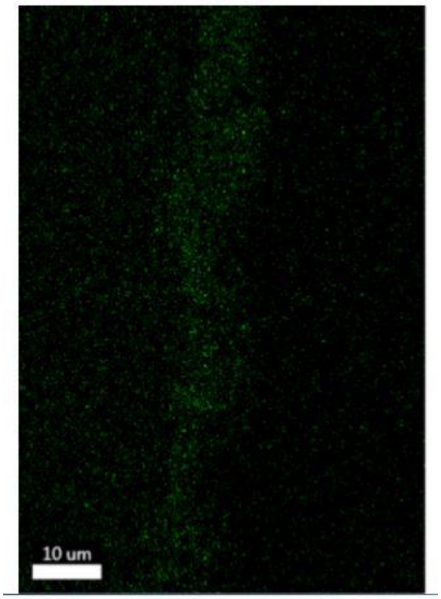

Figure A5.41: Mapping result showing the calcium content of sample 6 from series 3 in area 2. Sample not anodically polarized prior to inspection

AREA 3

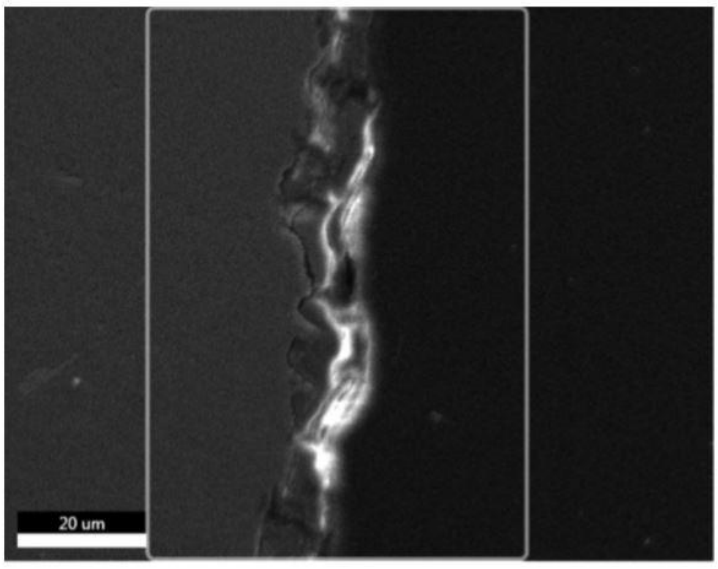

Figure A5.42: Secondary electron image of sample 6 in series 3 from area 3. Sample not anodically polarized prior to inspection

Figure A5.43: Element overlay from the cross section of sample 6 from series 3 in area 3. Sample not anodically polarized prior to inspection.

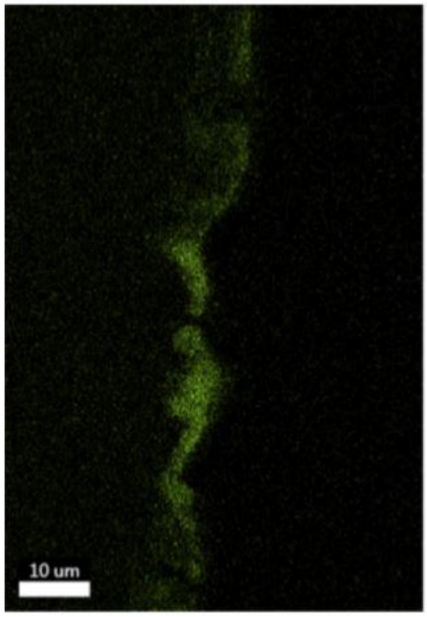

Figure A5.44: Mapping result showing the calcium content of sample 6 from series 3 in area 3. Sample not anodically polarized prior to inspection

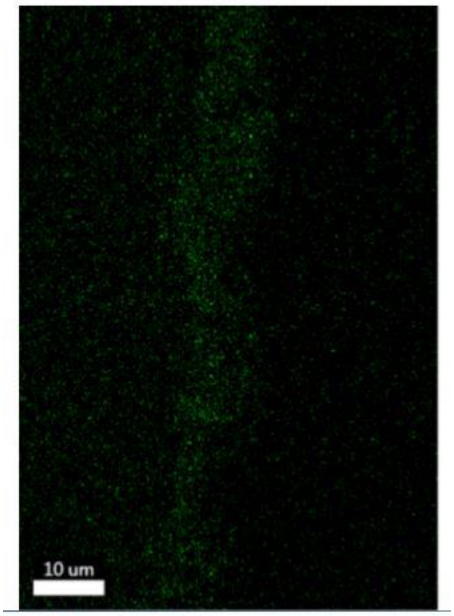

Figure A5.45: Mapping result showing the calcium content of sample 6 from series 3 in area 3. Sample not anodically polarized prior to inspection

Anders Opheim Heggseth

Passivation and Reactivation of Aluminium Sacrificial Anodes

NTNU
Norwegian University of
Science and Technology